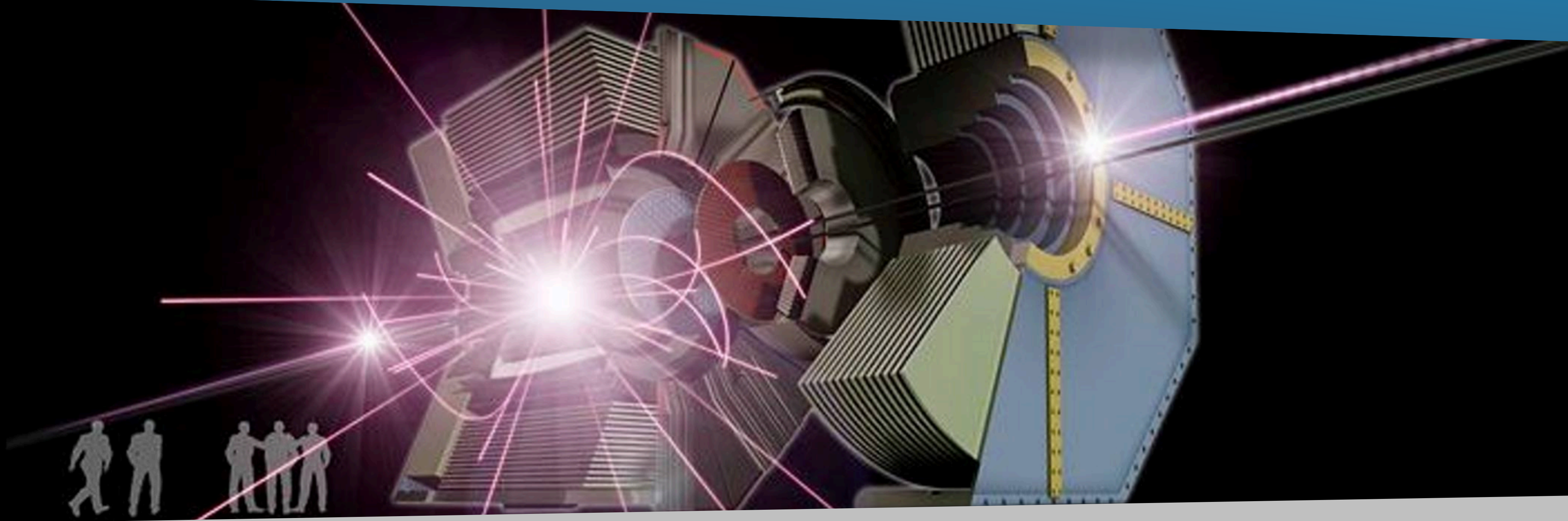


Status and Recent Highlights of Belle II



Lu Cao

(for the Belle II Collaboration)

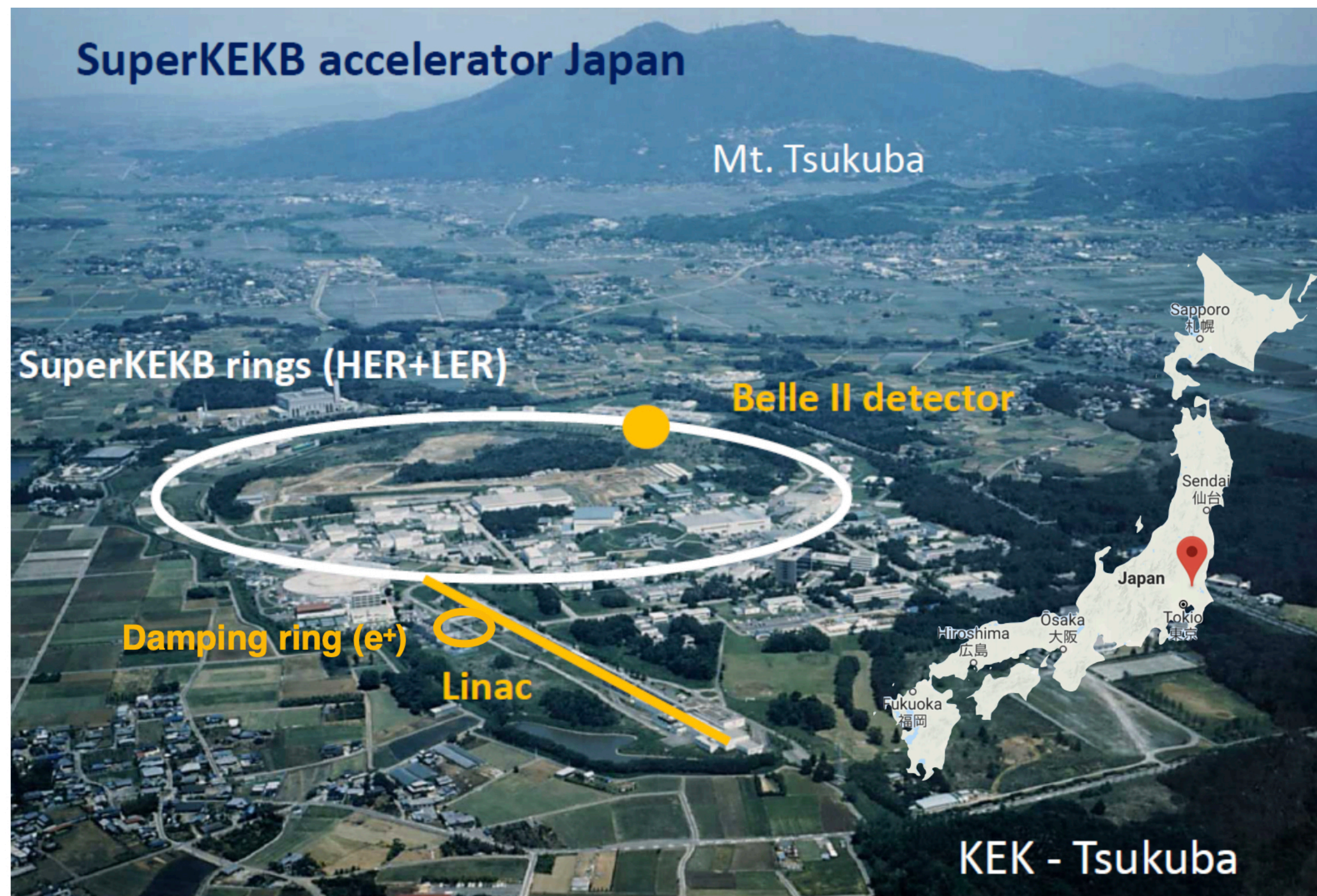
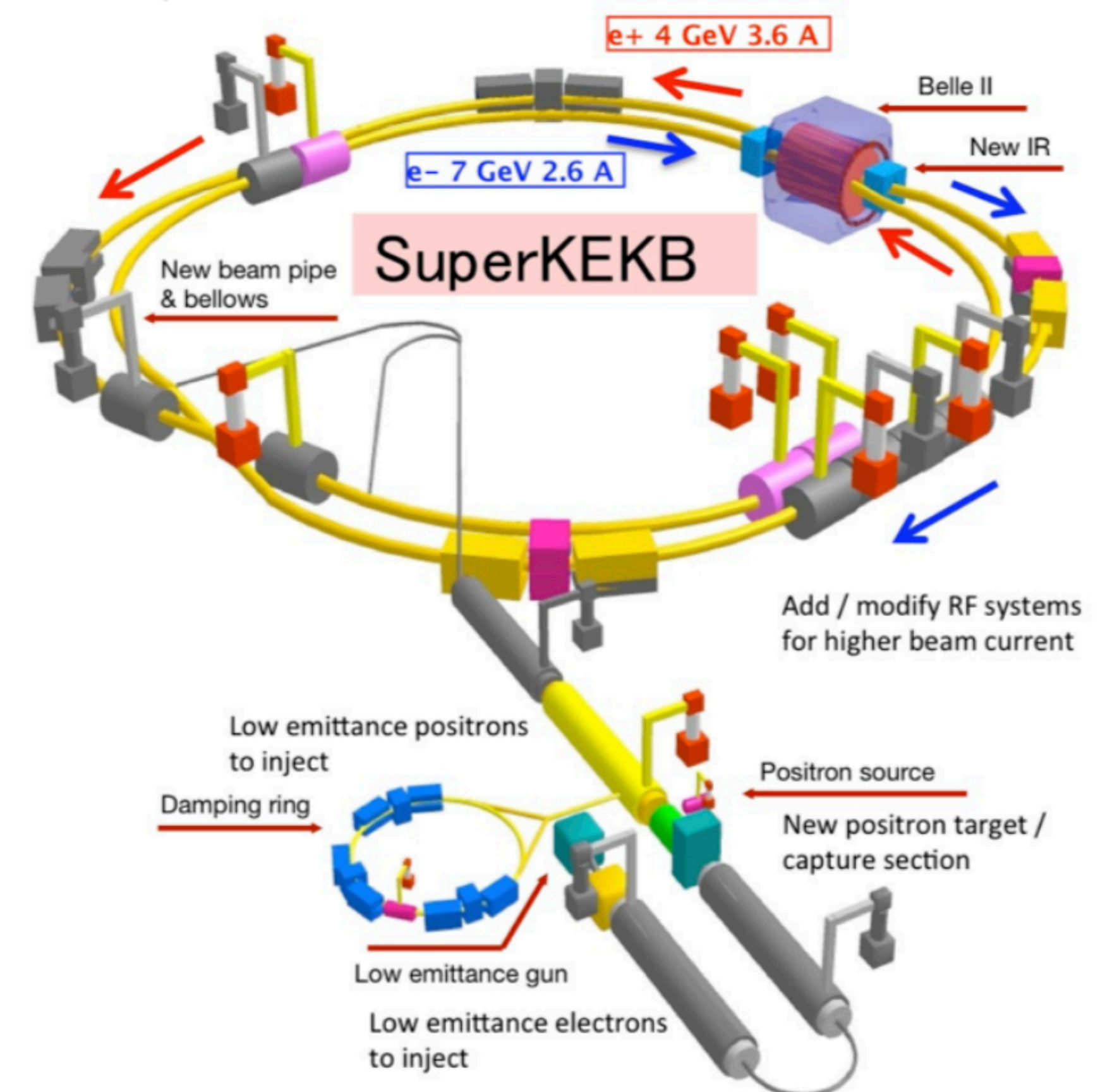
CEA (Paris-Saclay), 05-22-2023



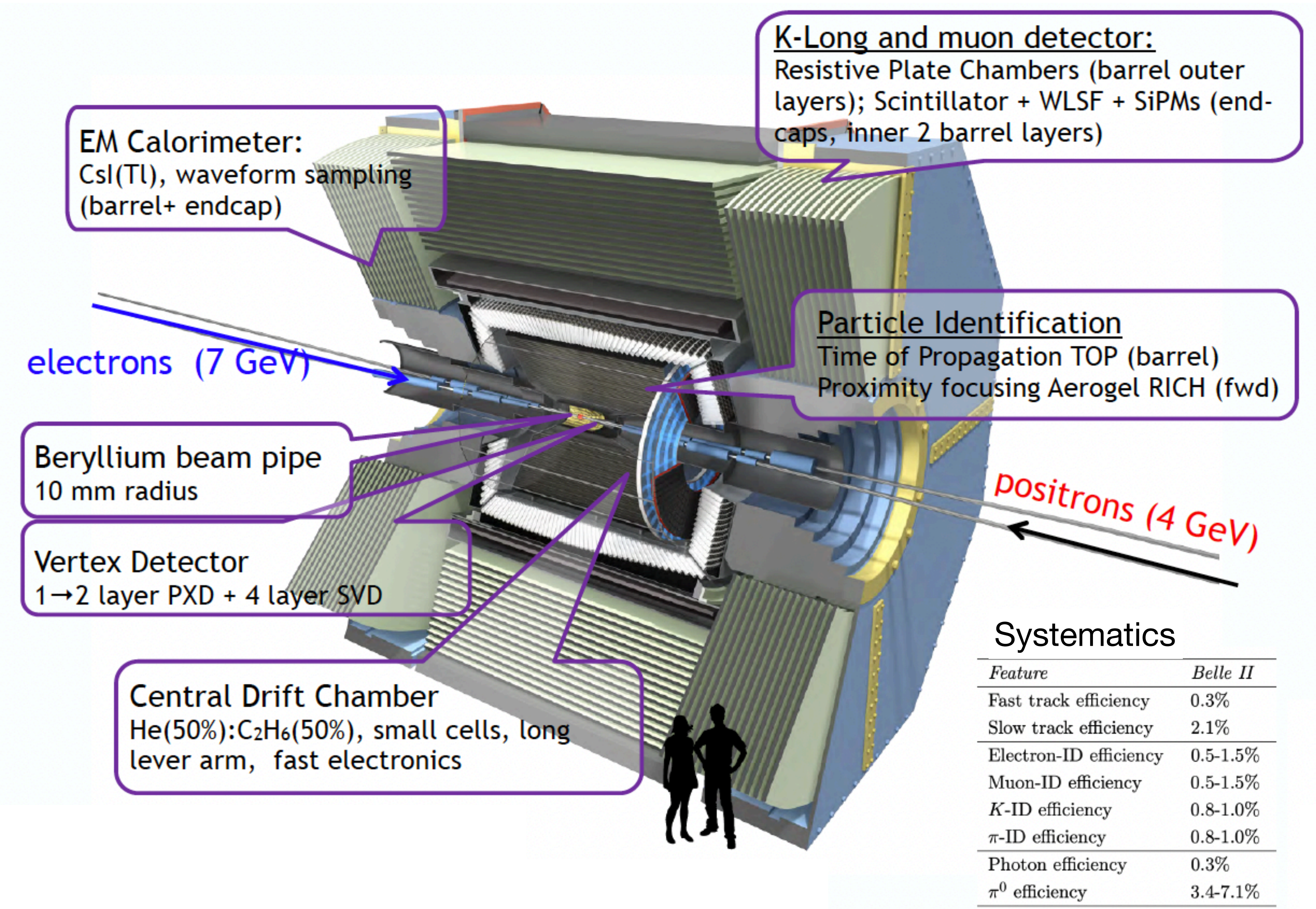
Belle II Experiment @ SuperKEKB

- Asymmetric-energy e^+e^- collider operating near $\Upsilon(4S)$ mass peak
- KEKB => **SuperKEKB**; Belle => **Belle II**
- Goal is to collect **50 billion $B\bar{B}$ pairs!**

Upgraded detector and accelerator



Belle II Detector

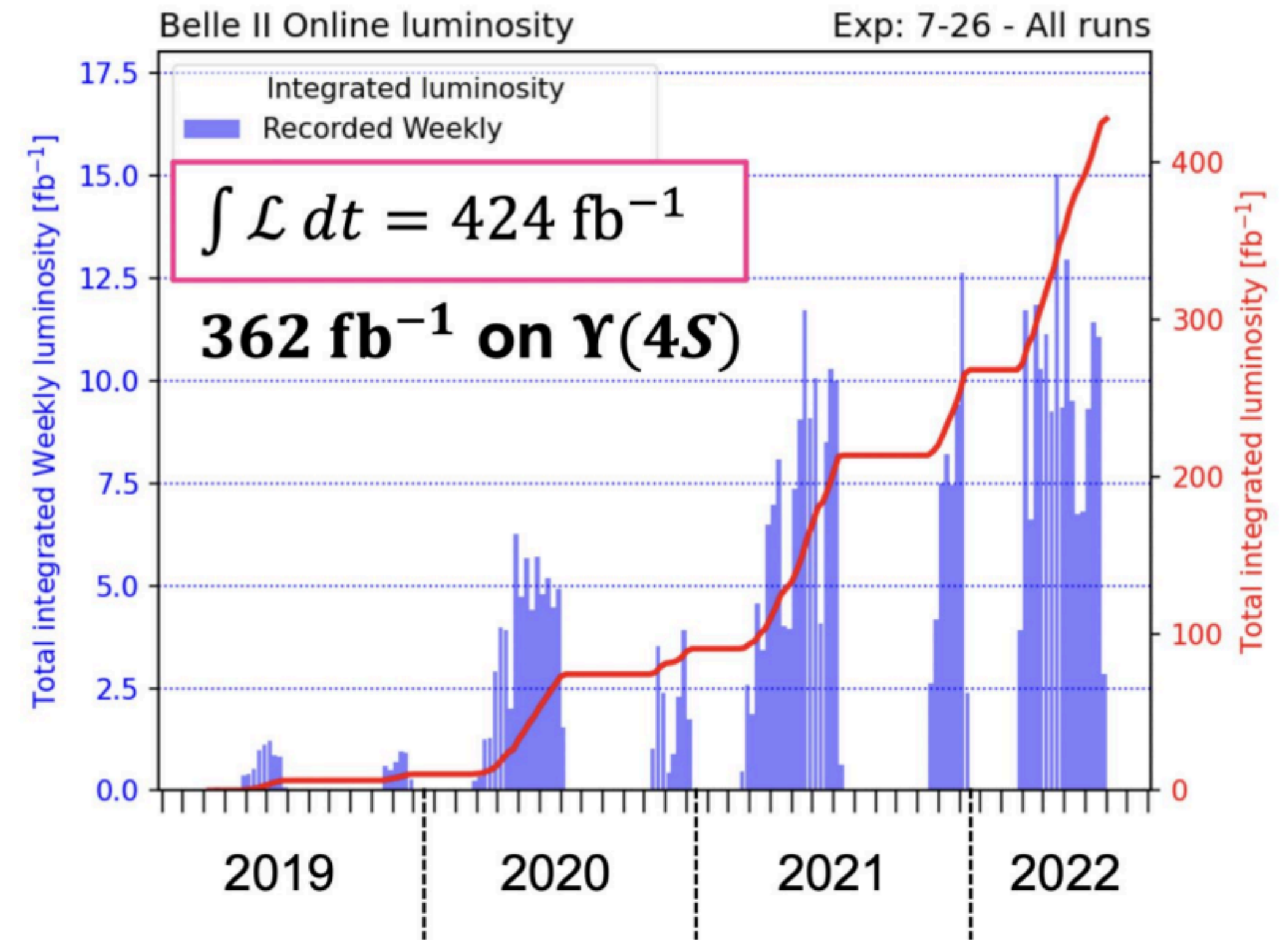
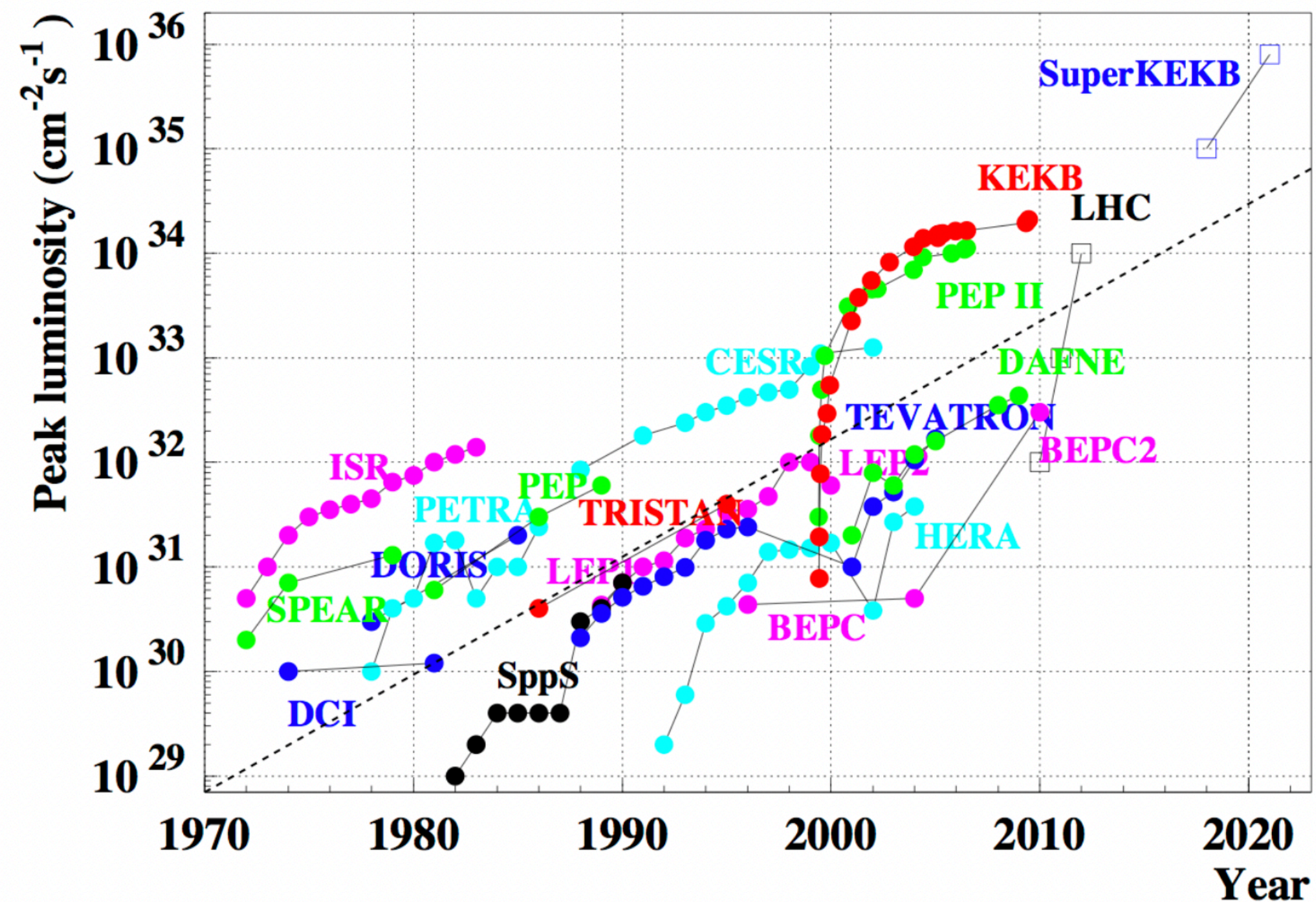


Systematics

| Feature | Belle II |
|------------------------|----------|
| Fast track efficiency | 0.3% |
| Slow track efficiency | 2.1% |
| Electron-ID efficiency | 0.5-1.5% |
| Muon-ID efficiency | 0.5-1.5% |
| K-ID efficiency | 0.8-1.0% |
| π -ID efficiency | 0.8-1.0% |
| Photon efficiency | 0.3% |
| π^0 efficiency | 3.4-7.1% |

Status of Belle II Experiment

- Max instantaneous luminosity $L_{\text{peak}} = 4.7 \times 10^{34} \text{ cm}^{-2}\text{s}^{-1}$ (world record)
- By summer 2022, $L_{\text{int}} = 424 \text{ fb}^{-1}$ accumulated (similar to full dataset of BaBar, ~1/2 of Belle's)
- Ultimate goal: reach 50 ab^{-1} by operating at instantaneous lumi. of $6 \times 10^{35} \text{ cm}^{-2}\text{s}^{-1}$



Status of Belle II Experiment

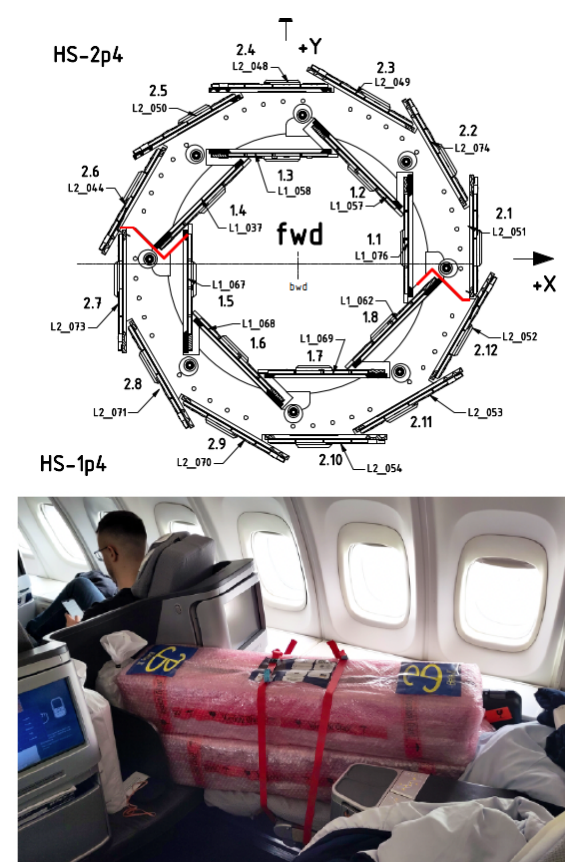
- Currently, we are in **LS1** (long shutdown 1) starting from summer 2022
- Operation will be resumed in the coming winter

We are working on:

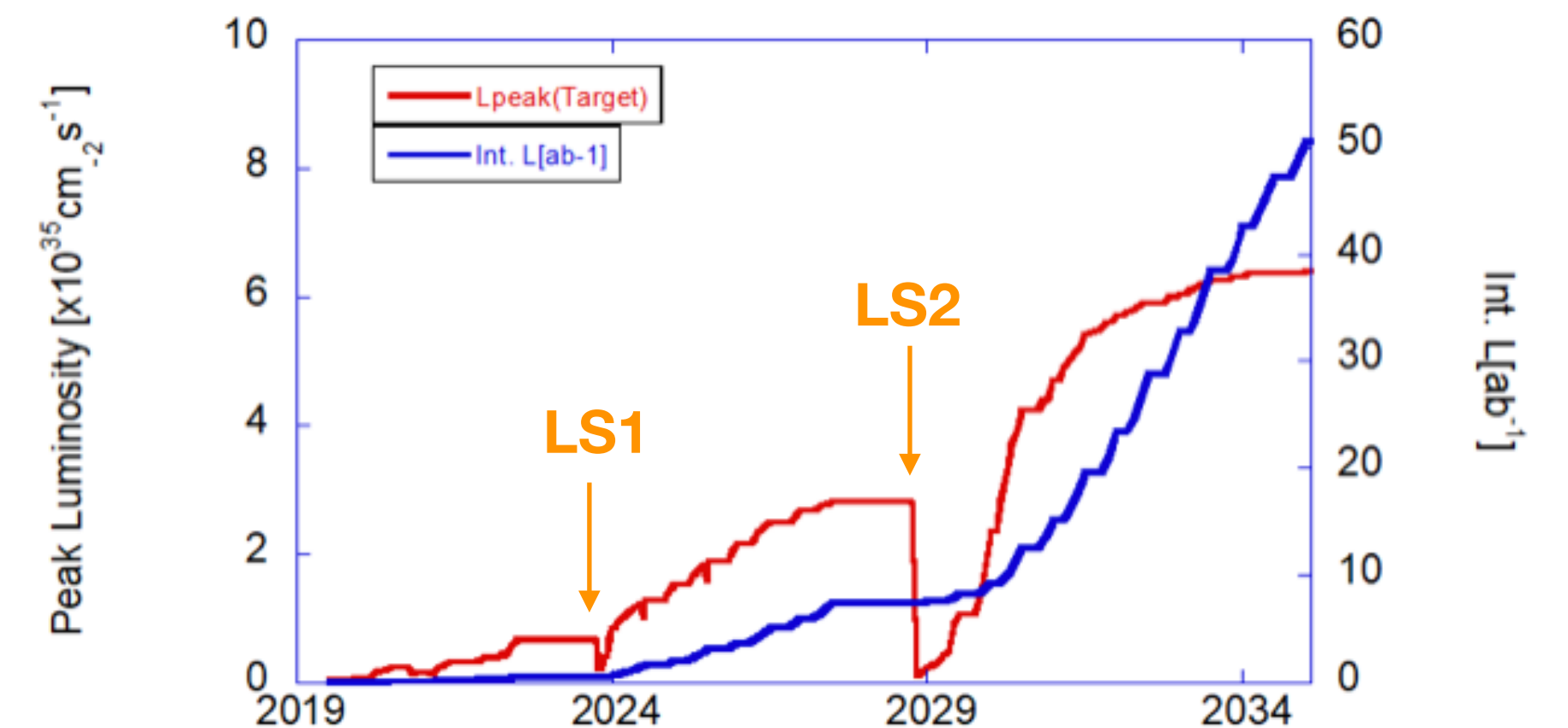
- Replacement of beam pipe
- Replacement of photomultipliers of the central PID detector (TOP)
- Installation of 2-layered pixel vertex detector
- Improvement of data-quality monitoring and alarm system
- Complete transition to new DAQ boards (PCIe40)
- Replacement of aging components
- Additional shielding and increased resilience against beam background



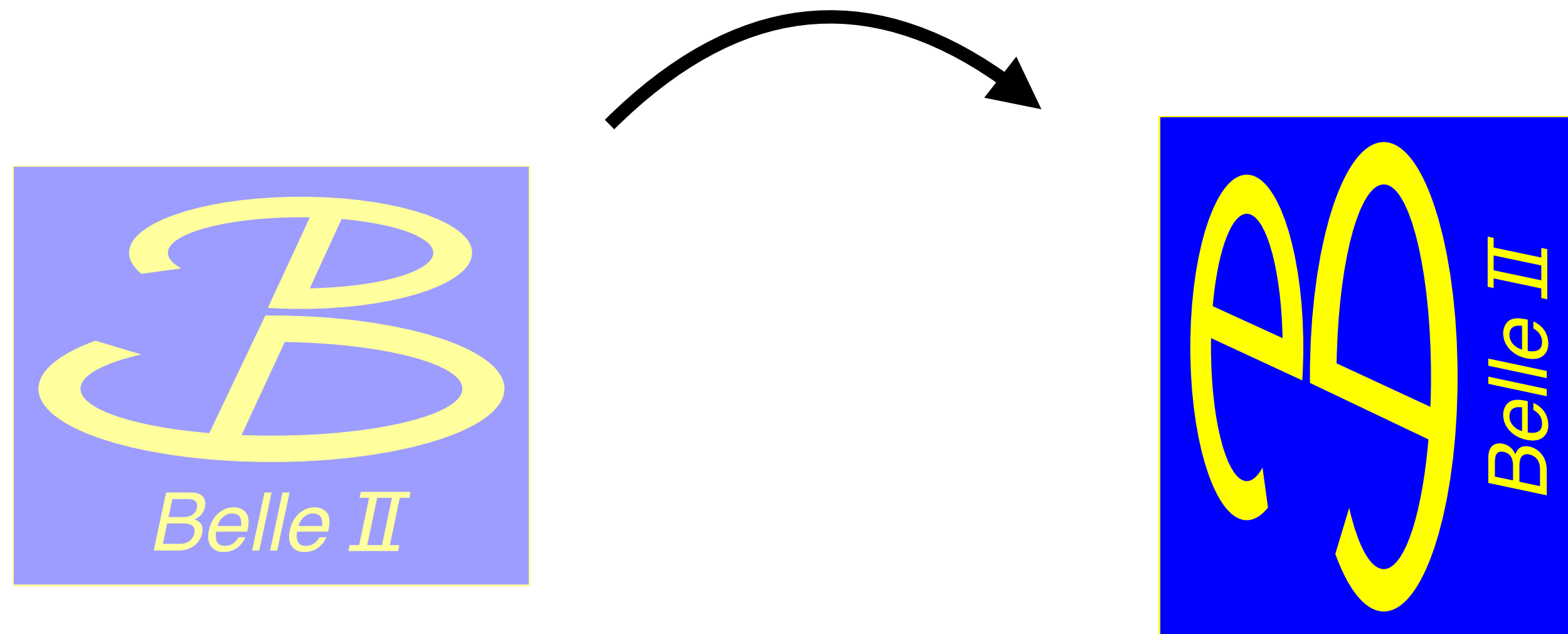
- Higher and more stable beam injection
- Longer beam lifetime and improved stability
- IR radiation shield modification, new collimation scheme and robust collimator head



PXD2 assembly completed in April @ KEK



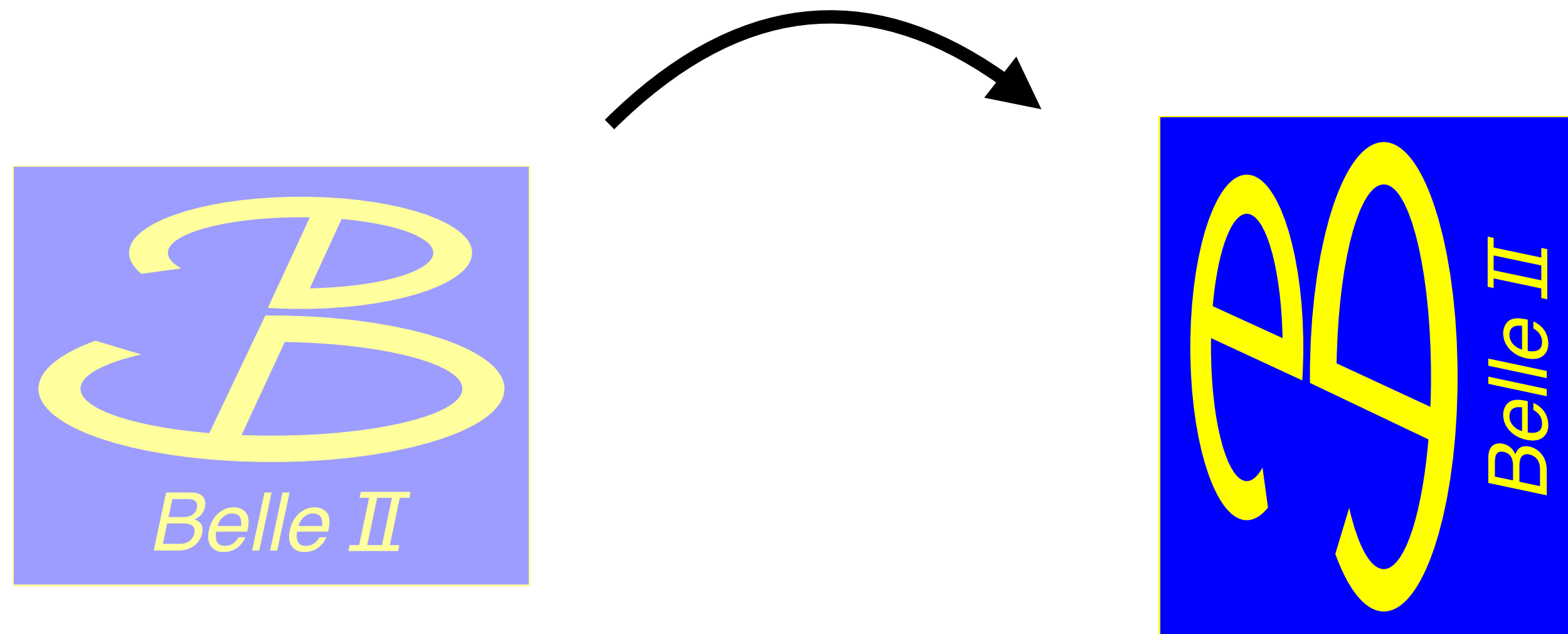
Belle II is maybe (?) the only experiment that explains how it works via its logo:



Plenty of Puns

- 1) Belle collides **electrons** and their **anti-particle positrons**
- 2) B breaks the symmetry between $e_l - l_e$
(i.e. between matter and antimatter)
- 3) Belle investigates **beauty** quarks, which are of course "belle"

Belle II is maybe (?) the only experiment that explains how it works via its logo:



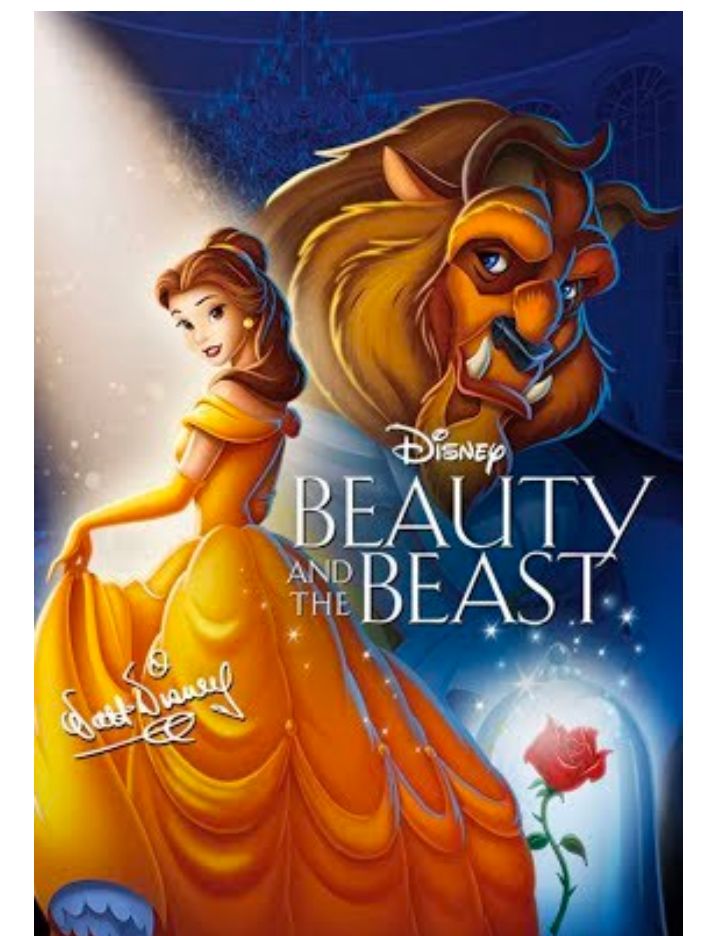
BEAST

(Beam Exorcism for A Stable BELLE Experiment)

The BEAST experiment: a background detector for the commissioning of the BELLE experiment

Plenty of Puns

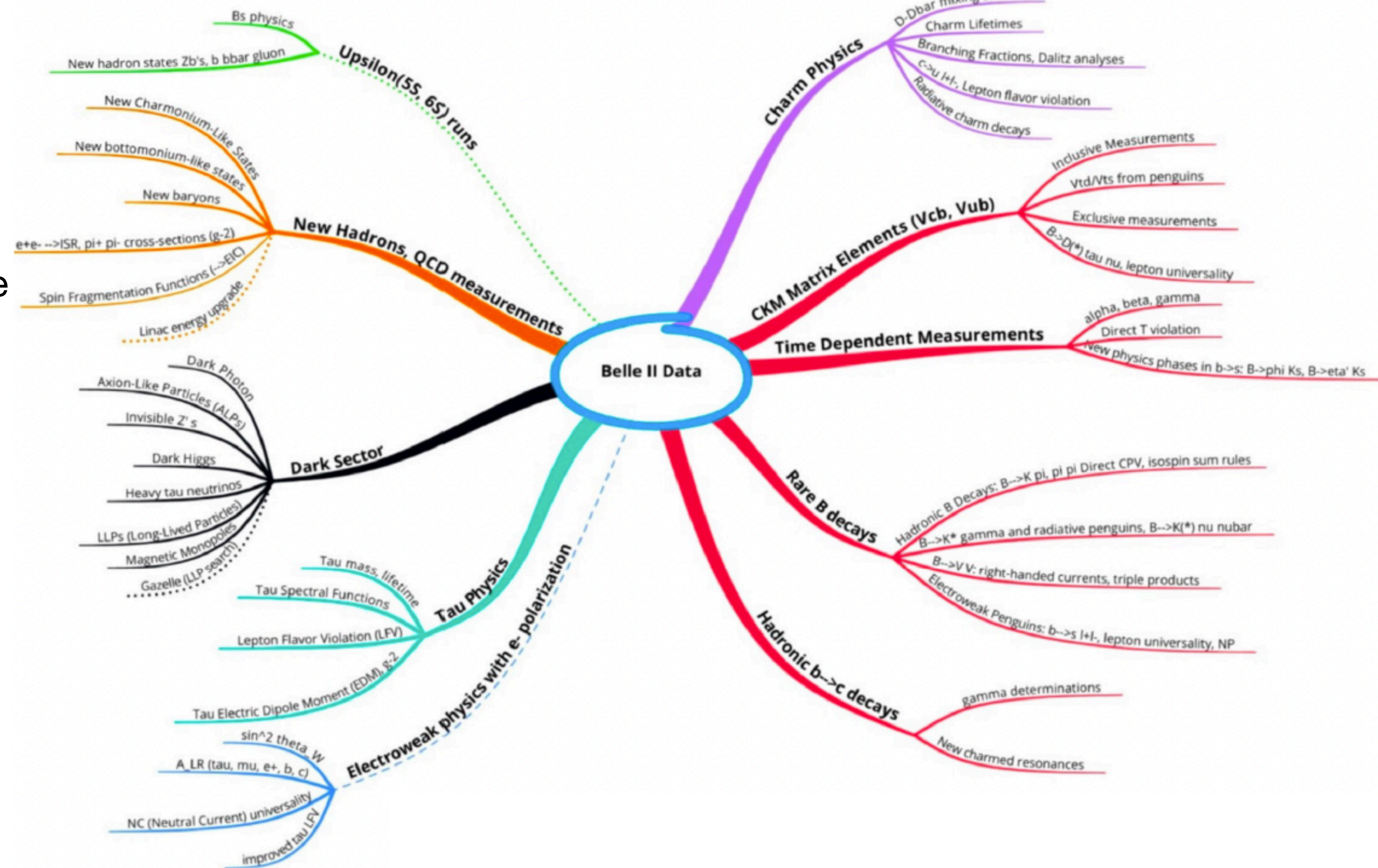
- 1) Belle collides **electrons** and their **anti-particle positrons**
- 2) B breaks the symmetry between $e_l - l_e$
(i.e. between matter and antimatter)
- 3) Belle investigates **beauty** quarks, which are of course "belle"



Picture: movies.disney.com

Belle II Physics Program

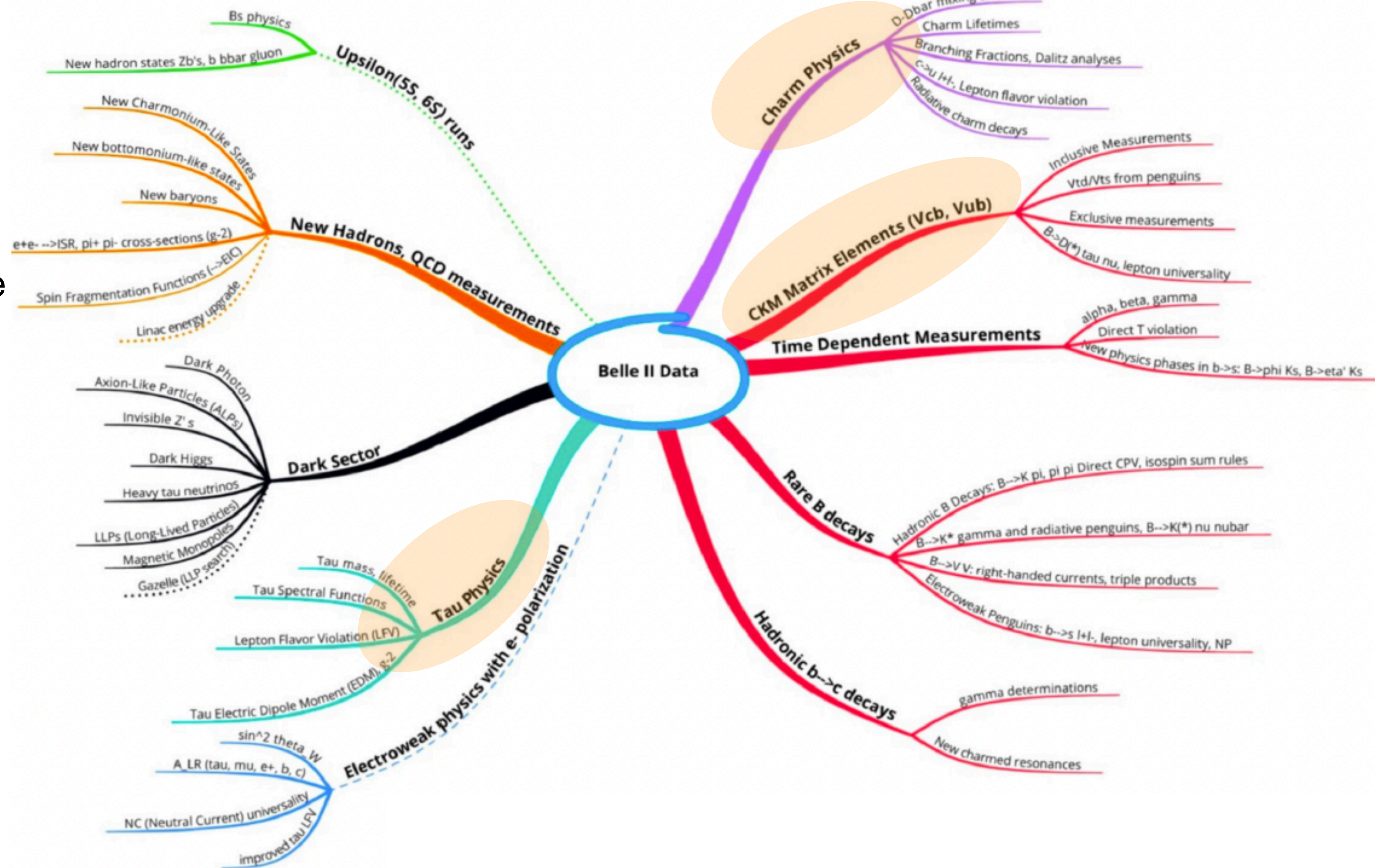
- Many sectors will be explored by analyzing Belle II data
- Unique advantages in inclusive analyses, decays involving multiple neutrals
- Full potential summarized in “Belle II Physics Book” [PTEP 2019 123C01, arXiv:1808.10567]



Belle II Physics Program

- Many sectors will be explored by analyzing Belle II data
- Unique advantages in inclusive analyses, decays involving multiple neutrals
- Full potential summarized in “Belle II Physics Book” [PTEP 2019 123C01, arXiv:1808.10567]

recent highlights covered in today's talk

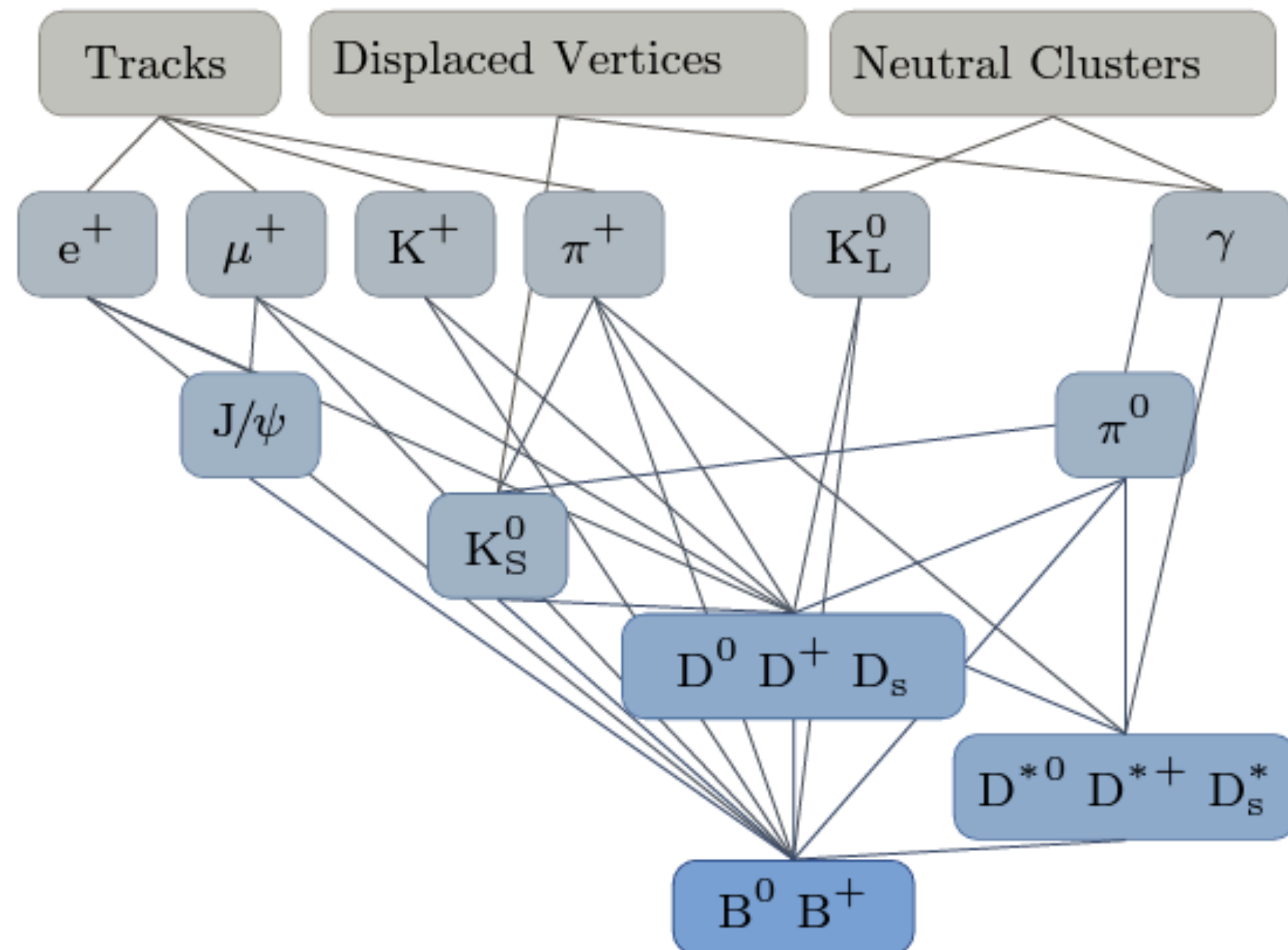
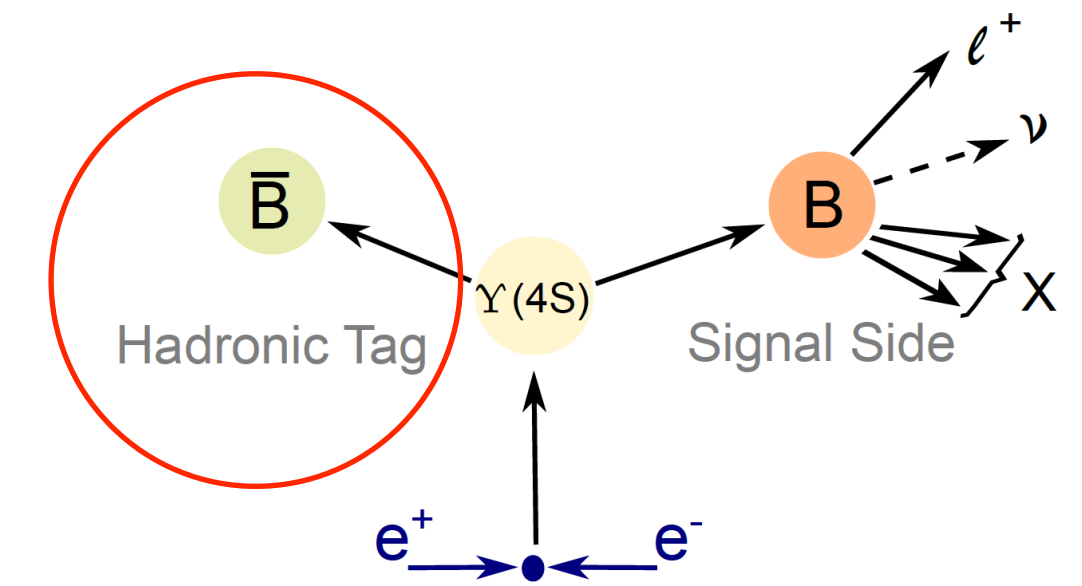


CKM matrix element $|V_{cb}|$

Inclusive $B \rightarrow X_c \ell \nu$ Decays and q^2 Moments

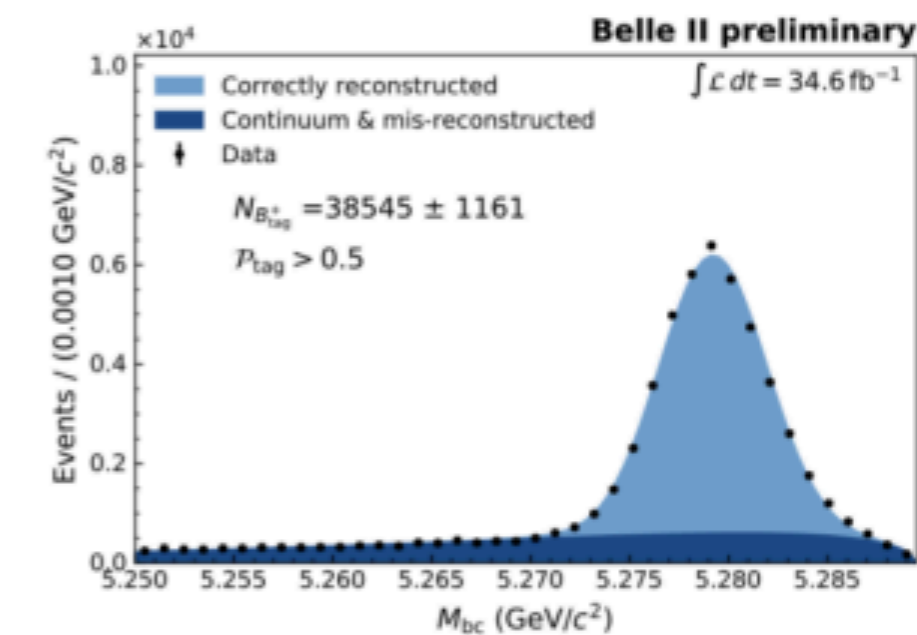
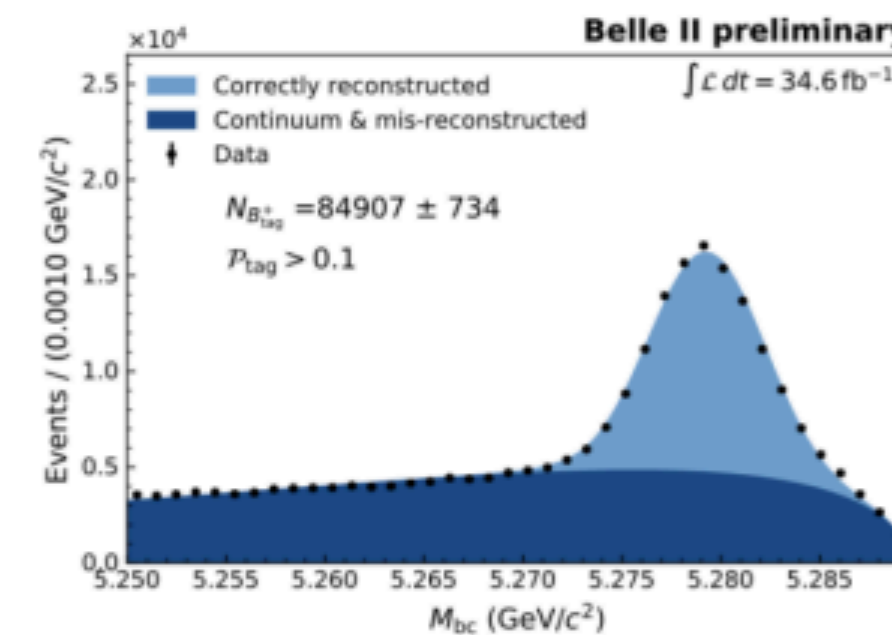
- Measurement of q^2 moments allows new approach to extract inclusive $|V_{cb}|$
- Analysis Belle II dataset of 62.8 fb^{-1} , $\ell = e, \mu$
- Hadronic tagging with **Full Event Interpretation** algorithm [Comput Softw Big Sci 3, 6(2019)] to reconstruct B_{tag}
 - Reconstruct B candidate with all combination of daughters
 - Calculate signal probability with multivariate classifiers

PRD 107, 072002 (2023)



Hadronic FEI

- Over 200 BDTs to reconstruct $\mathcal{O}(10000)$ distinct decay chains
- Efficiency $\epsilon_{B^+} \approx 0.5\%$, $\epsilon_{B^0} \approx 0.3\%$ at $\sim 15\%$ purity

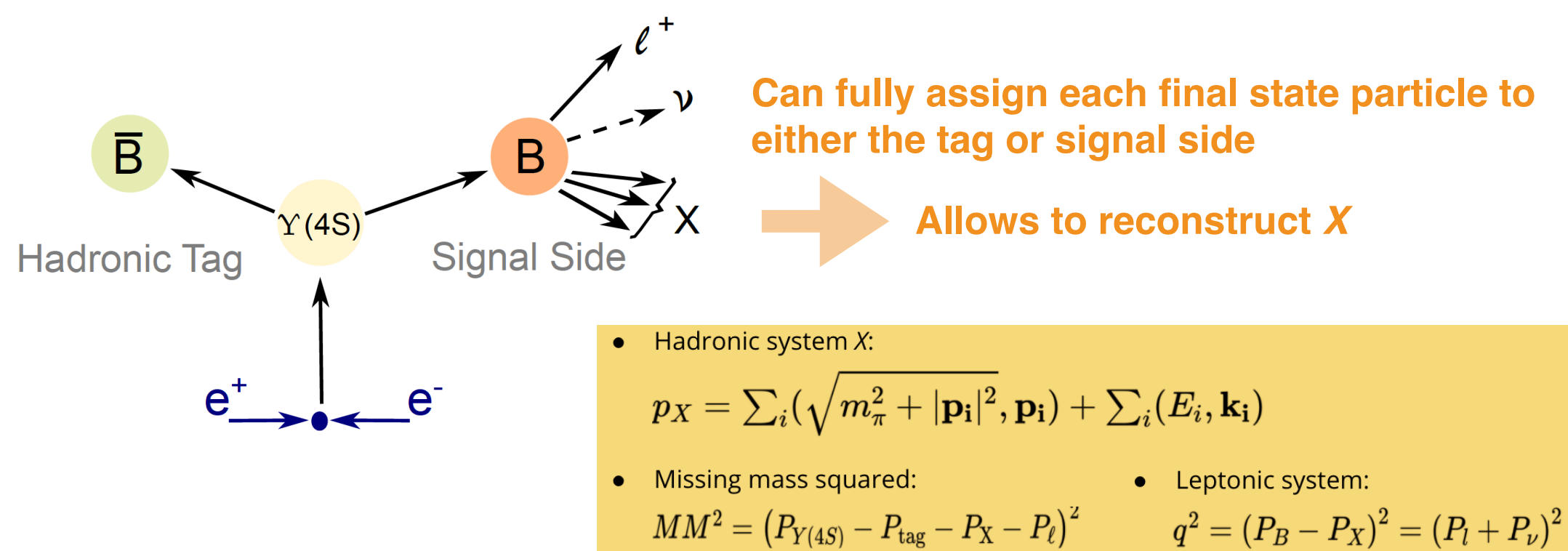


$$M_{bc} = \sqrt{E_{\text{beam}}^2/4 - (p_{B_{\text{tag}}}^{\text{cm}})^2} > 5.27 \text{ GeV}/c^2$$

Inclusive $B \rightarrow X_c \ell \nu$ Decays and q^2 Moments

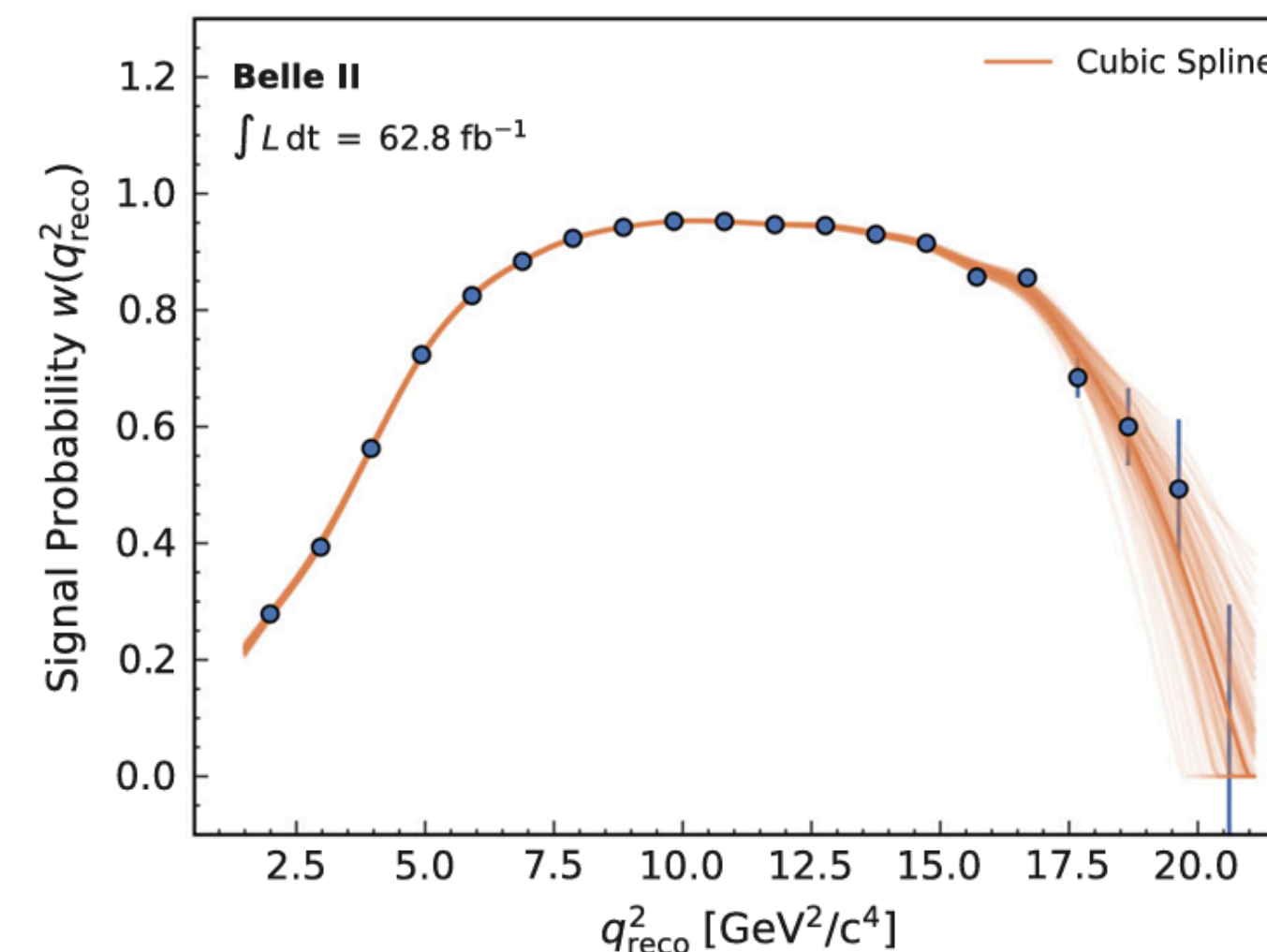
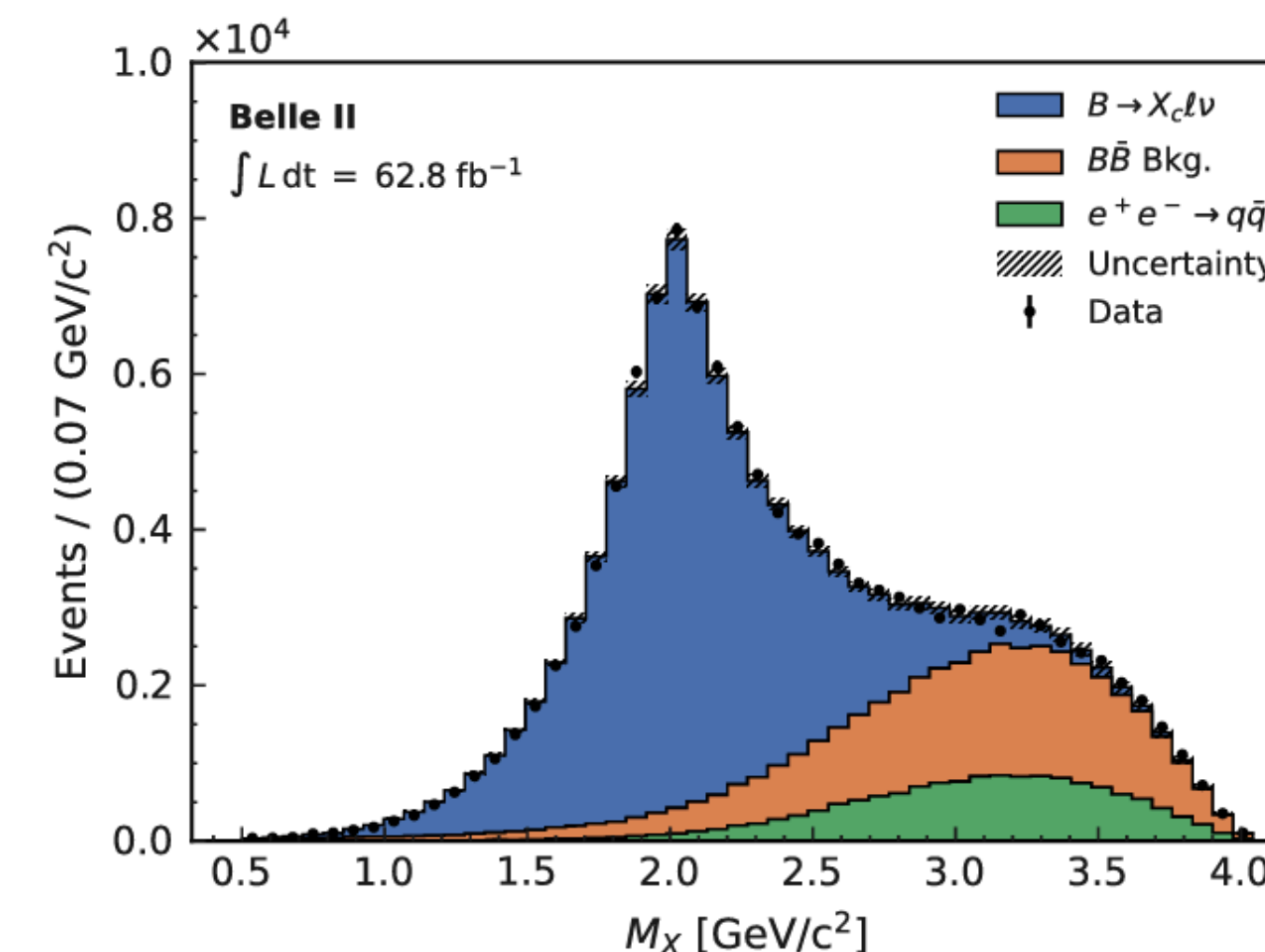
- Measurement of q^2 moments allows new approach to extract inclusive IV_{cb}
- Analysis Belle II dataset of 62.8 fb^{-1} , $\ell = e, \mu$
- Hadronic tagging with **Full Event Interpretation** algorithm [Comput Softw Big Sci 3, 6(2019)] to reconstruct B_{tag}
- Background suppressed in hadronic mass M_X and converted to signal prob. on q^2

PRD 107, 072002 (2023)



- **First to fourth moments (m=1~4)** measured at a progression of cuts on q^2
- Spectra corrected for **linear distortions**, **eff. & acc.** & **residual bias**

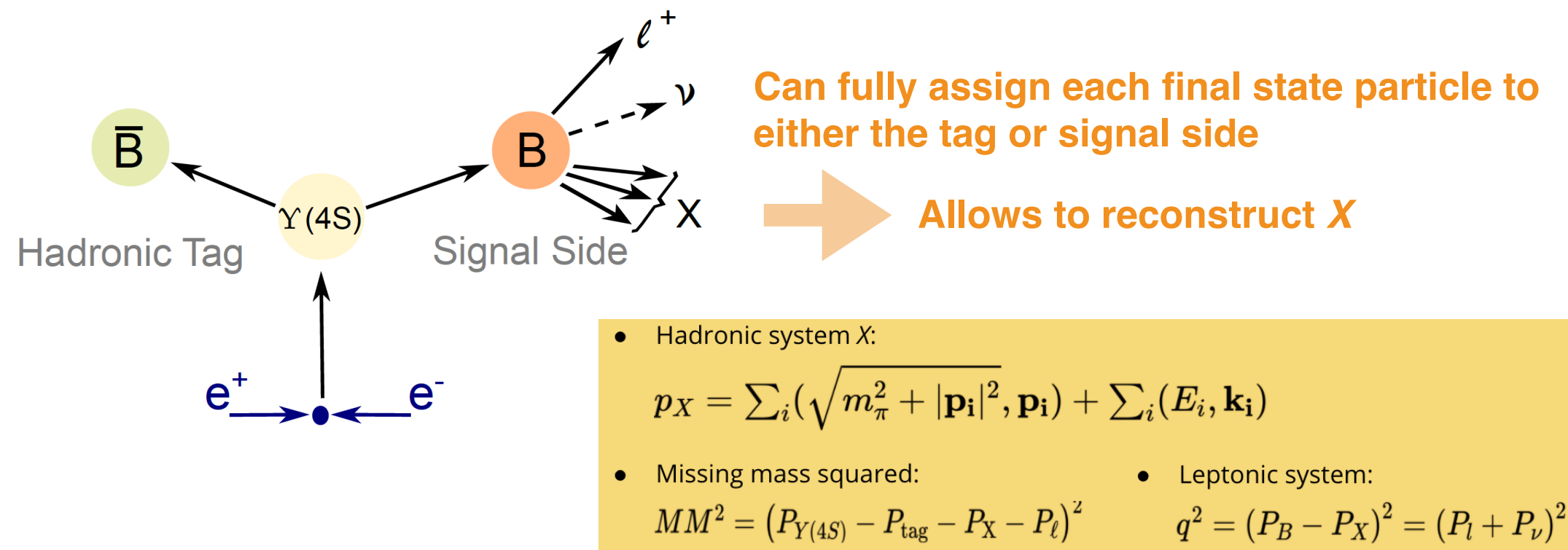
$$\langle q^{2m} \rangle = \frac{C_{\text{cal}} \cdot C_{\text{acc}}}{\sum_i^{\text{events}} w(q_i^2)} \times \sum_i^{\text{events}} w(q_i^2) \cdot q_{\text{cal } i}^{2m}$$



Inclusive $B \rightarrow X_c \ell \nu$ Decays and q^2 Moments

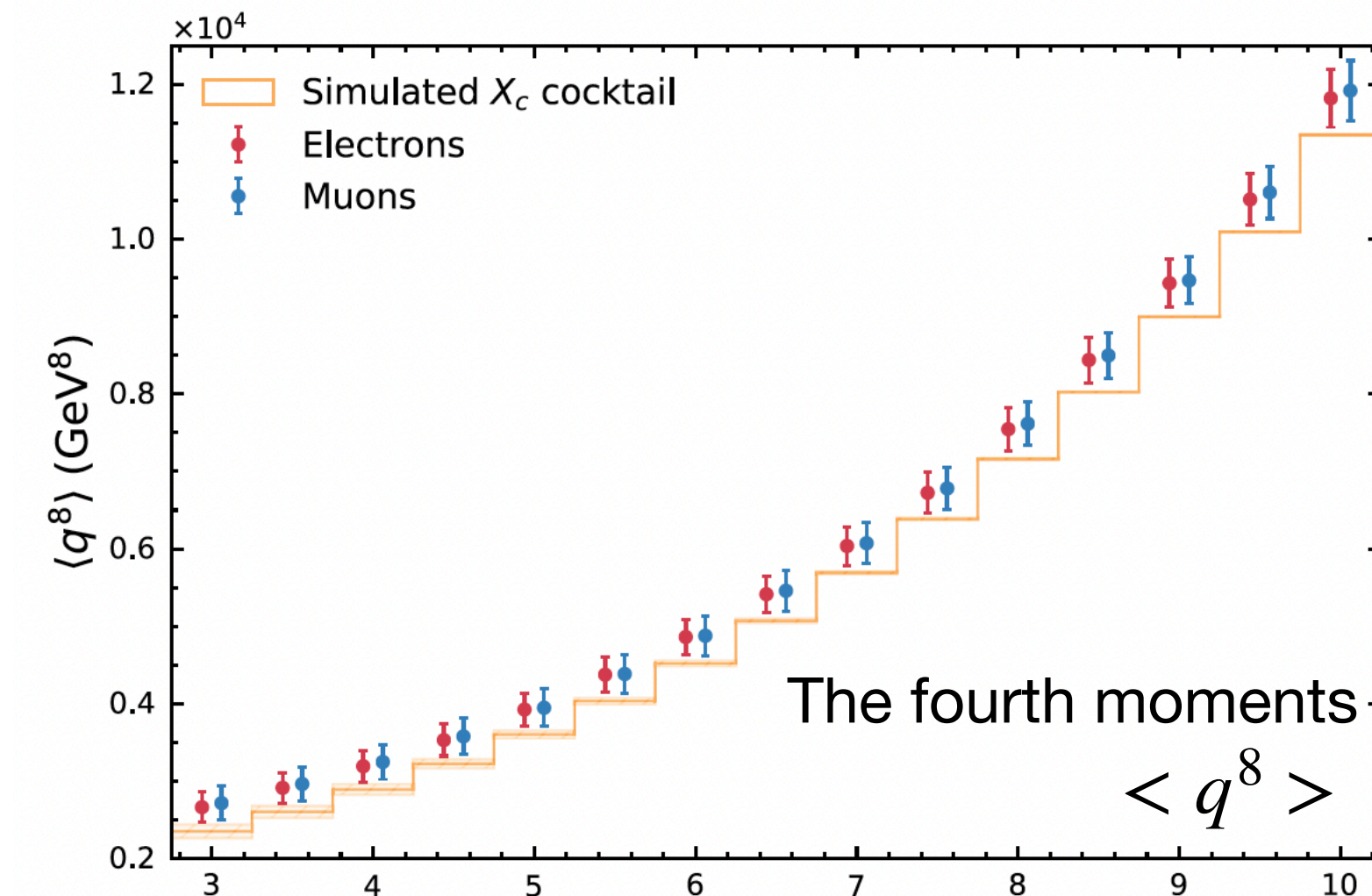
- Measurement of q^2 moments allows new approach to extract inclusive $|V_{cb}|$
- Analysis Belle II dataset of 62.8 fb^{-1} , $\ell = e, \mu$
- Hadronic tagging with **Full Event Interpretation** algorithm [Comput Softw Big Sci 3, 6(2019)] to reconstruct B_{tag}
- Background suppressed in hadronic mass M_X and converted to signal prob. on q^2
- Measured phase space of $q^2 = [1.5, 8.5] \text{ GeV}^2$

PRD 107, 072002 (2023)

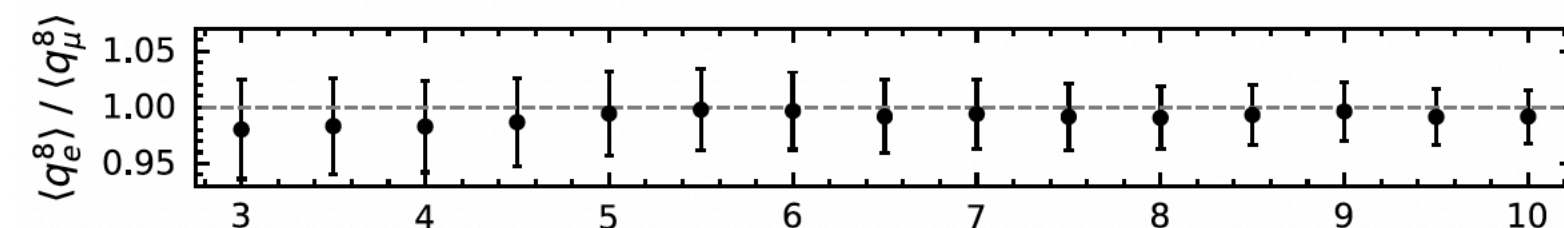


- **First to fourth moments (m=1~4)** measured at a progression of cuts on q^2
- Spectra corrected for **linear distortions**, **eff. & acc.** & **residual bias**

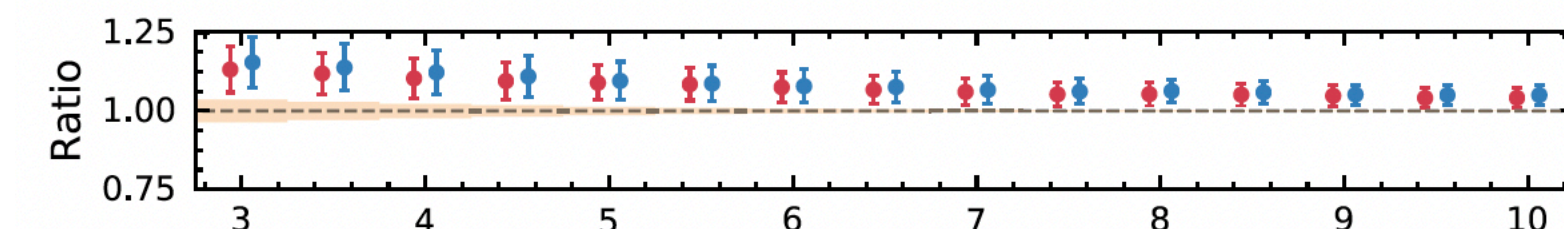
$$\langle q^{2m} \rangle = \frac{C_{\text{cal}} \cdot C_{\text{acc}}}{\sum_i^{\text{events}} w(q_i^2)} \times \sum_i^{\text{events}} w(q_i^2) \cdot q_{\text{cal } i}^{2m}$$



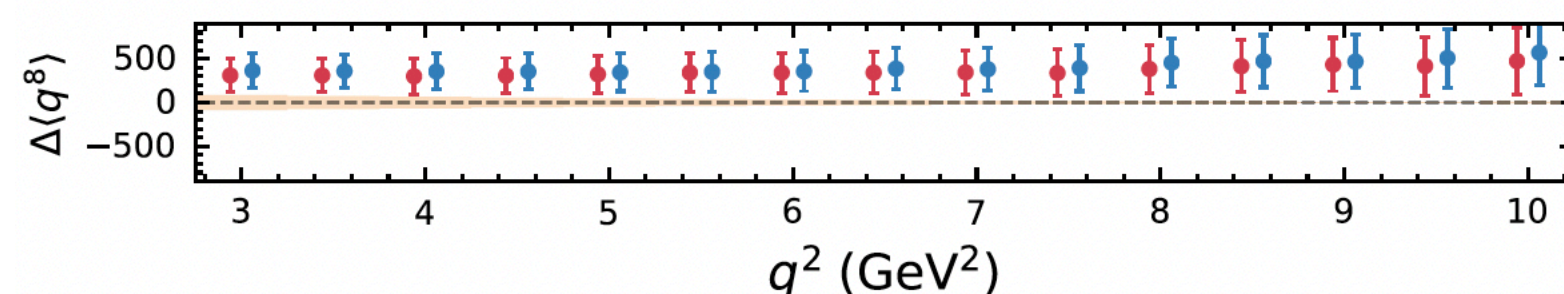
← Extract $|V_{cb}|$



← LFUV test



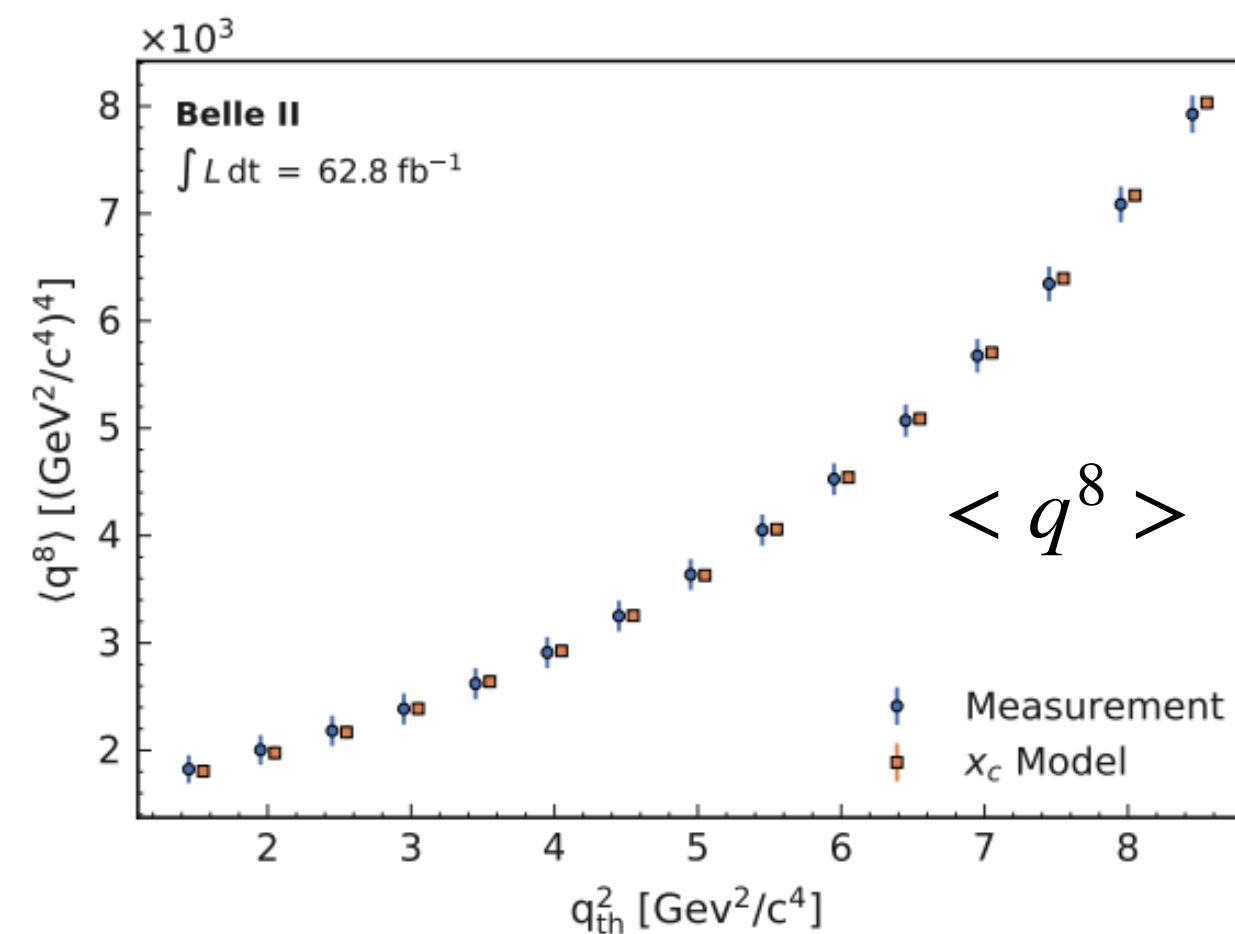
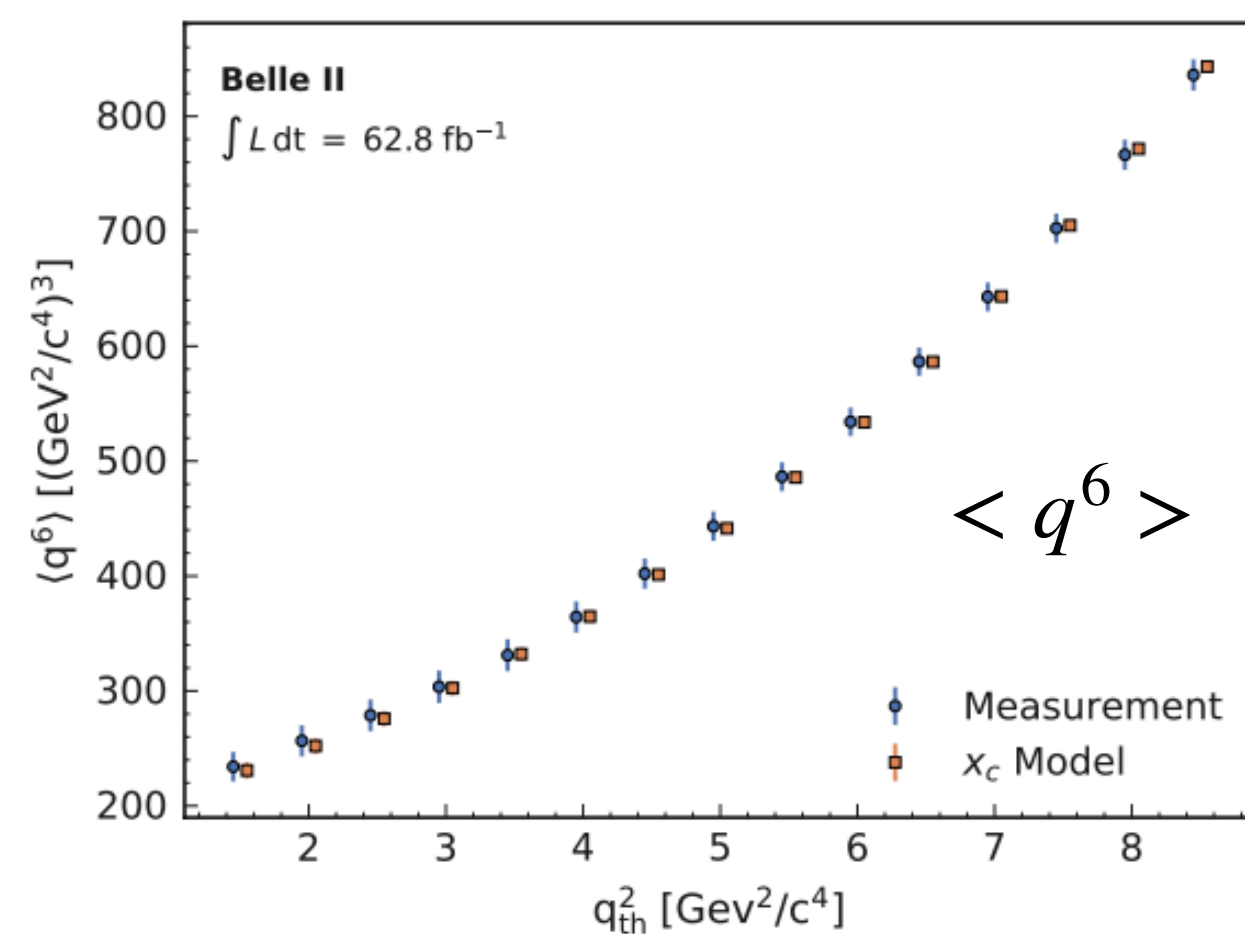
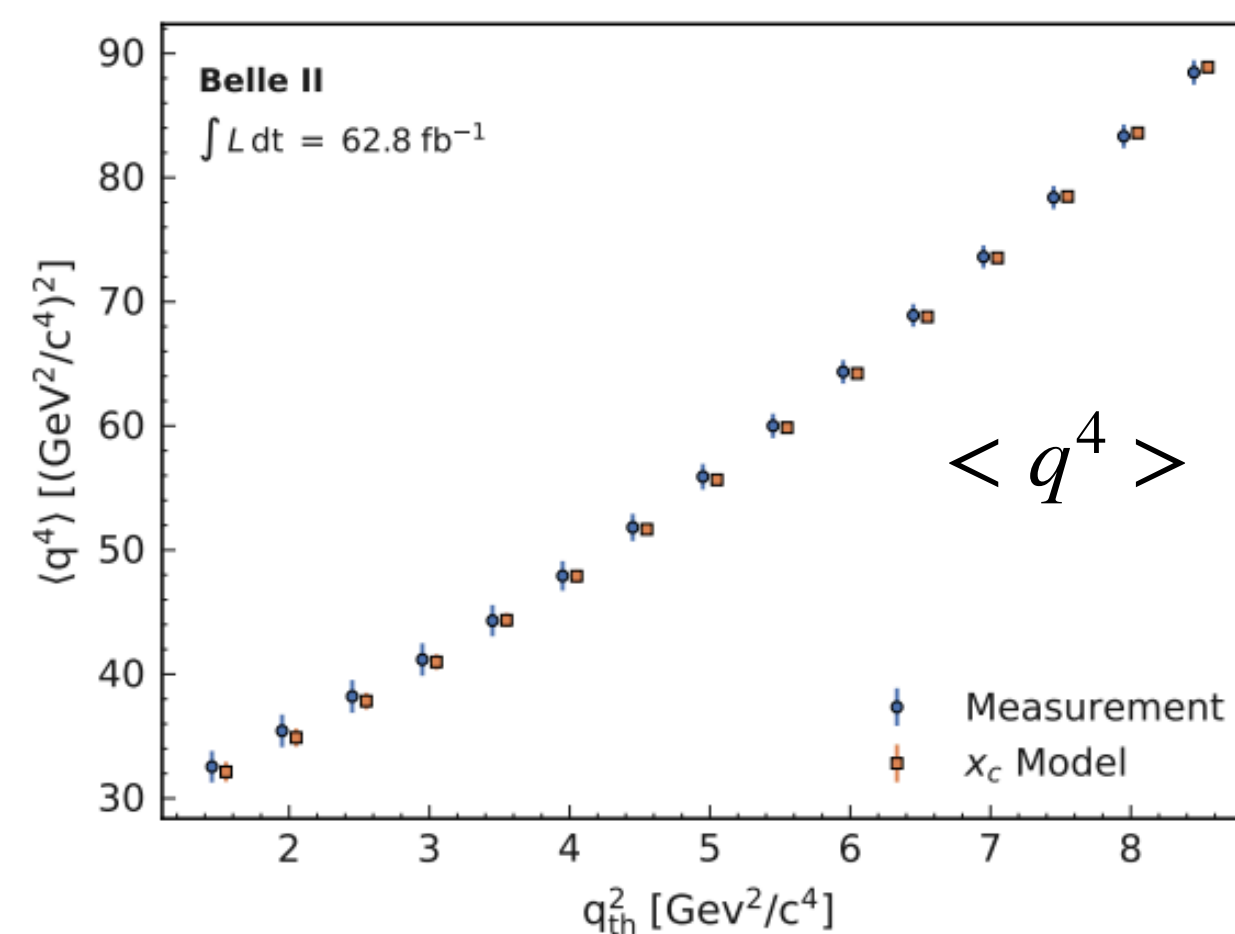
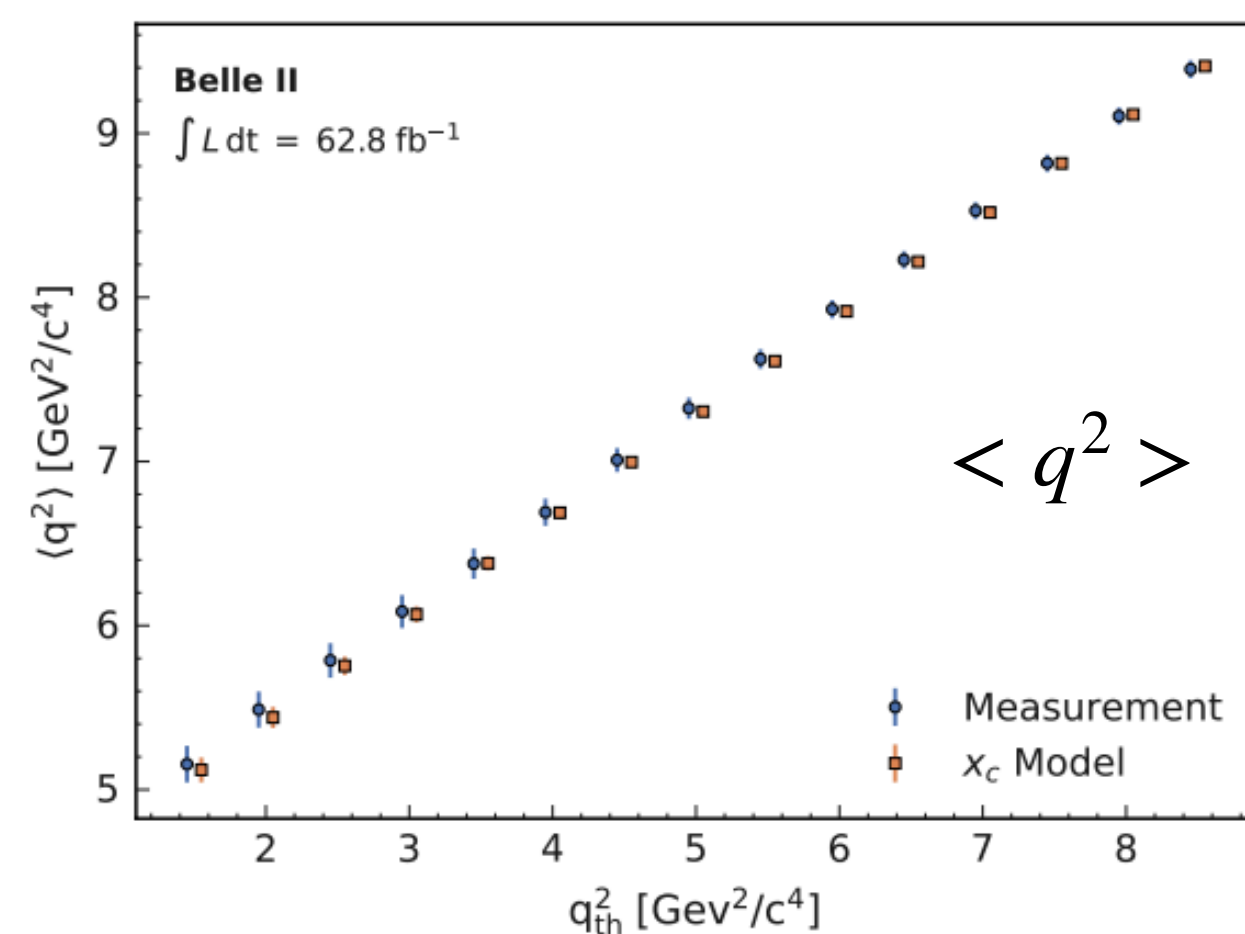
← Mea. / Sim.



← Mea. - Sim.

Inclusive $B \rightarrow X_c \ell \nu$ Decays and q^2 Moments

PRD 107, 072002 (2023)



A side remark on Inclusive $|V_{cb}|$ determination

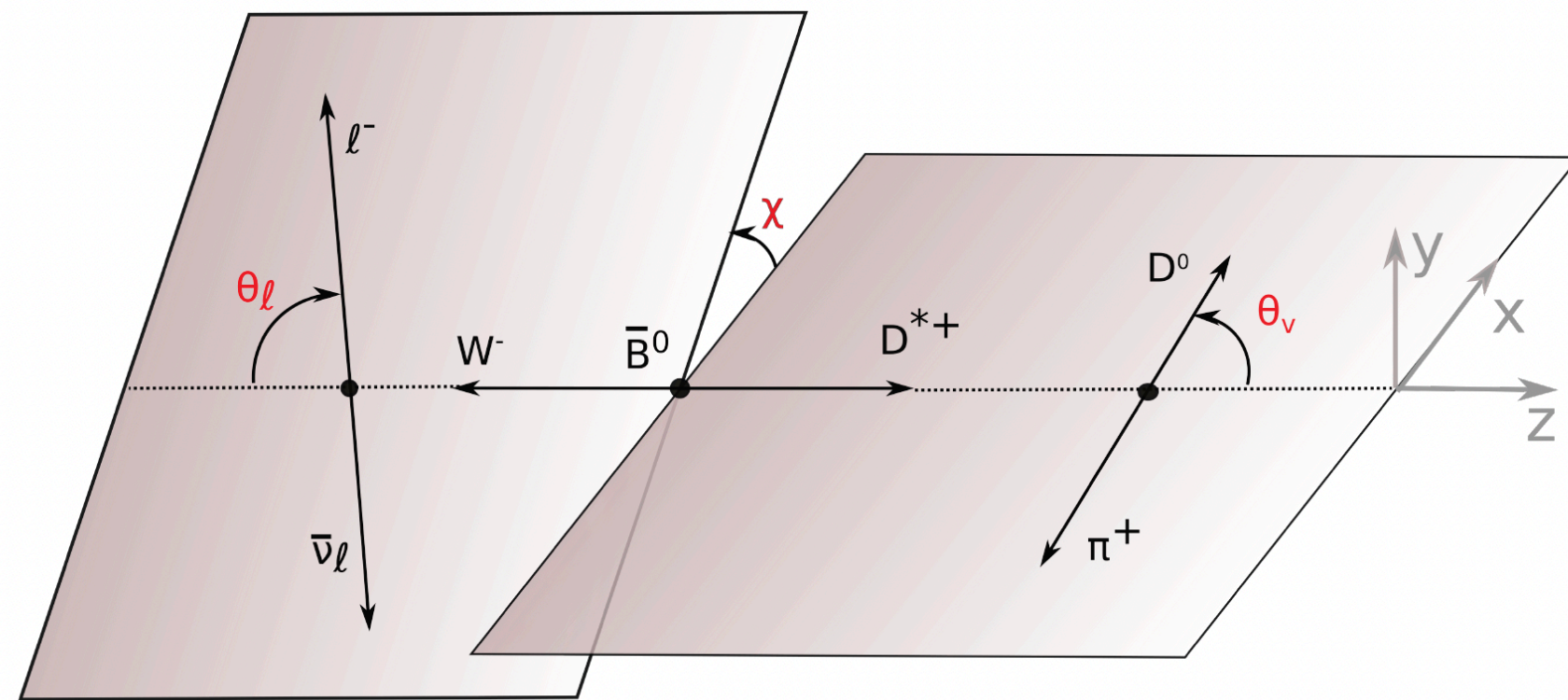
- Belle II & Belle $\langle q^{2m} \rangle$ results are used in novel approach to extract $|V_{cb}|$ [JHEP 10 (2022) 068]
- Benefit from reduced number of non-perturbative matrix elements
- Obtained consistent $|V_{cb}|$ with previous results using M_X, E_ℓ^B moments

$$|V_{cb}| = (41.69 \pm 0.63) \times 10^{-3}$$

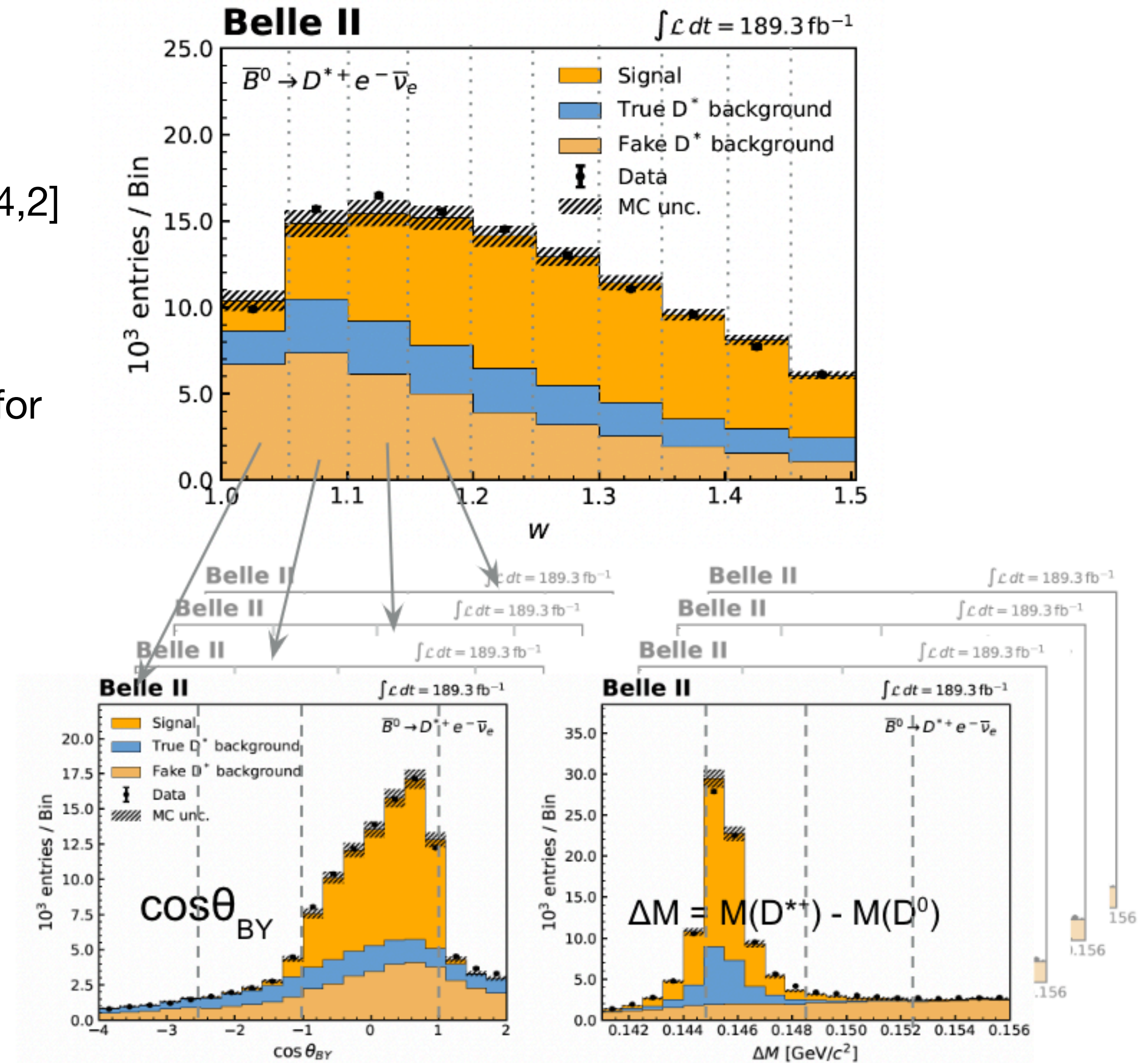
$|V_{cb}|$ in $B^0 \rightarrow D^* \ell \nu$ Decay

Preliminary

- Decay chain: $B^0 \rightarrow D^{*+} \ell \nu$, $D^{*+} \rightarrow D^0 \pi^+$, $D^0 \rightarrow K^- \pi^+$
- Untagged strategy (higher efficiency than tagged)
- Select energetic signal lepton $p^{\text{CM}} > 1.2 \text{ GeV}$
- $M(D^0) = m_{\text{PDG}} \pm 15 \text{ MeV}$, $M(D^{*+}) - M(D^0) = [0.141, 0.156] \text{ GeV}$, $\cos\theta_{BY} = [-4, 2]$
- 2D binned likelihood fit on $(\cos\theta_{BY}, \Delta M)$ for each bin of kinematic variables: recoil parameter w , and angles $\cos\theta_\ell$, $\cos\theta_\nu$, χ
- Systematic shape variations incorporated as bin-wise Nuisance para. for each fit template



$$\cos\theta_{BY} = \frac{2E_B^{\text{CM}} E_Y^{\text{CM}} - m_B^2 - m_Y^2}{2|\vec{p}_B^{\text{CM}}| |\vec{p}_Y^{\text{CM}}|}$$



integral projection

$|V_{cb}|$ in $B^0 \rightarrow D^* \ell \nu$ Decay

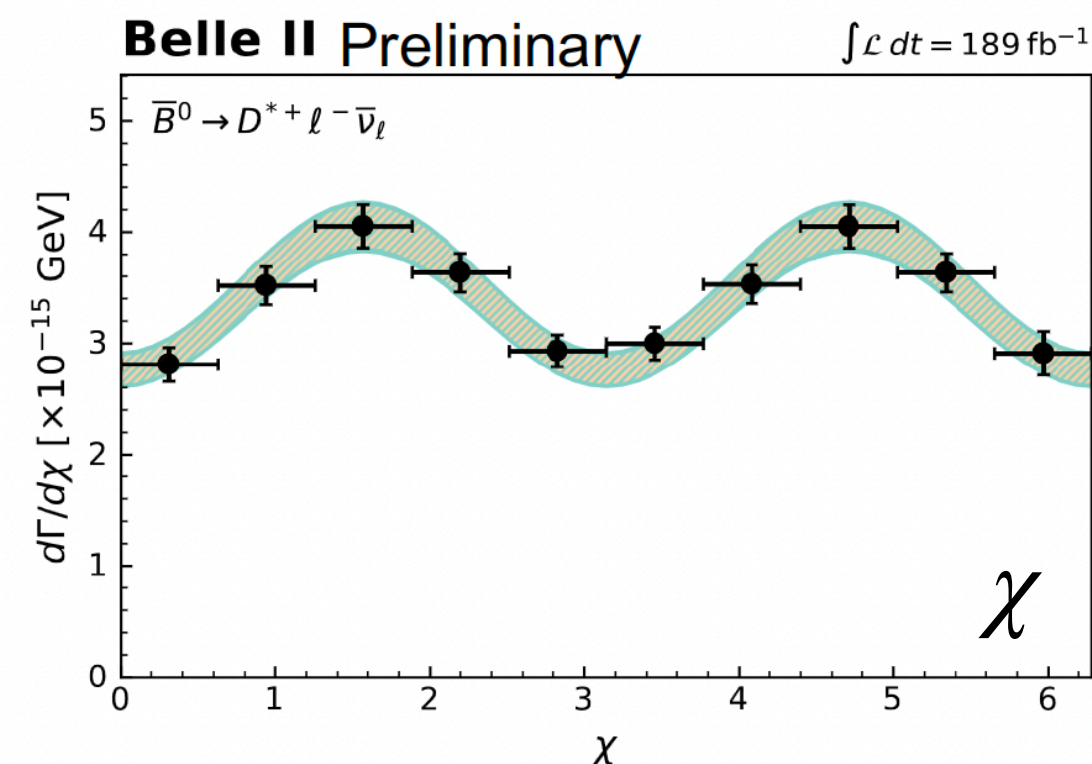
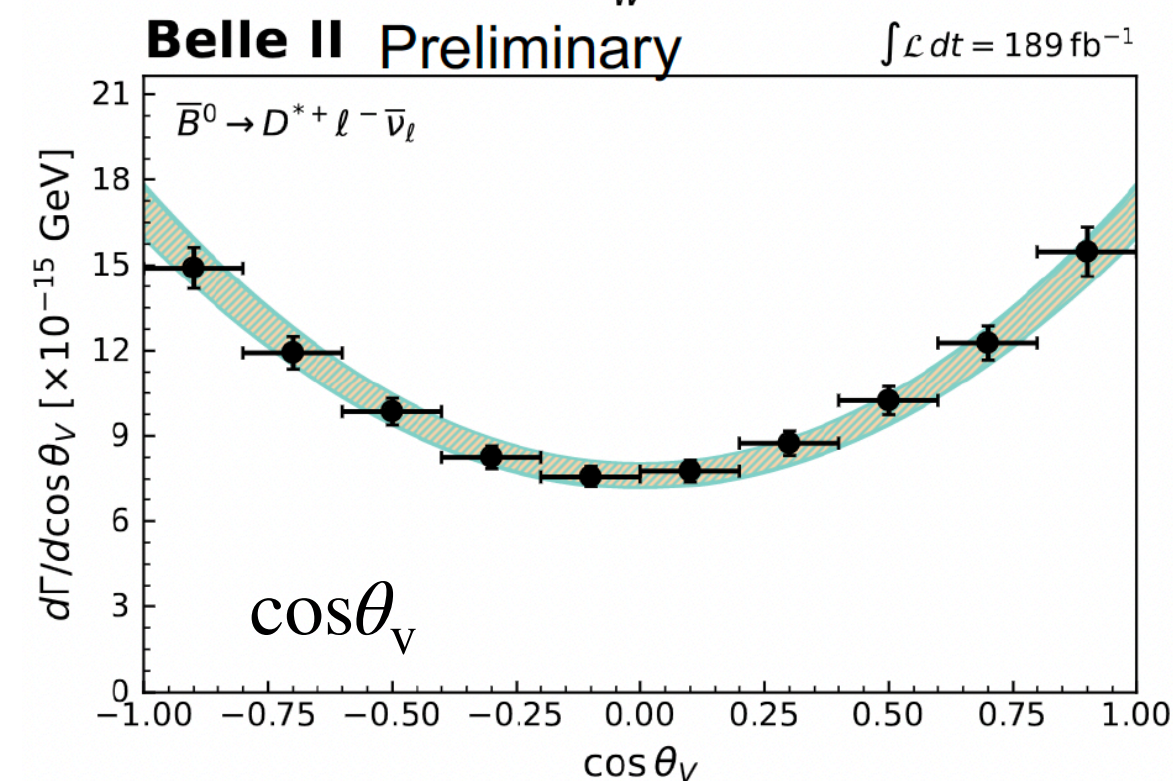
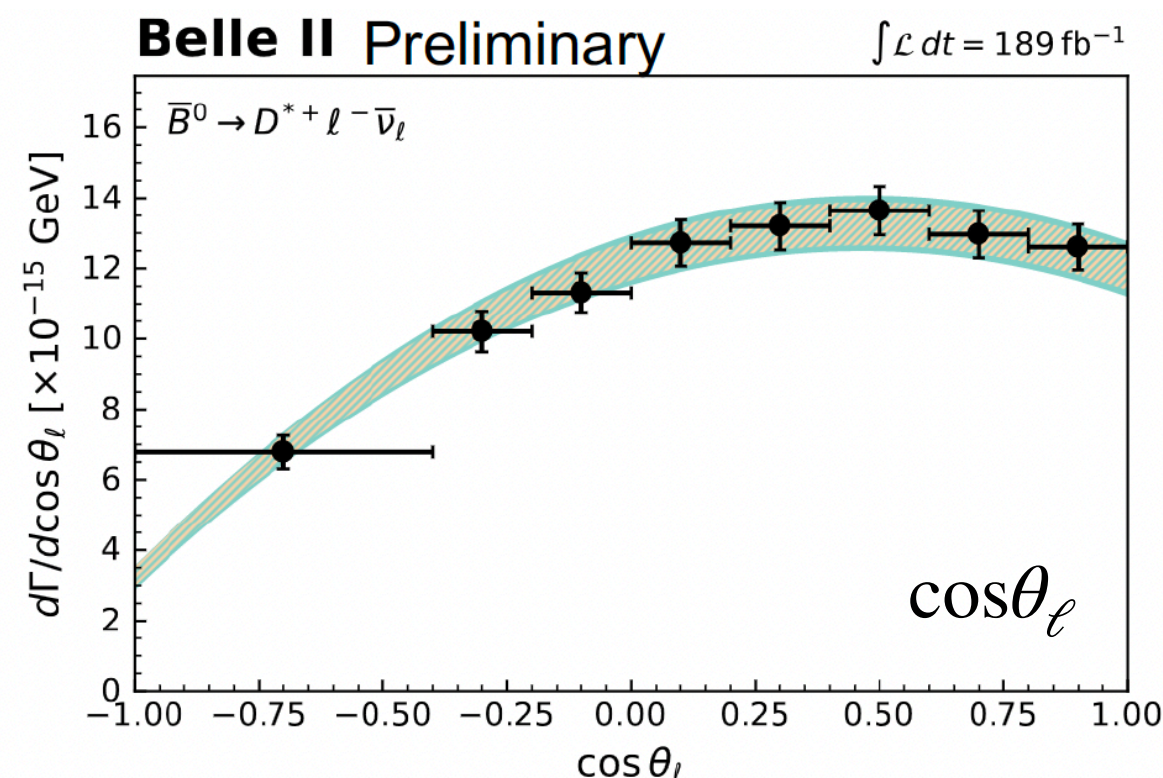
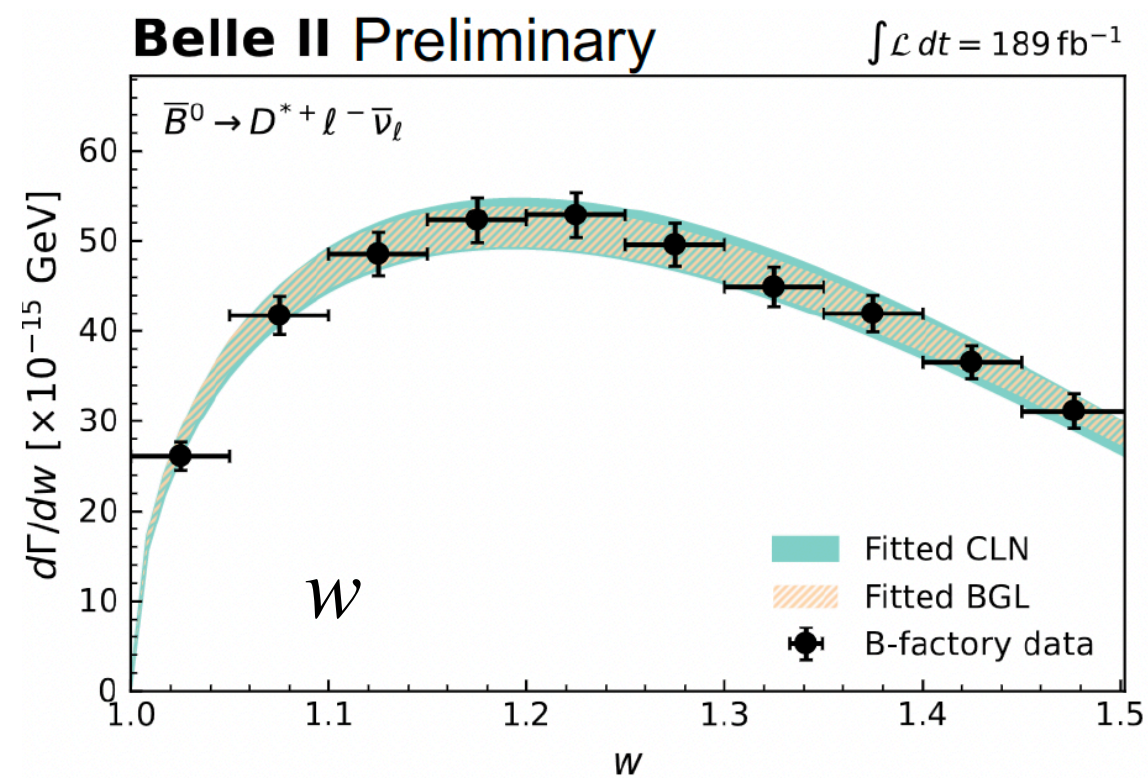
Preliminary

- Unfold signal yields using **singular-value-decomposition (SVD)** method within `pyRooUnfold`, regularization para. optimised for low bias & stable result
- Full post-unfolding stat. & syst. covariance propagated into partial decay rate

$$\Delta\Gamma_i = \frac{\text{reco. eff \& acc.} \cdot y_i^{\text{unfolded}}}{\epsilon_i N_{B^0} \mathcal{B}(D^{*+} \rightarrow D^0 \pi^+) \mathcal{B}(D^0 \rightarrow K^- \pi^+) \tau_{B^0}}$$

input of PDG2022

$$\Gamma = \left(\sum_{i=1}^{10} \Delta\Gamma_i^w + \sum_{i=1}^8 \Delta\Gamma_i^{\cos\theta_\ell} + \sum_{i=1}^{10} \Delta\Gamma_i^{\cos\theta_V} + \sum_{i=1}^{10} \Delta\Gamma_i^\chi \right) / 4$$



$|V_{cb}|$ in $B^0 \rightarrow D^* \ell \nu$ Decay

Preliminary

- Unfold signal yields using **singular-value-decomposition (SVD)** method within `pyRooUnfold`, regularization para. optimised for low bias & stable result
- Full post-unfolding stat. & syst. covariance propagated into partial decay rate

$$\Delta\Gamma_i = \frac{\text{reco. eff \& acc.} \cdot y_i^{\text{unfolded}}}{\epsilon_i N_{B^0} \mathcal{B}(D^{*+} \rightarrow D^0 \pi^+) \mathcal{B}(D^0 \rightarrow K^- \pi^+) \tau_{B^0}} \quad \text{input of PDG2022}$$

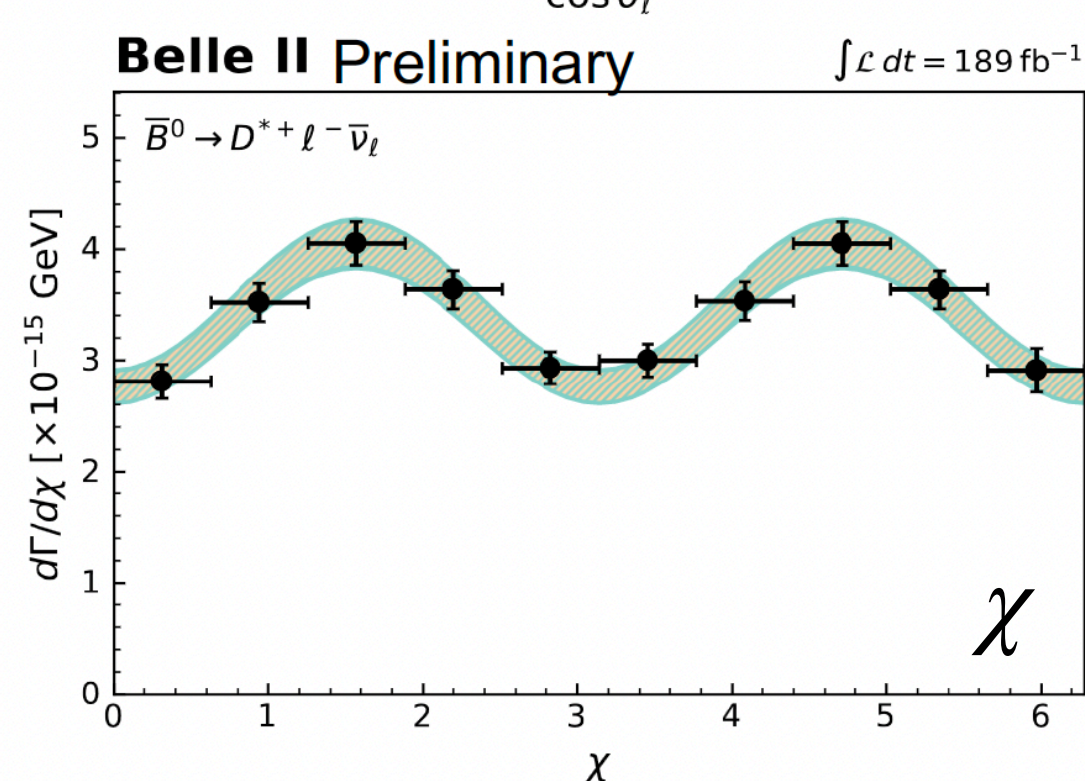
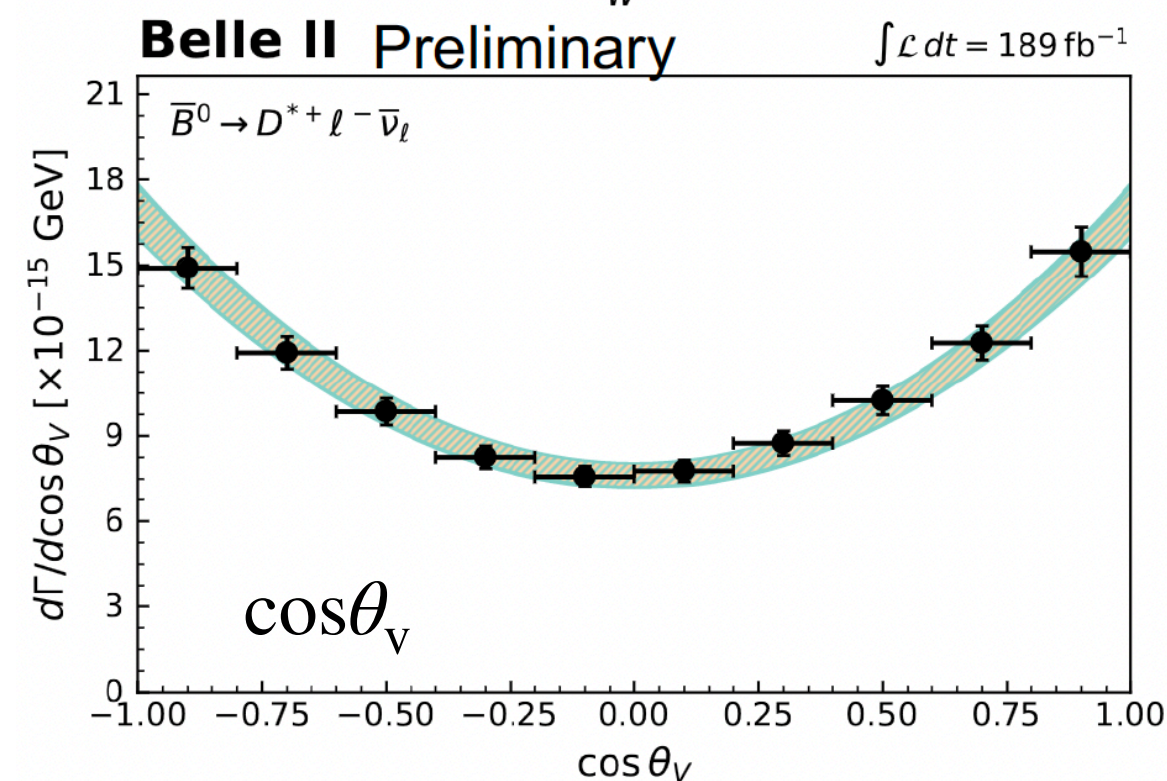
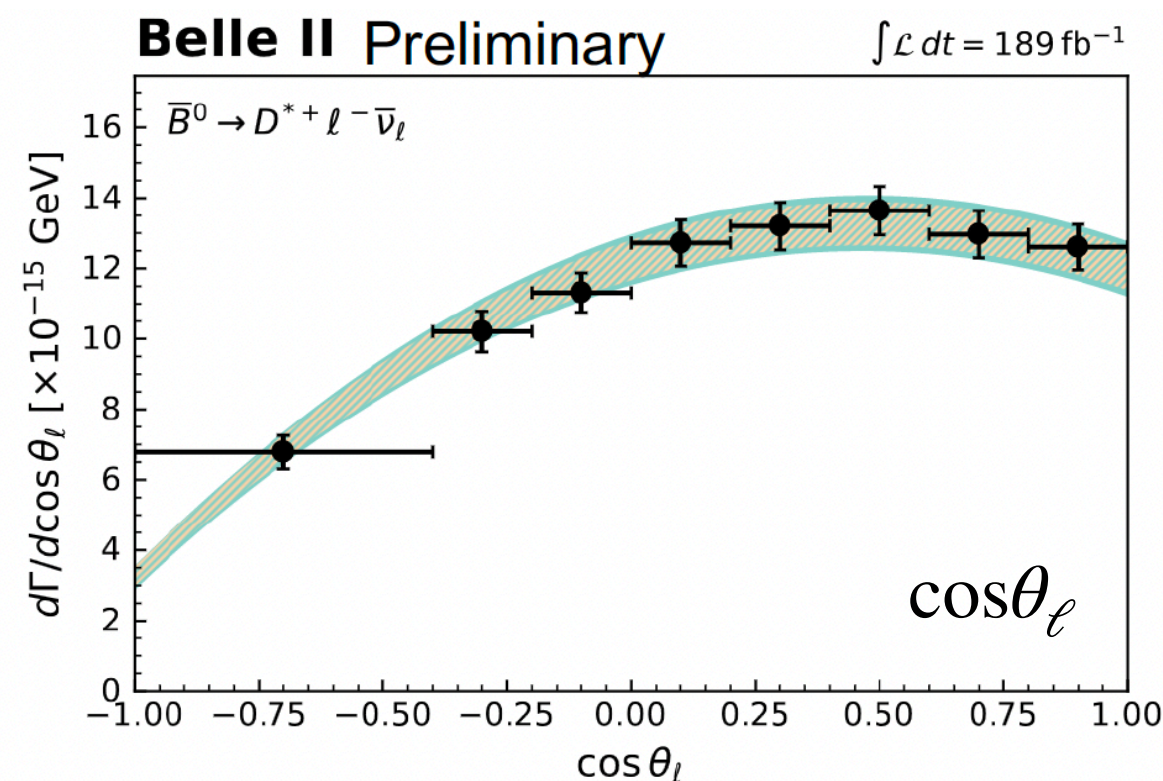
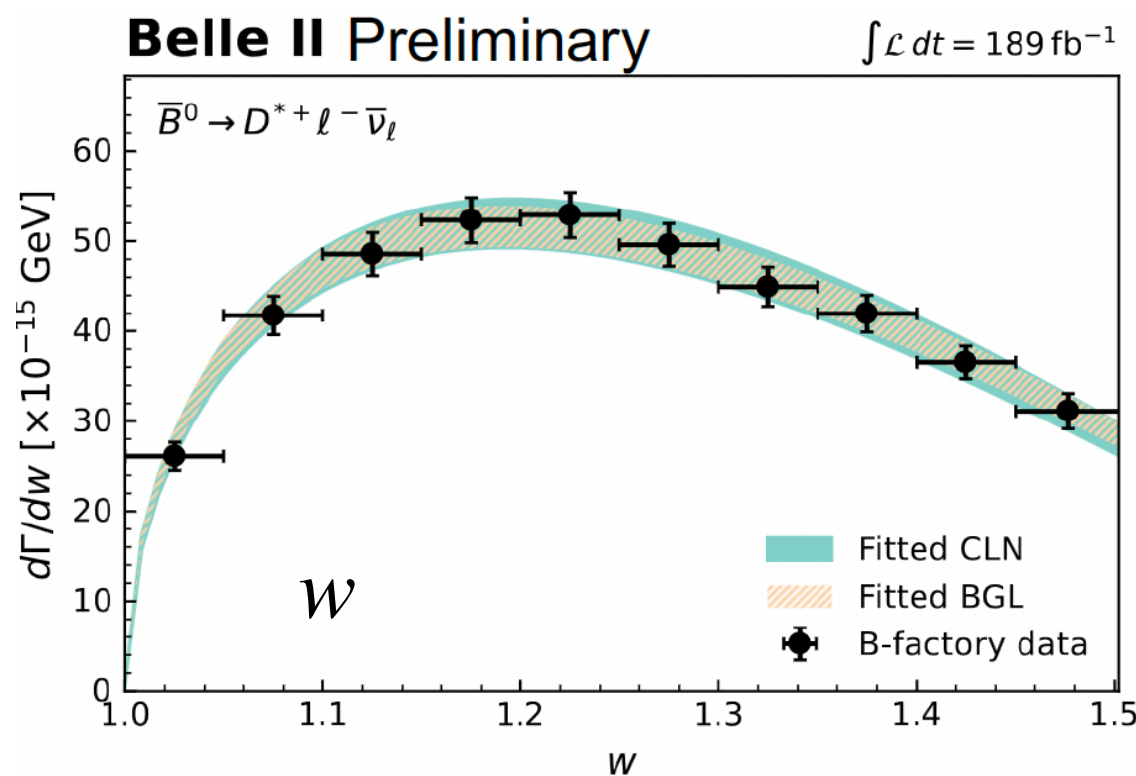
$$\Gamma = \left(\sum_{i=1}^{10} \Delta\Gamma_i^w + \sum_{i=1}^8 \Delta\Gamma_i^{\cos\theta_\ell} + \sum_{i=1}^{10} \Delta\Gamma_i^{\cos\theta_V} + \sum_{i=1}^{10} \Delta\Gamma_i^\chi \right) / 4$$

Branching fraction extracted by the **total rate** summing over partial decay rates and averaging all kin. variables

e mode: $\mathcal{B}(\bar{B}^0 \rightarrow D^{*+} e^- \bar{\nu}_e) = (4.94 \pm 0.03 \pm 0.22)\%$

mu mode: $\mathcal{B}(\bar{B}^0 \rightarrow D^{*+} \mu^- \bar{\nu}_\mu) = (4.94 \pm 0.03 \pm 0.24)\%$

average: $\mathcal{B}(\bar{B}^0 \rightarrow D^{*+} \ell^- \bar{\nu}_\ell) = (4.94 \pm 0.02 \pm 0.22)\%$

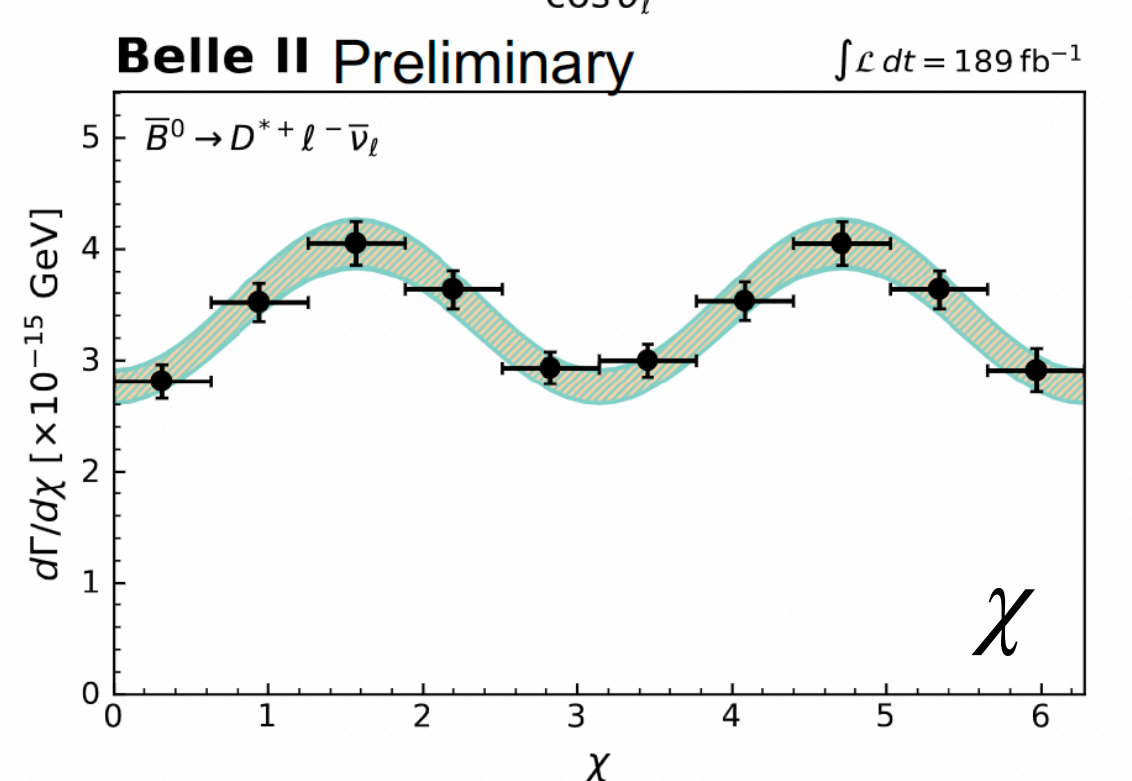
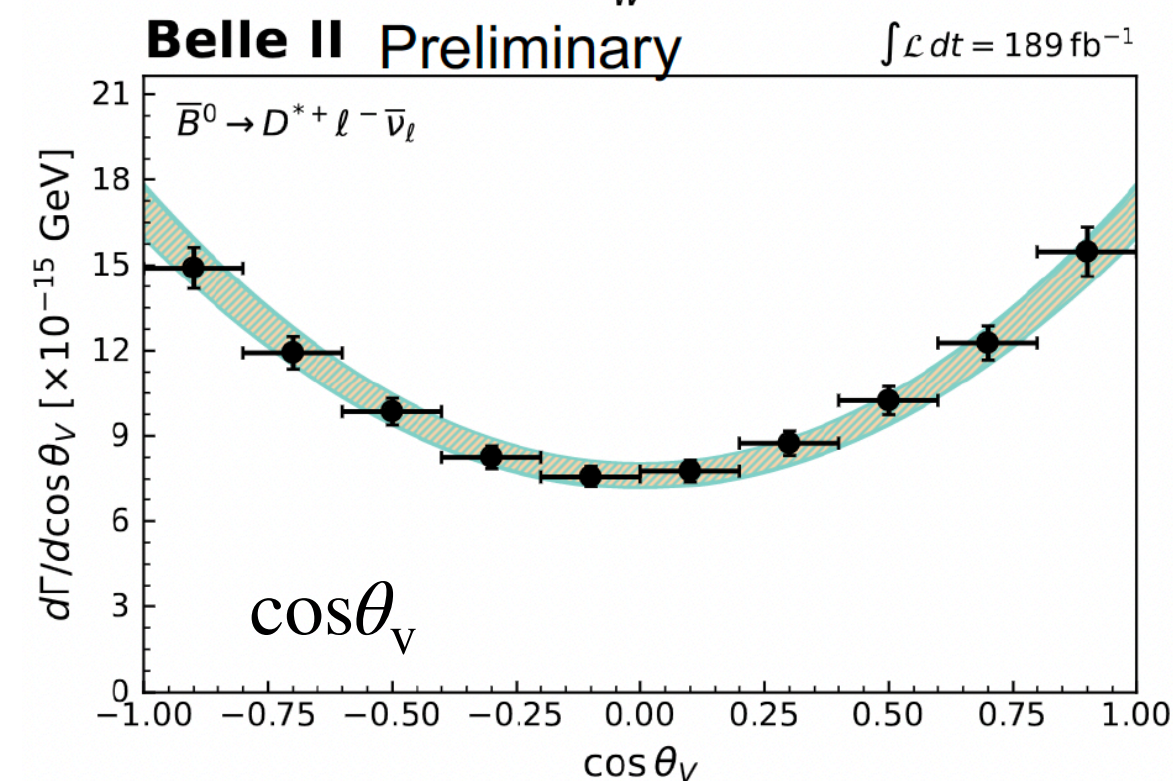
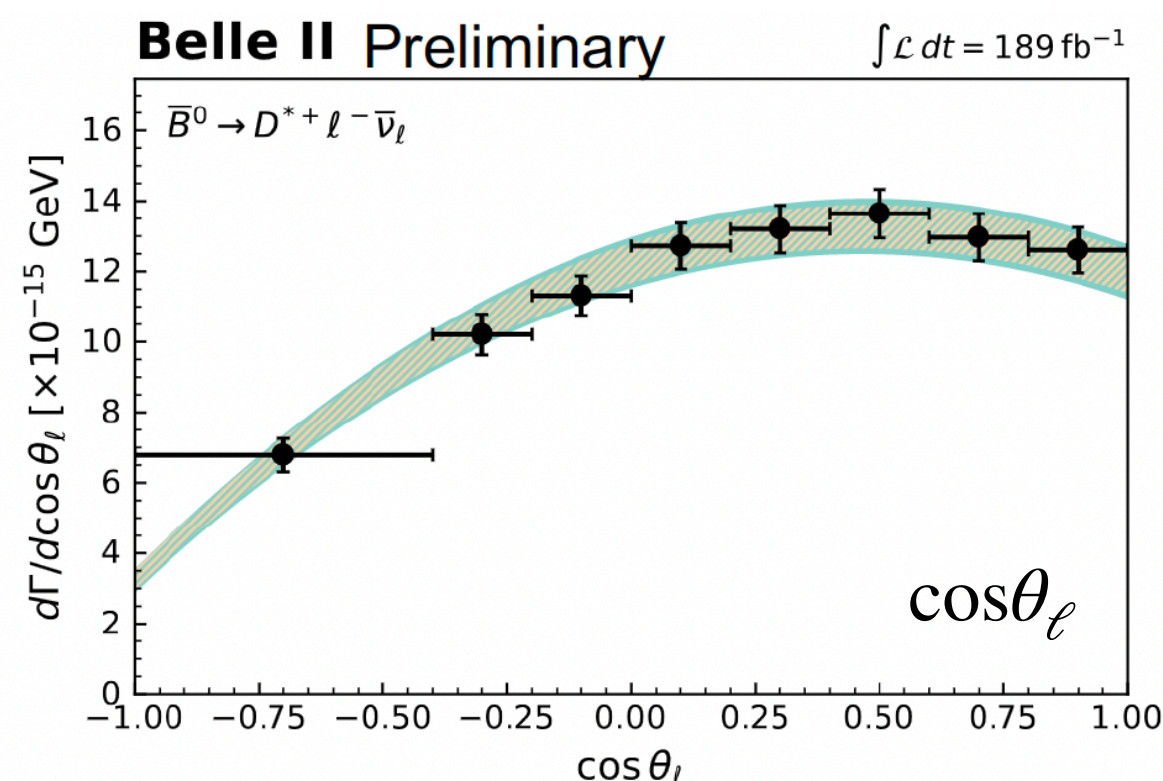
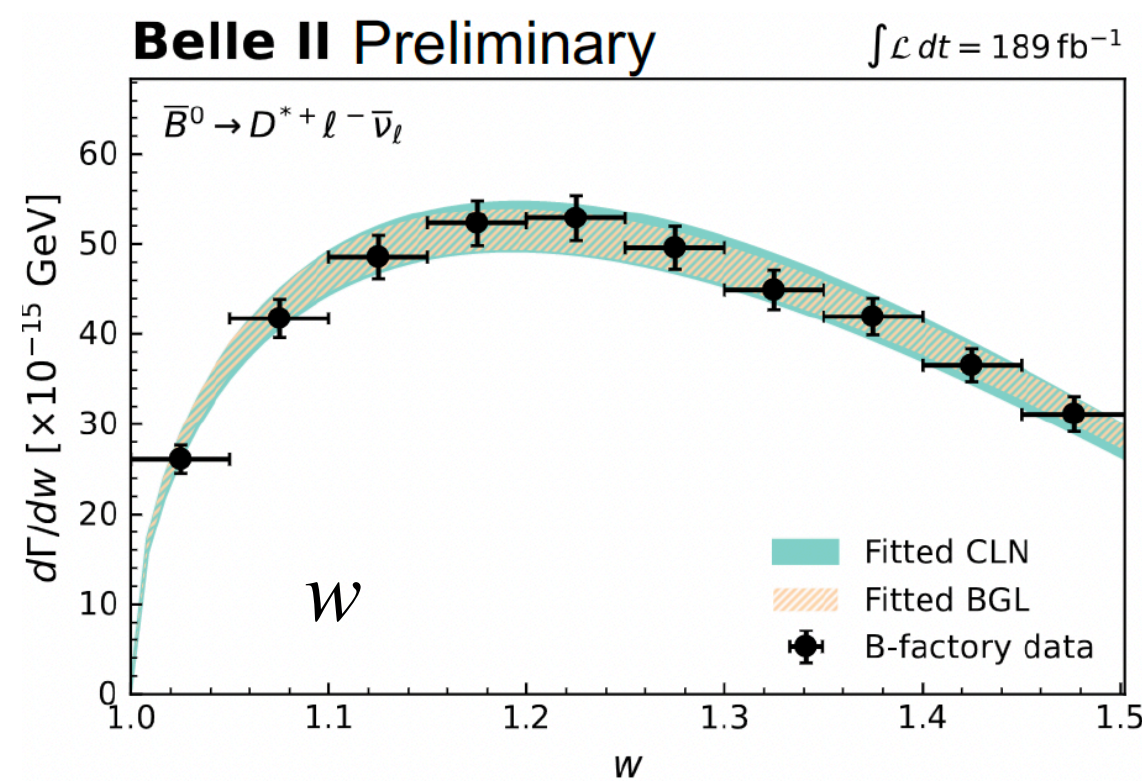


$|V_{cb}|$ in $B^0 \rightarrow D^* \ell \nu$ Decay

Preliminary

- Include all measured w , $\cos\theta_\ell$, $\cos\theta_\nu$, χ to extract form factor & $|V_{cb}|$
- Fit with form factor expansion based on **CLN & BGL (truncation tested)**
- Reredundant degrees of freedom removed by using **normalized partial rates** on each variable together with the **averaged total rate** (ndf = 34+1)

$$\chi^2 = \sum_{i,j} \left(\frac{\Delta\Gamma_i^{\text{obs}}}{\Gamma^{\text{obs}}} - \frac{\Delta\Gamma_i^{\text{pre}}}{\Gamma^{\text{pre}}} \right) C_{ij}^{-1} \left(\frac{\Delta\Gamma_j^{\text{obs}}}{\Gamma^{\text{obs}}} - \frac{\Delta\Gamma_j^{\text{pre}}}{\Gamma^{\text{pre}}} \right) + \frac{(\Gamma^{\text{obs}} - \Gamma^{\text{pre}})^2}{\sigma_\Gamma^2}$$



$$|V_{cb}| \eta_{\text{EW}} \mathcal{F}(1) = \frac{1}{\sqrt{m_B m_{D^*}}} \left(\frac{|\tilde{b}_0|}{P_f(0) \phi_f(0)} \right)$$

$$|V_{cb}|_{\text{BGL}} = (40.9 \pm 0.3 \pm 1.0 \pm 0.6) \times 10^{-3}$$

$$|V_{cb}|_{\text{CLN}} = (40.4 \pm 0.3 \pm 1.0 \pm 0.6) \times 10^{-3}$$

Slow pion eff. plays leading role in syst.

Input from LQCD at zero-recoil $\mathcal{F}(1)$

$|V_{cb}|$ in $B^0 \rightarrow D^* \ell \bar{\nu}$ Decay

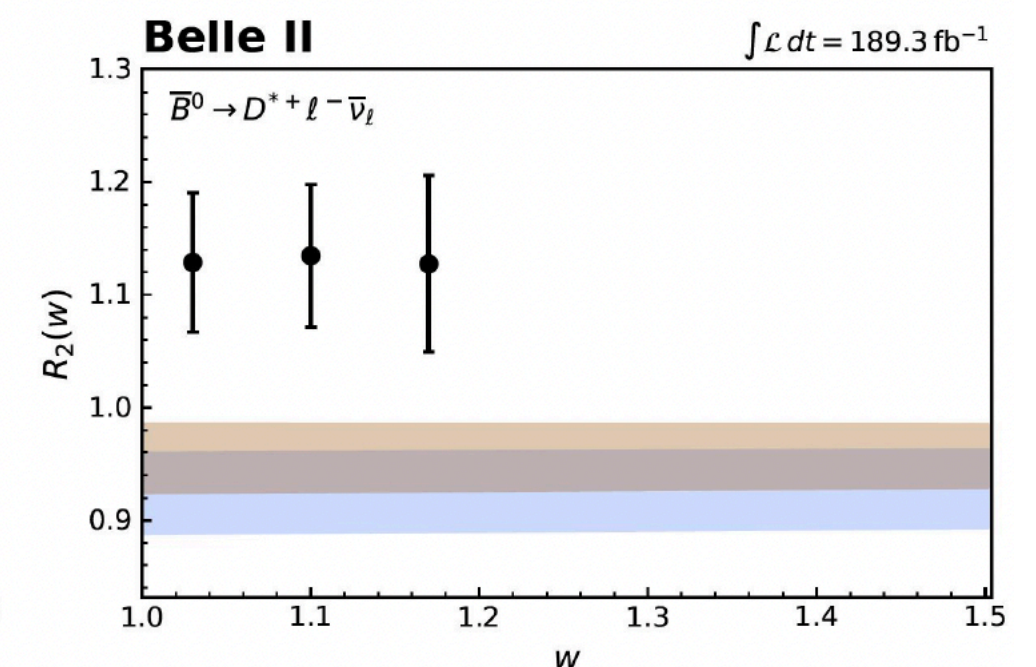
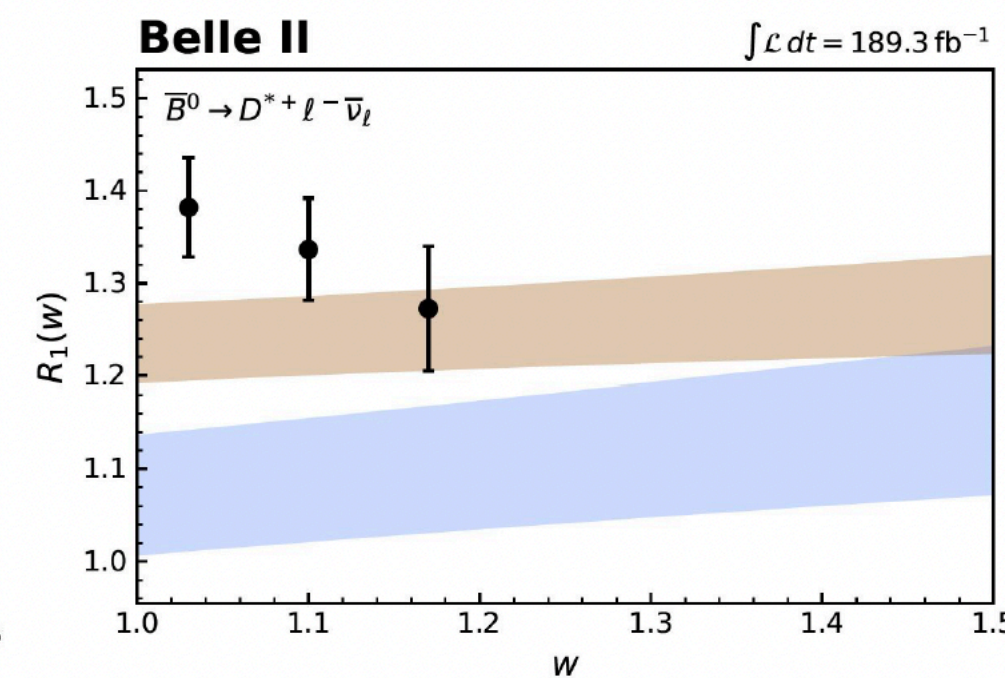
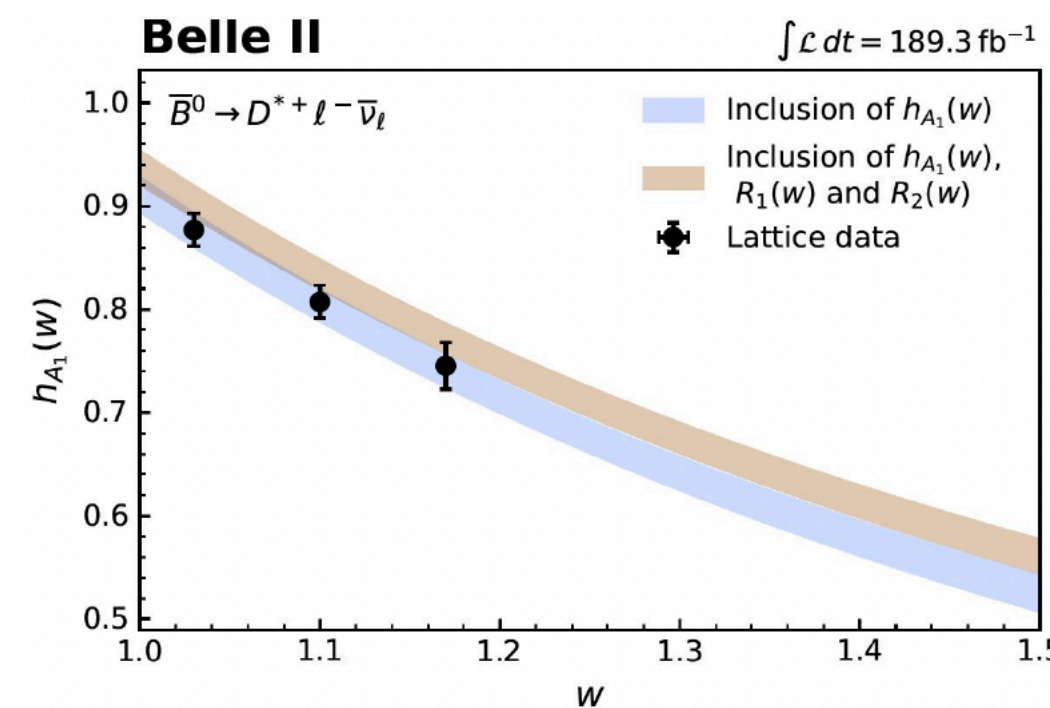
Preliminary

- Include all measured w , $\cos\theta_\ell$, $\cos\theta_\nu$, χ to extract form factor & $|V_{cb}|$
- Fit with form factor expansion based on **CLN & BGL (truncation tested)**
- Reredundant degrees of freedom removed by using **normalized partial rates** on each variable together with the **averaged total rate** (ndf = 34+1)
- Inclusion of LQCD constraint [arxiv:2105.14019] at beyond zero-recoil ($w = [1.03, 1.10, 1.17]$) in two scenarios

$$\chi^2 = \sum_{i,j} \left(\frac{\Delta\Gamma_i^{\text{obs}}}{\Gamma^{\text{obs}}} - \frac{\Delta\Gamma_i^{\text{pre}}}{\Gamma^{\text{pre}}} \right) C_{ij}^{-1} \left(\frac{\Delta\Gamma_j^{\text{obs}}}{\Gamma^{\text{obs}}} - \frac{\Delta\Gamma_j^{\text{pre}}}{\Gamma^{\text{pre}}} \right) + \frac{(\Gamma^{\text{obs}} - \Gamma^{\text{pre}})^2}{\sigma_\Gamma^2} + \sum_{ij} (F_i^{\text{LQCD}} - F_i^{\text{exp}}) C_{ij}^{-1} (F_j^{\text{LQCD}} - F_j^{\text{exp}})$$

| BGL | Constraints on $h_{A_1}(w)$ | Constraints on $h_{A_1}(w), R_1(w), R_2(w)$ |
|------------------------|-----------------------------|---|
| $a_0 \times 10^3$ | 21.7 ± 1.4 | 25.7 ± 0.8 |
| $b_0 \times 10^3$ | 13.20 ± 0.24 | 13.58 ± 0.23 |
| $b_1 \times 10^3$ | -7 ± 7 | 2 ± 6 |
| $c_1 \times 10^3$ | -1.1 ± 0.8 | -0.5 ± 0.8 |
| $ V_{cb} \times 10^3$ | 40.5 ± 1.2 | 38.6 ± 1.1 |
| χ^2/ndf | 40/33 | 74/39 |
| p -value | 0.18 | 0.001 |

$|V_{cb}|$ shifts when include LQCD full constraints



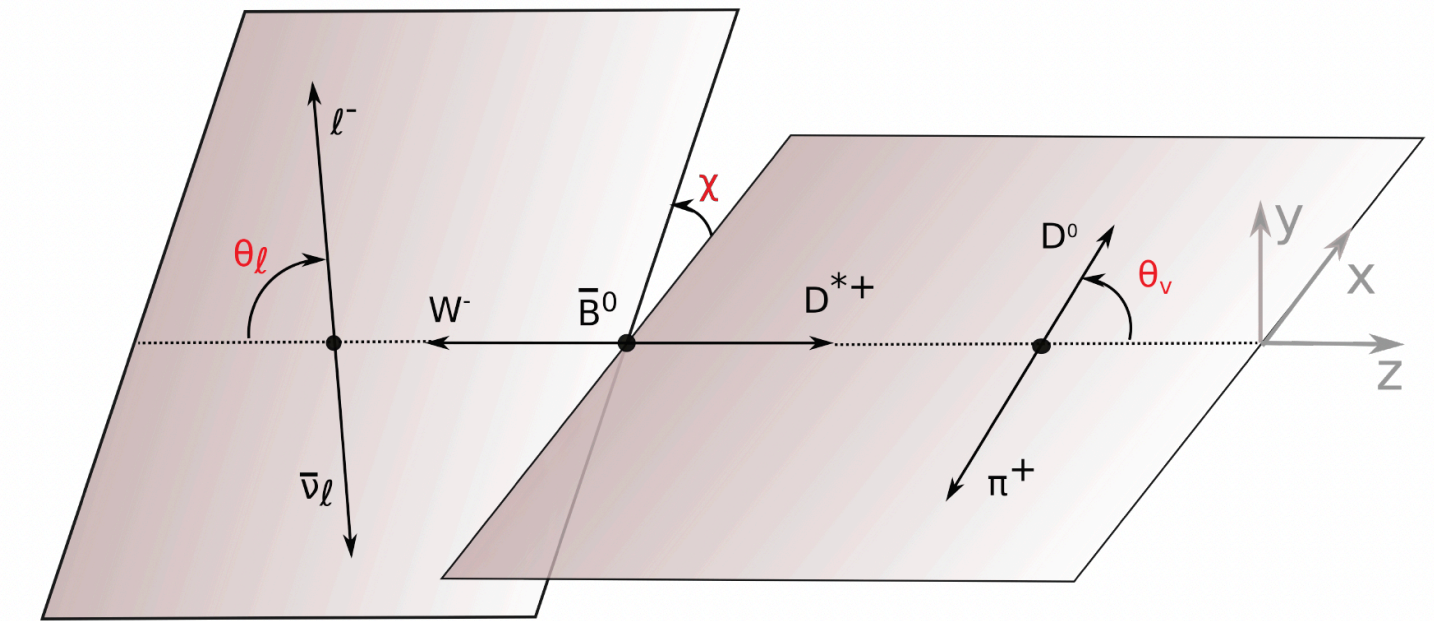
Consistent with recent Belle (2023) measurement [arXiv:2301.07529]
 \Rightarrow Both found large disagreements wrt LQCD results on R_2

$|V_{cb}|$ in $B^0 \rightarrow D^* \ell \nu$ Decay

Preliminary

- Lepton-flavor-universality tested with separate results on e- & mu-mode
- All in **good agreement with SM expectations**

Test on branching fraction ratio: $R_{e/\mu} = 1.001 \pm 0.009 \pm 0.021$



Test on forward-backward asymmetry:

$$\mathcal{A}_{\text{FB}} = \frac{\int_0^1 d \cos \theta_\ell d\Gamma/d \cos \theta_\ell - \int_{-1}^0 d \cos \theta_\ell d\Gamma/d \cos \theta_\ell}{\int_0^1 d \cos \theta_\ell d\Gamma/d \cos \theta_\ell + \int_{-1}^0 d \cos \theta_\ell d\Gamma/d \cos \theta_\ell}$$

$$\Delta \mathcal{A}_{\text{FB}} = \mathcal{A}_{\text{FB}}^\mu - \mathcal{A}_{\text{FB}}^e$$

$$\mathcal{A}_{\text{FB}}^e = 0.219 \pm 0.011 \pm 0.020,$$

$$\mathcal{A}_{\text{FB}}^\mu = 0.215 \pm 0.011 \pm 0.022,$$

$$\Delta \mathcal{A}_{\text{FB}} = (-4 \pm 16 \pm 18) \times 10^{-3}$$

Test on D^* longitudinal polarization fraction:

$$\frac{1}{\Gamma} \frac{d\Gamma}{d \cos \theta_V} = \frac{3}{2} \left(F_L \cos^2 \theta_V + \frac{1 - F_L}{2} \sin^2 \theta_V \right)$$

$$\Delta F_L = F_L^\mu - F_L^e$$

$$F_L^e = 0.521 \pm 0.005 \pm 0.007$$

$$F_L^\mu = 0.534 \pm 0.005 \pm 0.006$$

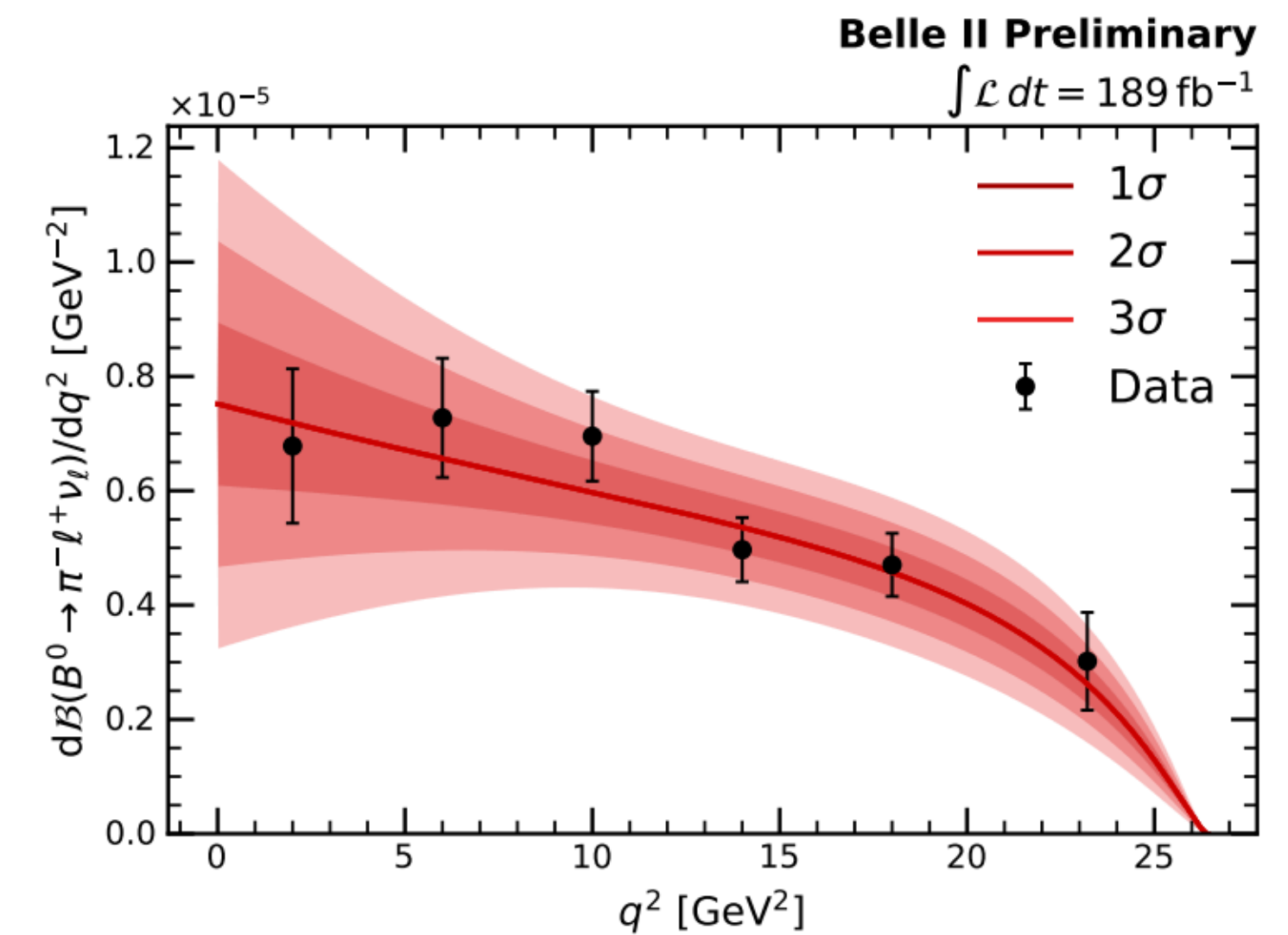
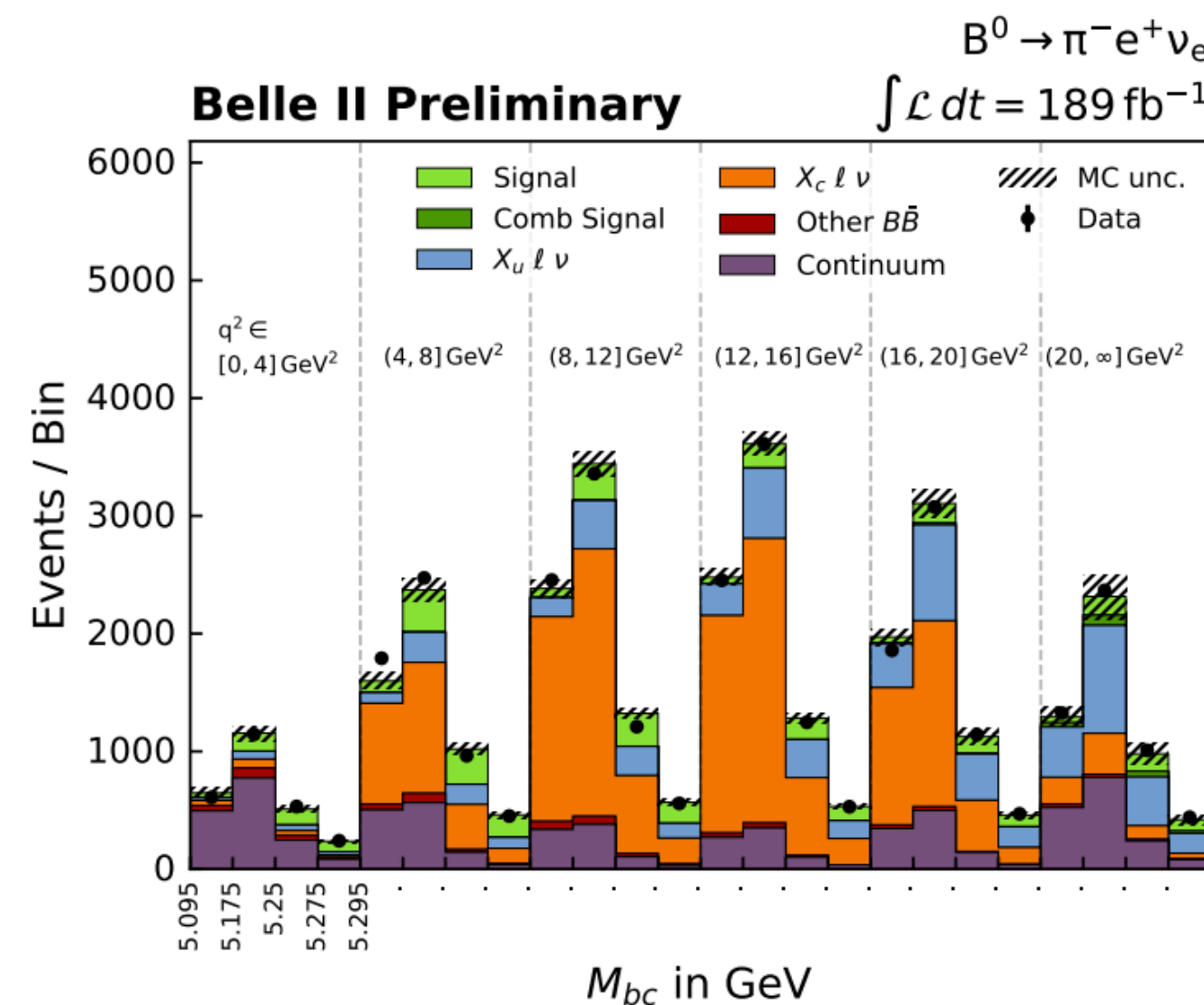
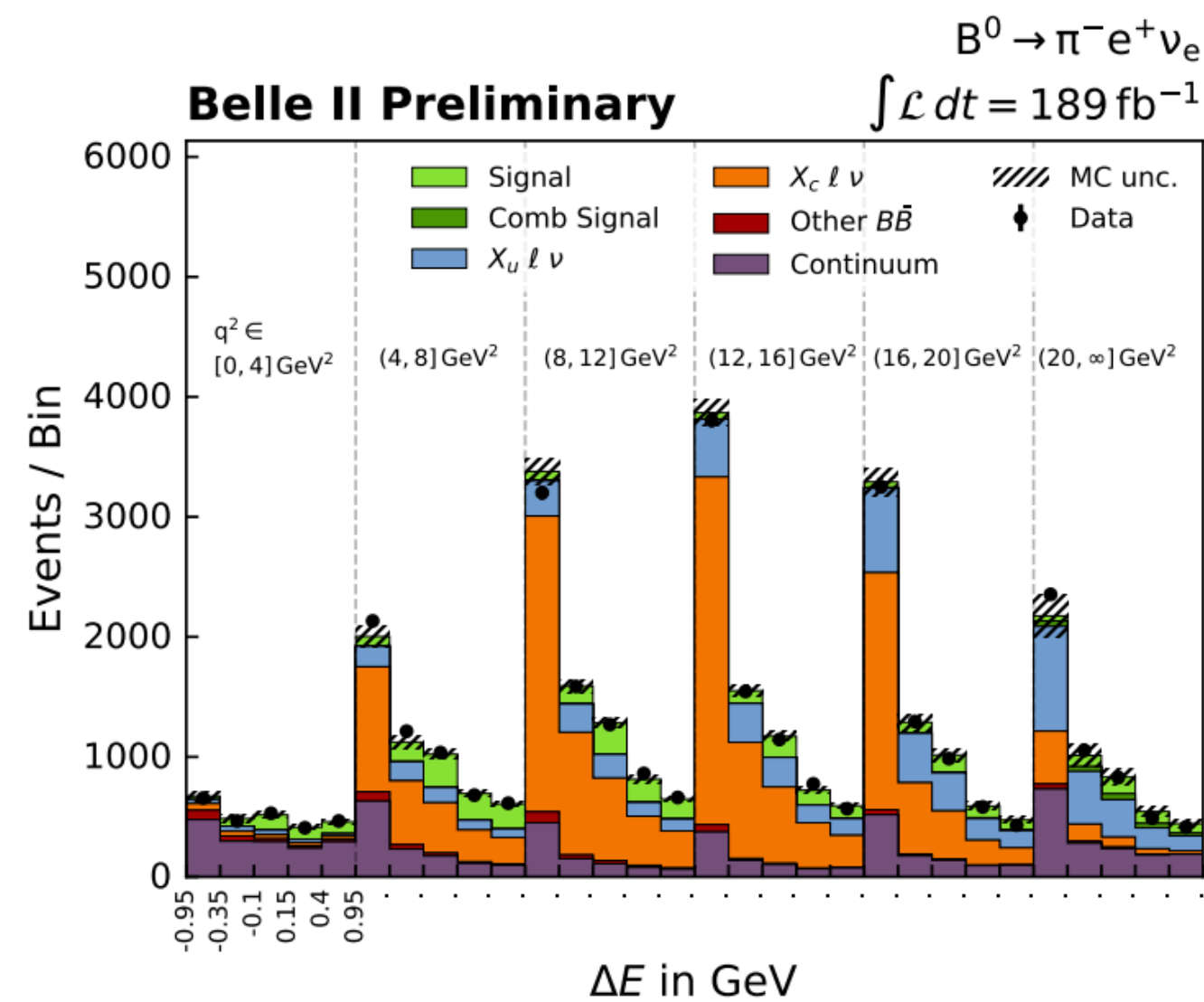
$$\Delta F_L = 0.013 \pm 0.007 \pm 0.007$$

CKM matrix element $|V_{ub}|$

$|V_{ub}|$ in $B^0 \rightarrow \pi^- \ell^+ \nu$ with Belle II data

arXiv: 2210.04224

- Data set of 189.3 fb^{-1} with untagged analysis strategy
- Extract signal in beam-constrained mass M_{bc} and energy difference ΔE for each bin of q^2
- $|V_{ub}|$ fitted with BCL expansion including LQCD constraints (FNAL/MILC)



$$\mathcal{B} = (1.426 \pm 0.056_{\text{stat}} \pm 0.125_{\text{syst}}) \times 10^{-4}$$

$$|V_{ub}| = (3.55 \pm 0.12_{\text{stat}} \pm 0.13_{\text{syst}} \pm 0.17_{\text{theo}}) \times 10^{-3}$$

dominated by background modelling (continuum, $B \rightarrow \rho \ell \nu$)

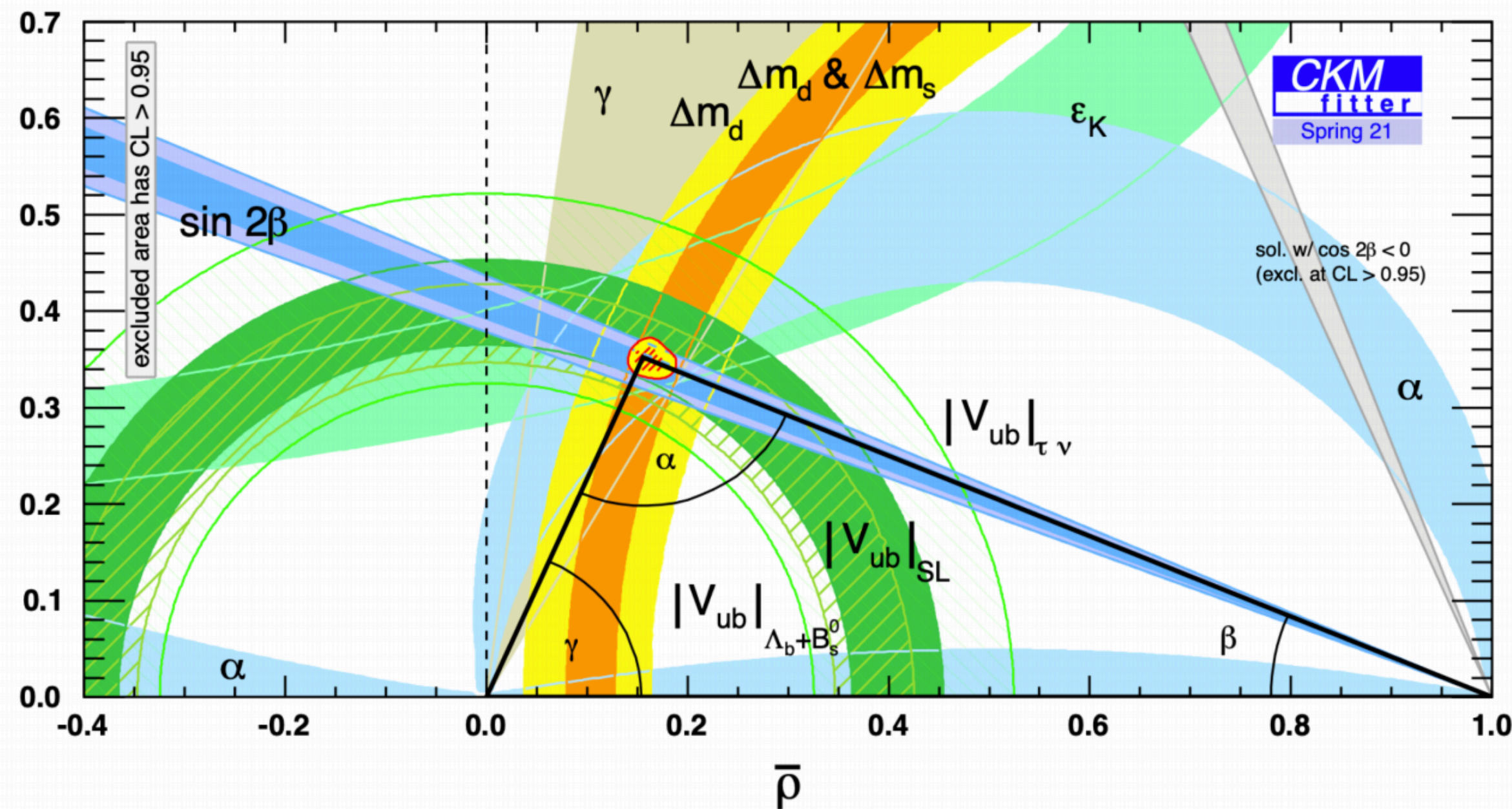
$$\Delta E = E_B^* - E_{\text{beam}}^* = E_B^* - \frac{\sqrt{s}}{2}$$

$$M_{bc} = \sqrt{E_{\text{beam}}^{*2} - |\vec{p}_B^*|^2} = \sqrt{\left(\frac{\sqrt{s}}{2}\right)^2 - |\vec{p}_B^*|^2}$$

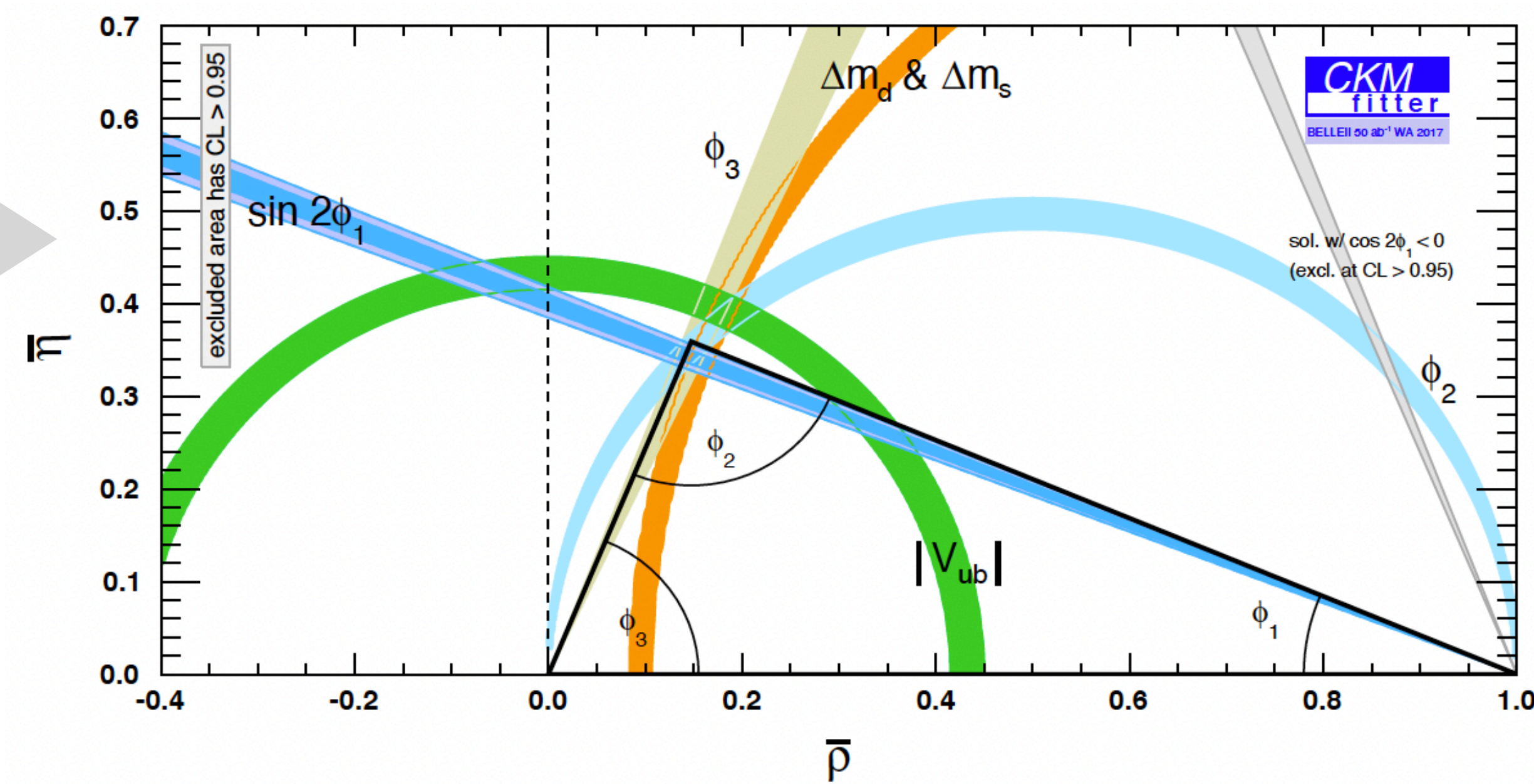
Ultimate Precision with Belle II

- UT lengths and angles can be explored with coming largest B dataset
- High statistics will shrink experimental uncertainties in global UT fit
- Many CKM measurements ($|V_{xb}|$, $\phi_{1,2,3}$) with Belle II data are on the way

Current



Projection to Belle II 50 ab^{-1} based on WA 2017

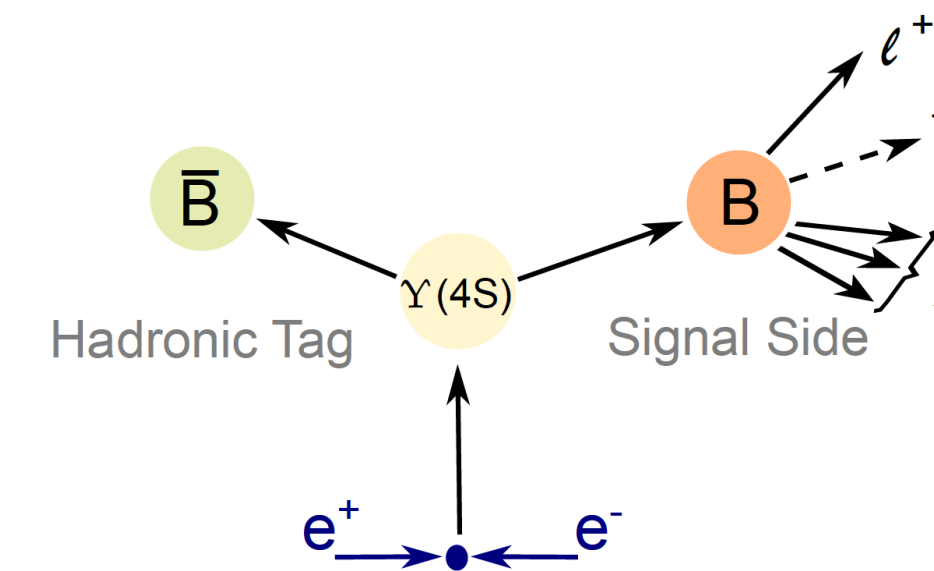


Light-lepton universality test in $B \rightarrow X\ell\nu$

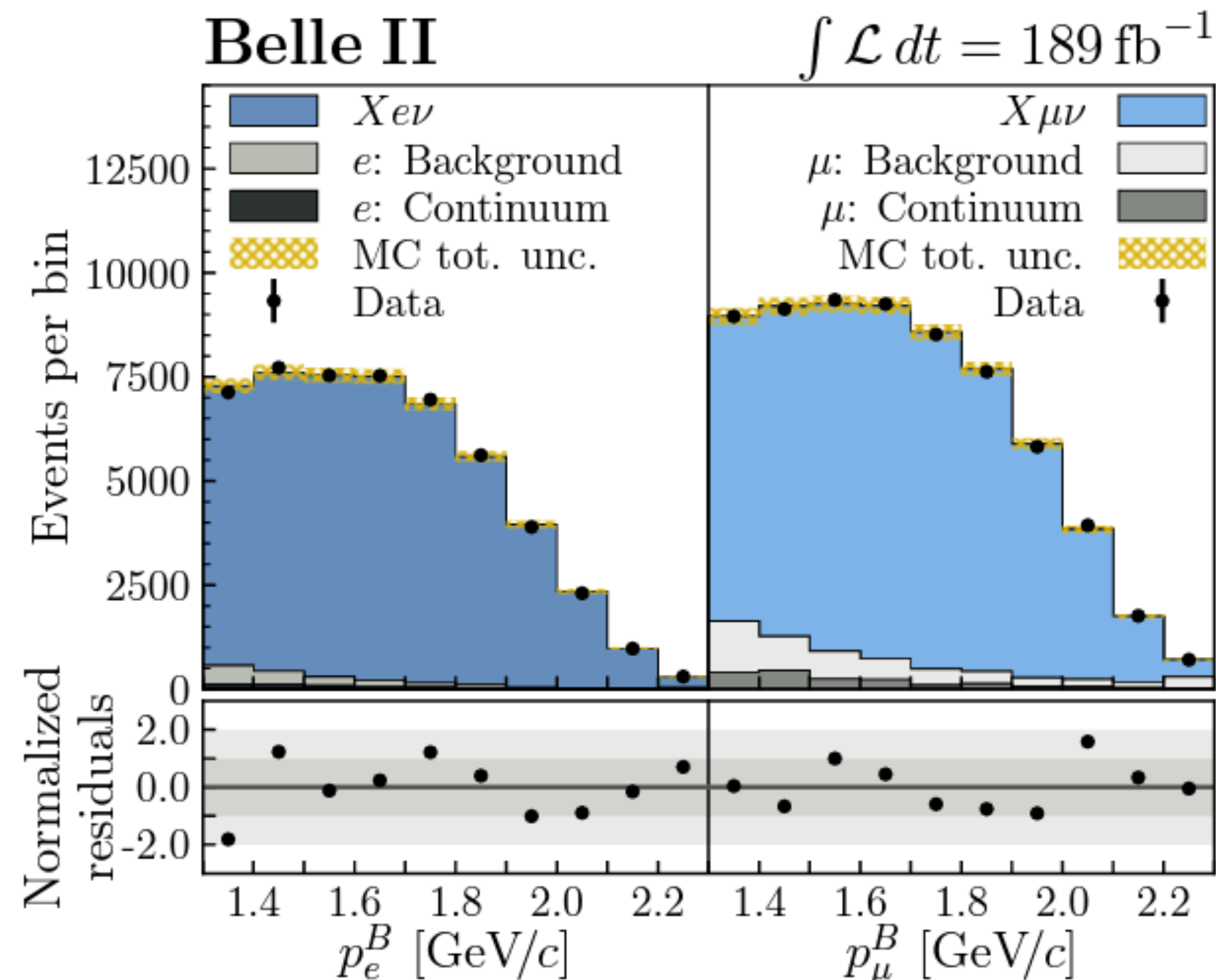
Measurement of $R(X)_{e\mu}$

- Use 189 fb⁻¹ dataset with hadronic tagging strategy
- Extract signal events above $p_\ell^B > 1.3$ GeV simultaneously for e- and μ -mode
- Calculate branching fraction ratio

$$R(X)_{e\mu} = \frac{\mathcal{B}(B \rightarrow Xe\nu)}{\mathcal{B}(B \rightarrow X\mu\nu)}$$



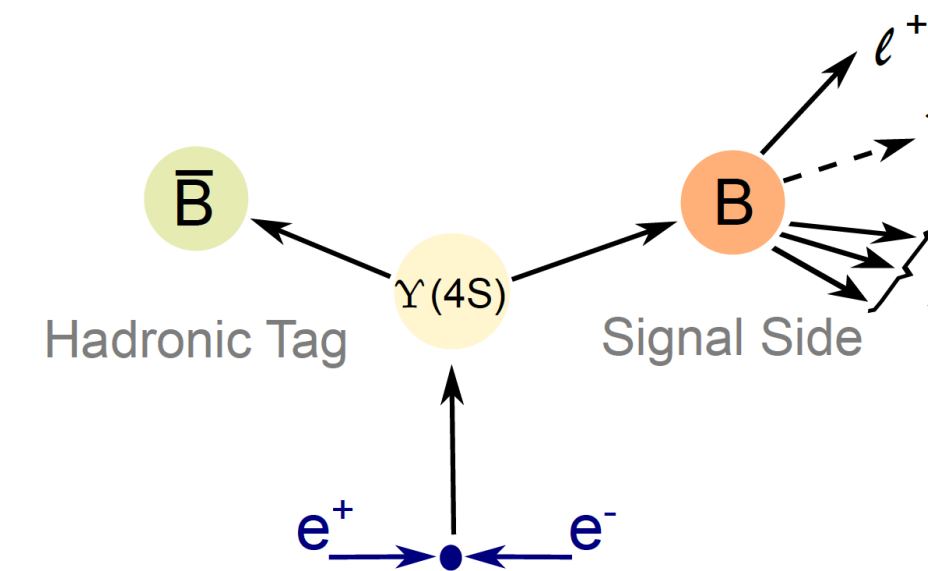
arXiv:2301.08266
(accepted by PRL)



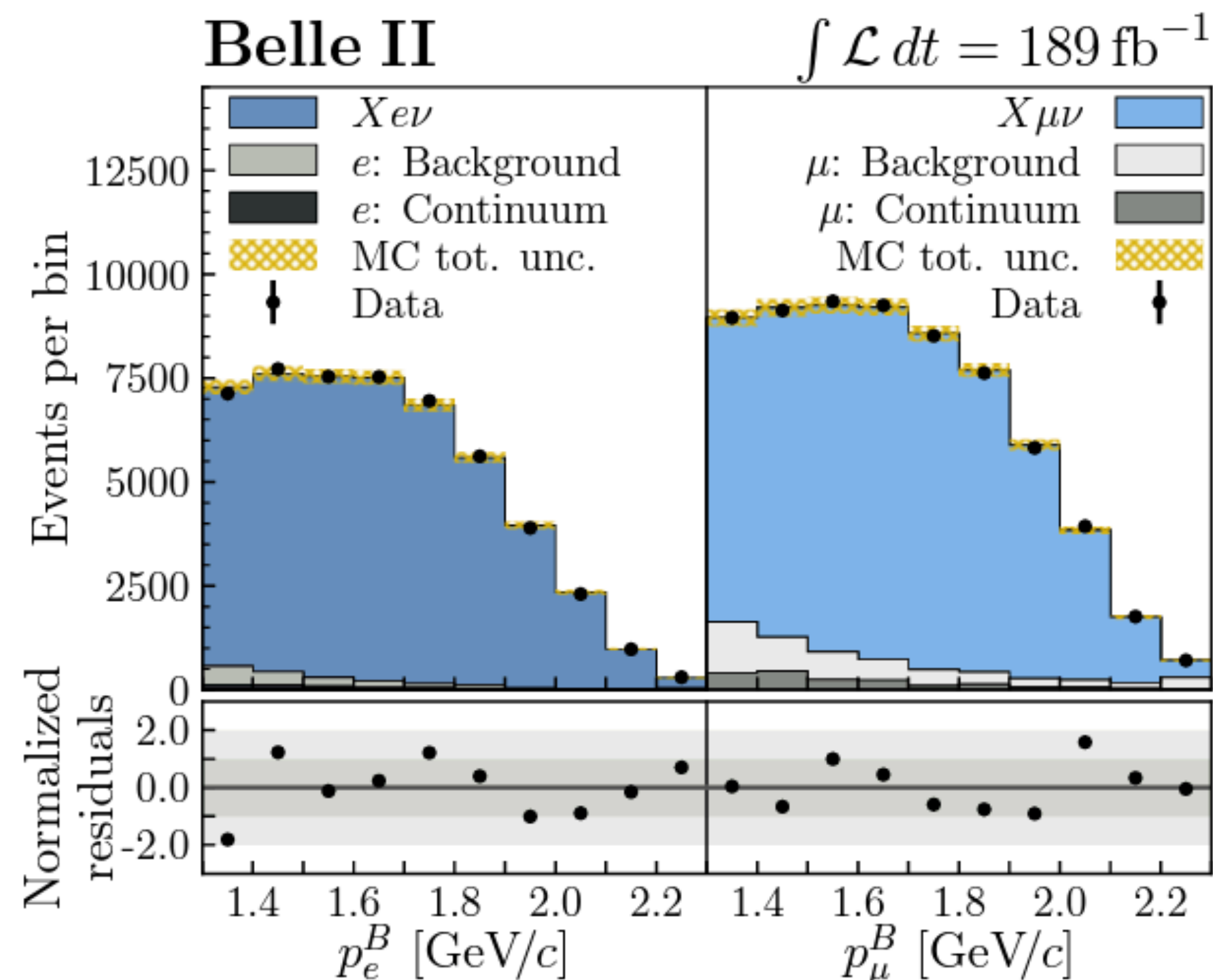
Measurement of $R(X)_{e\mu}$

- Use 189 fb⁻¹ dataset with hadronic tagging strategy
- Extract signal events above $p_\ell^B > 1.3$ GeV simultaneously for e- and μ -mode
- Calculate branching fraction ratio

$$R(X)_{e\mu} = \frac{\mathcal{B}(B \rightarrow Xe\nu)}{\mathcal{B}(B \rightarrow X\mu\nu)}$$



arXiv:2301.08266
(accepted by PRL)



- **Most precise** \mathcal{B} based LFU test in semileptonic B decays to date
- **World first** inclusive measurement
- Consistent with SM expectation within 1.2σ
- $R(X)_{\ell/\tau}$ is on the way

$$R(X)_{e\mu} = 1.033 \pm 0.010_{\text{stat}} \pm 0.019_{\text{syst}}$$

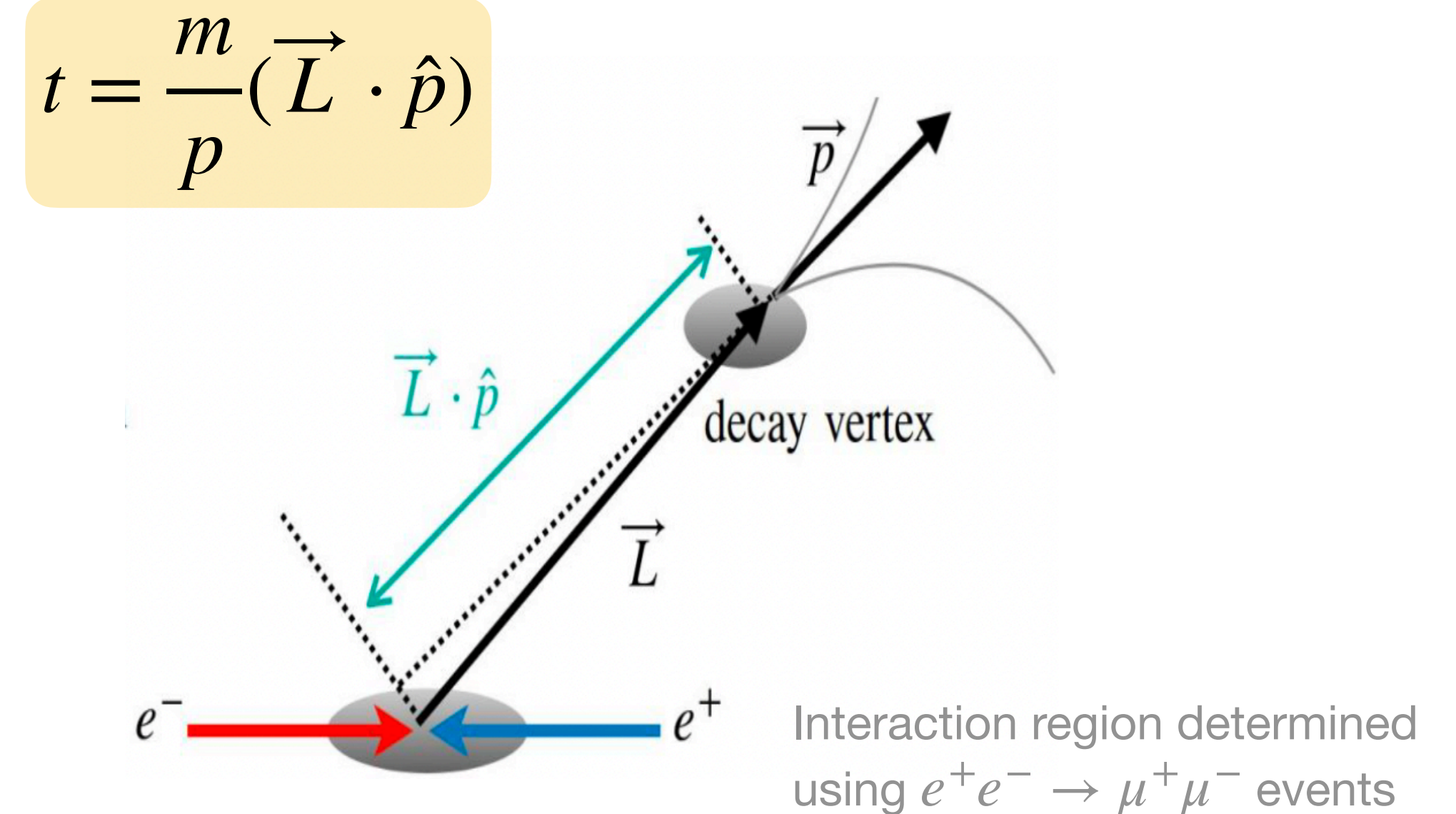
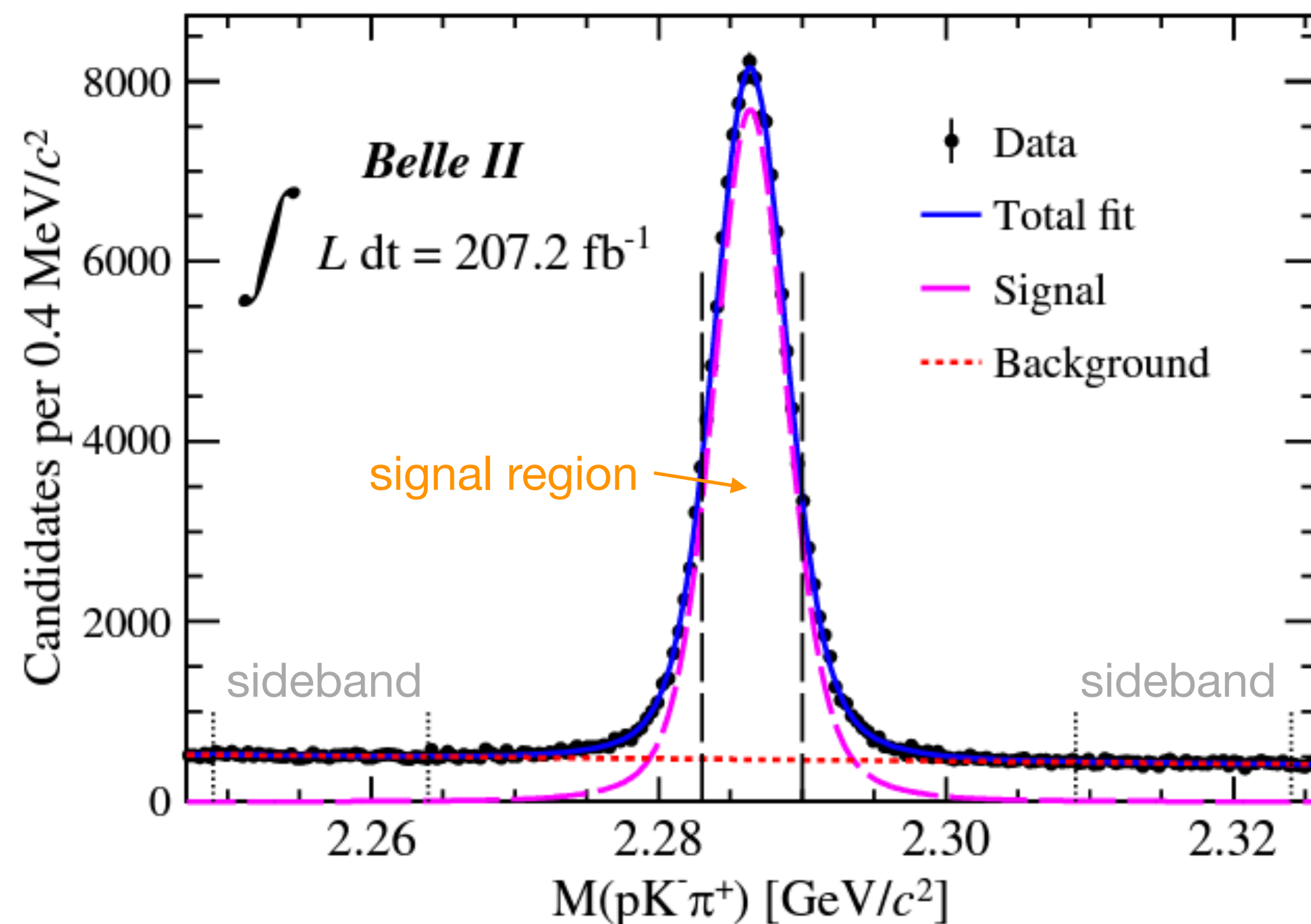
$$R(X|p_\ell^B > 1.3 \text{ GeV})_{e\mu} = 1.031 \pm 0.010_{\text{stat}} \pm 0.019_{\text{syst}}$$

Lifetime measurements of Λ_c^+ and Ω_c^0

Measurement of Λ_c^+ Lifetime

PRL 130, 071802 (2023)

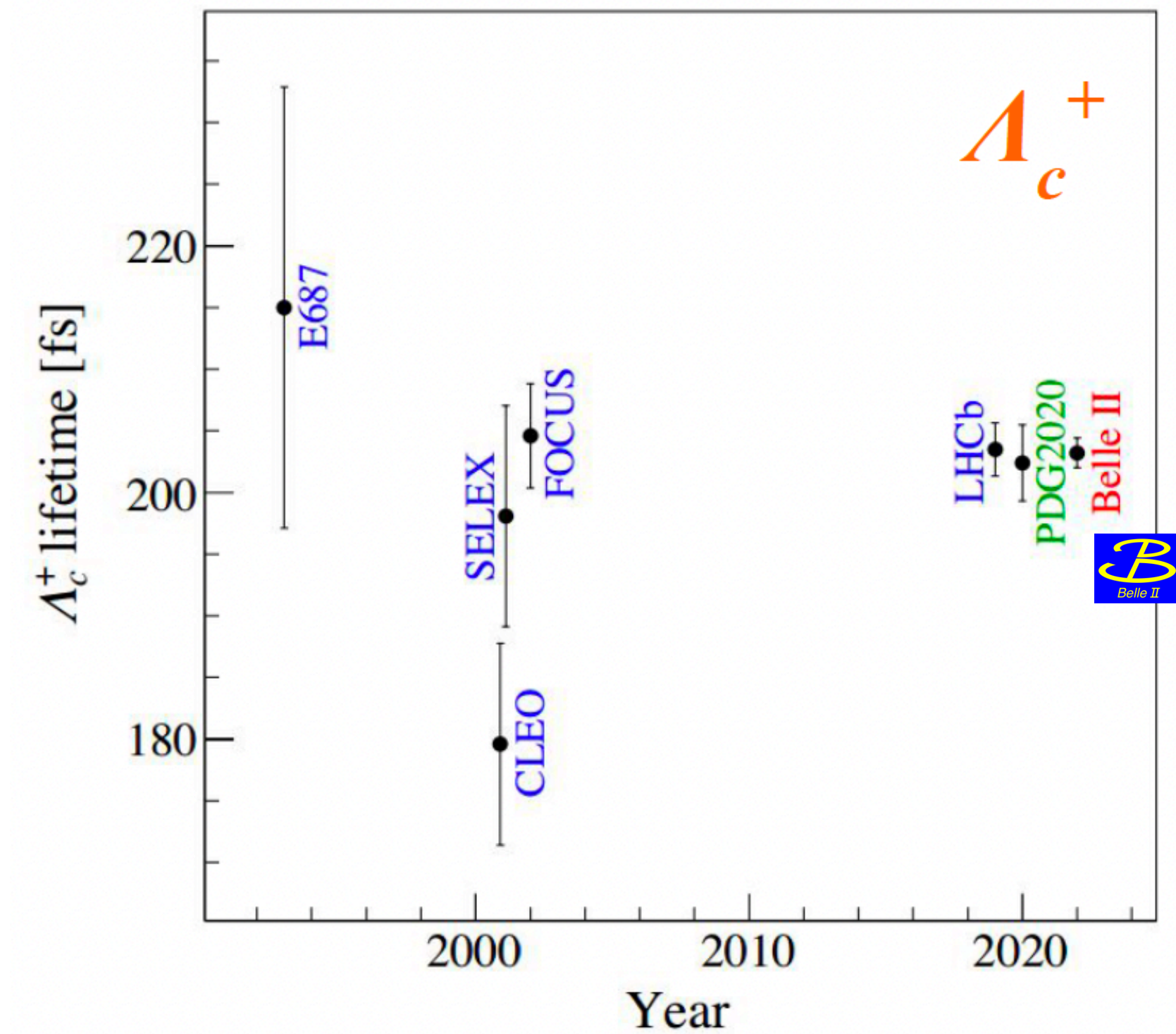
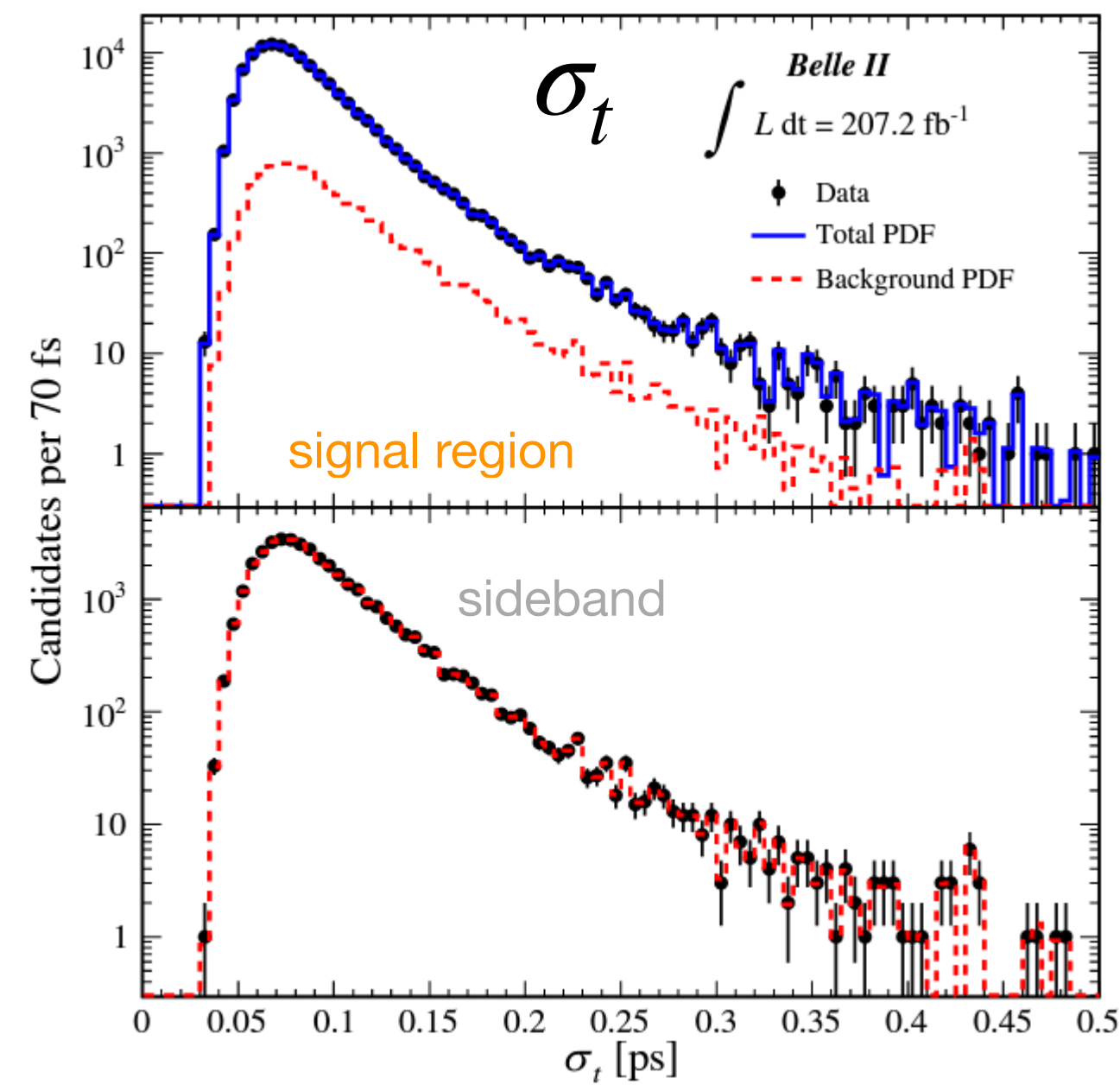
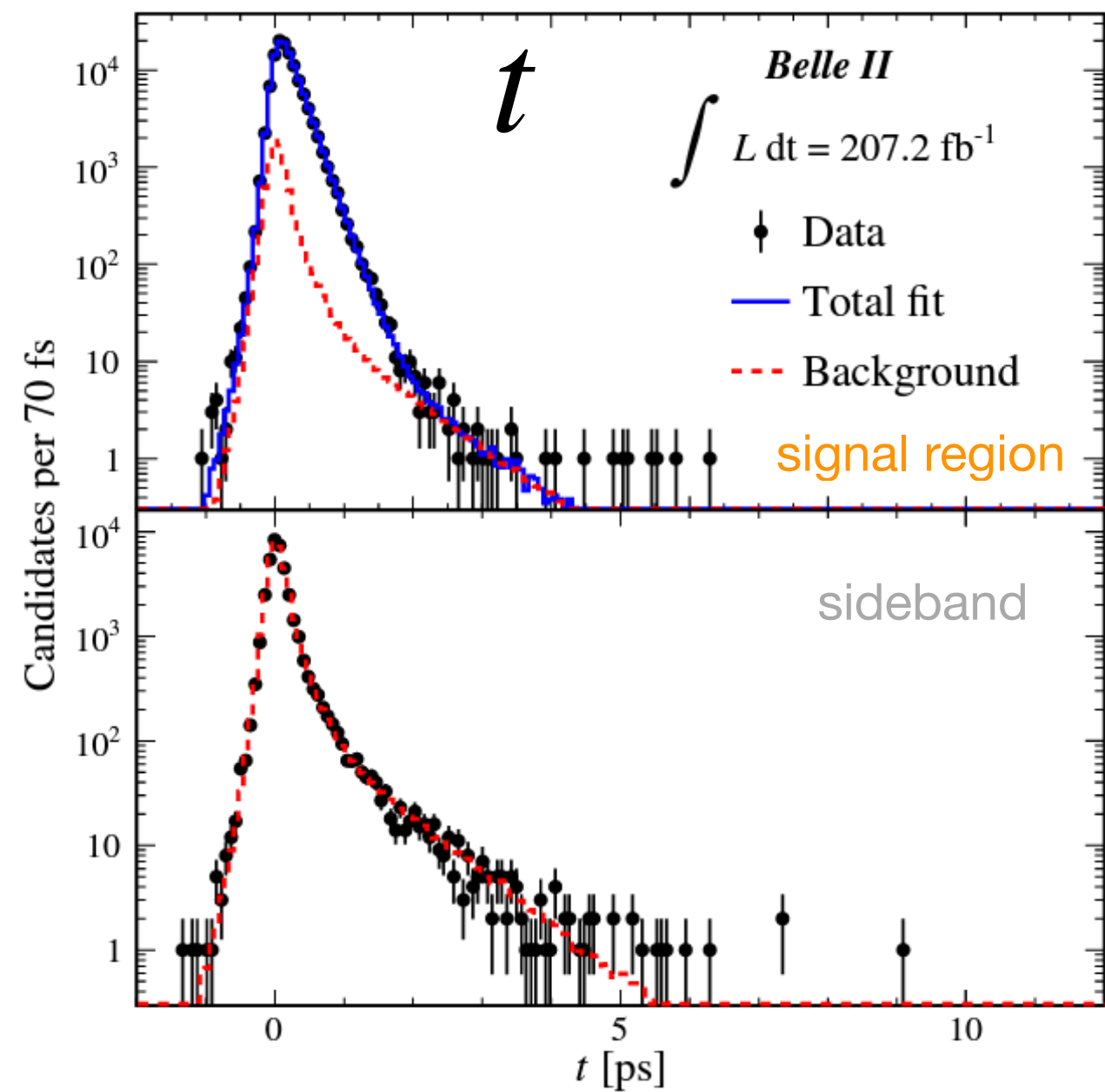
- Collision data of 207.2 fb^{-1} is used to reconstruct $\Lambda_c^+ \rightarrow pK^-\pi^+$
- Performed simultaneous fit to signal region and sidebands to better constrain bkg (Gaussian + Johnson functions with a common mode for signal shape)
- Decay time t calculated using displacement of Λ_c^+ decay vertex projected on its flying direction



Measurement of Λ_c^+ Lifetime

PRL 130, 071802 (2023)

- Unbinned likelihood fit to (t, σ_t) to extract lifetime
- Result consistent with WA and recent LHCb relative measurement [PRD 100, 032001(2019)] while show tension versus CLEO's result [PRL 86,2232(2001)]



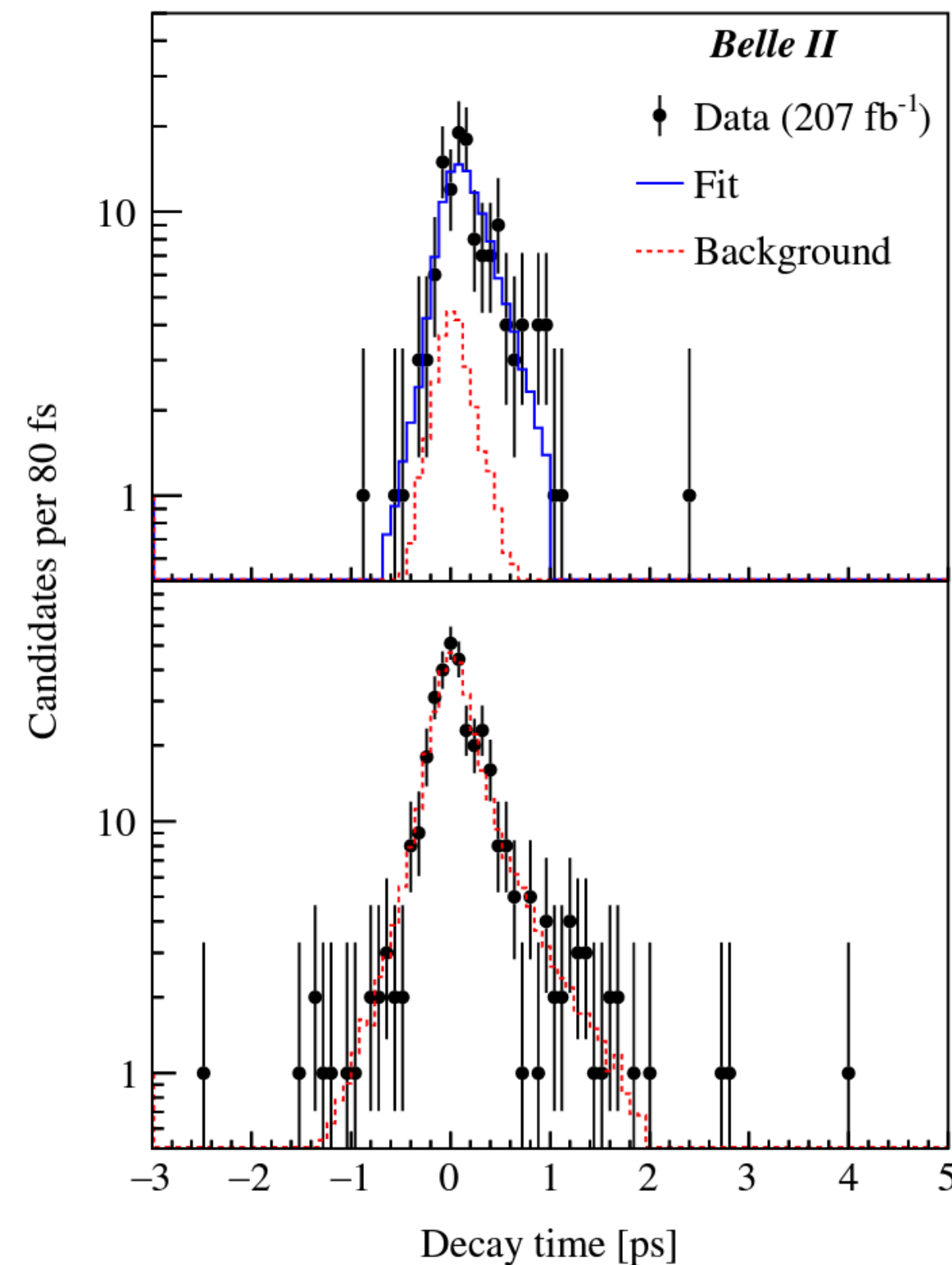
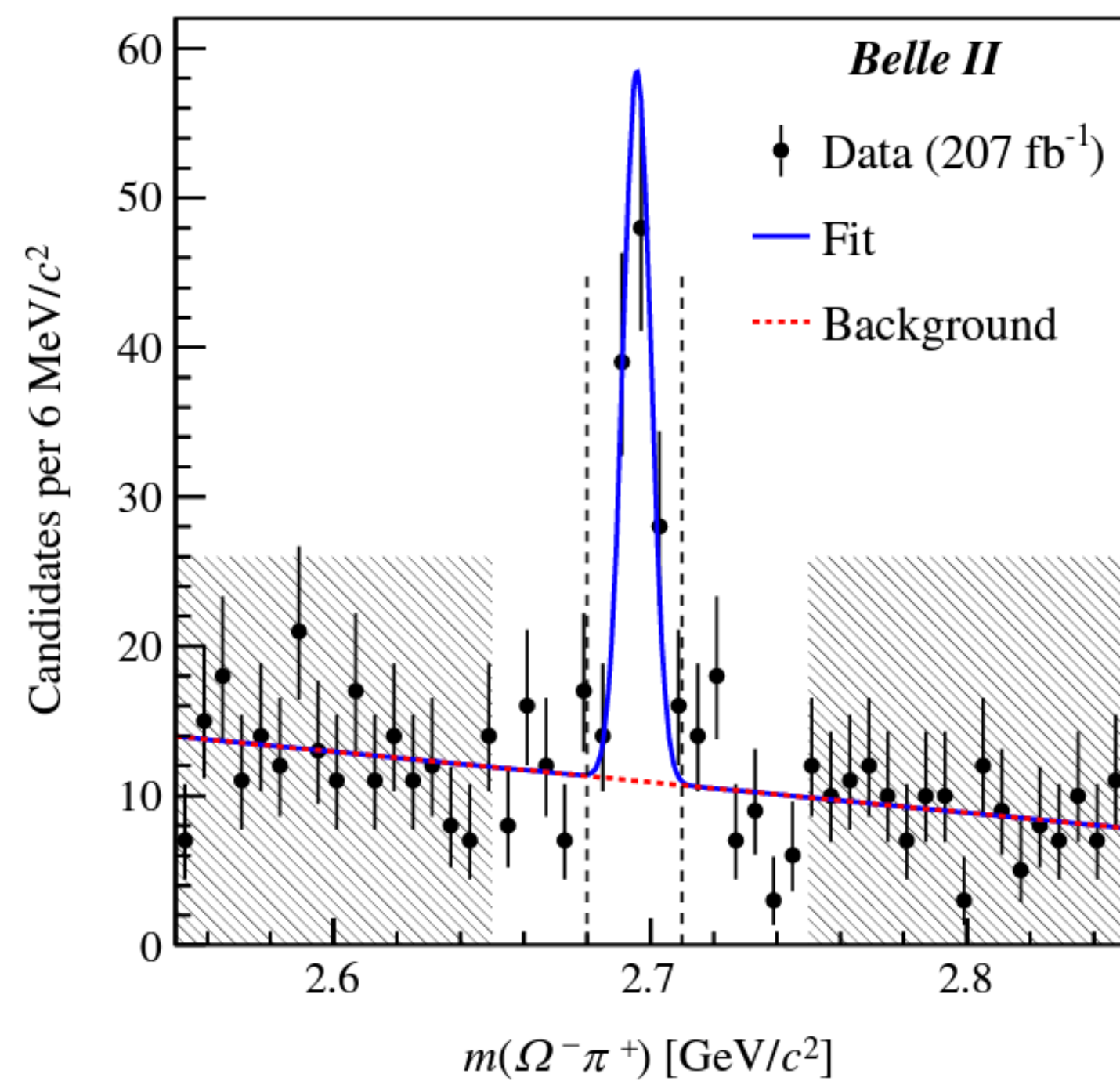
$$\tau(\Lambda_c^+) = 203.20 \pm 0.89_{\text{stat}} \pm 0.77_{\text{syst}} \text{ fs}$$

Most precise results to date!

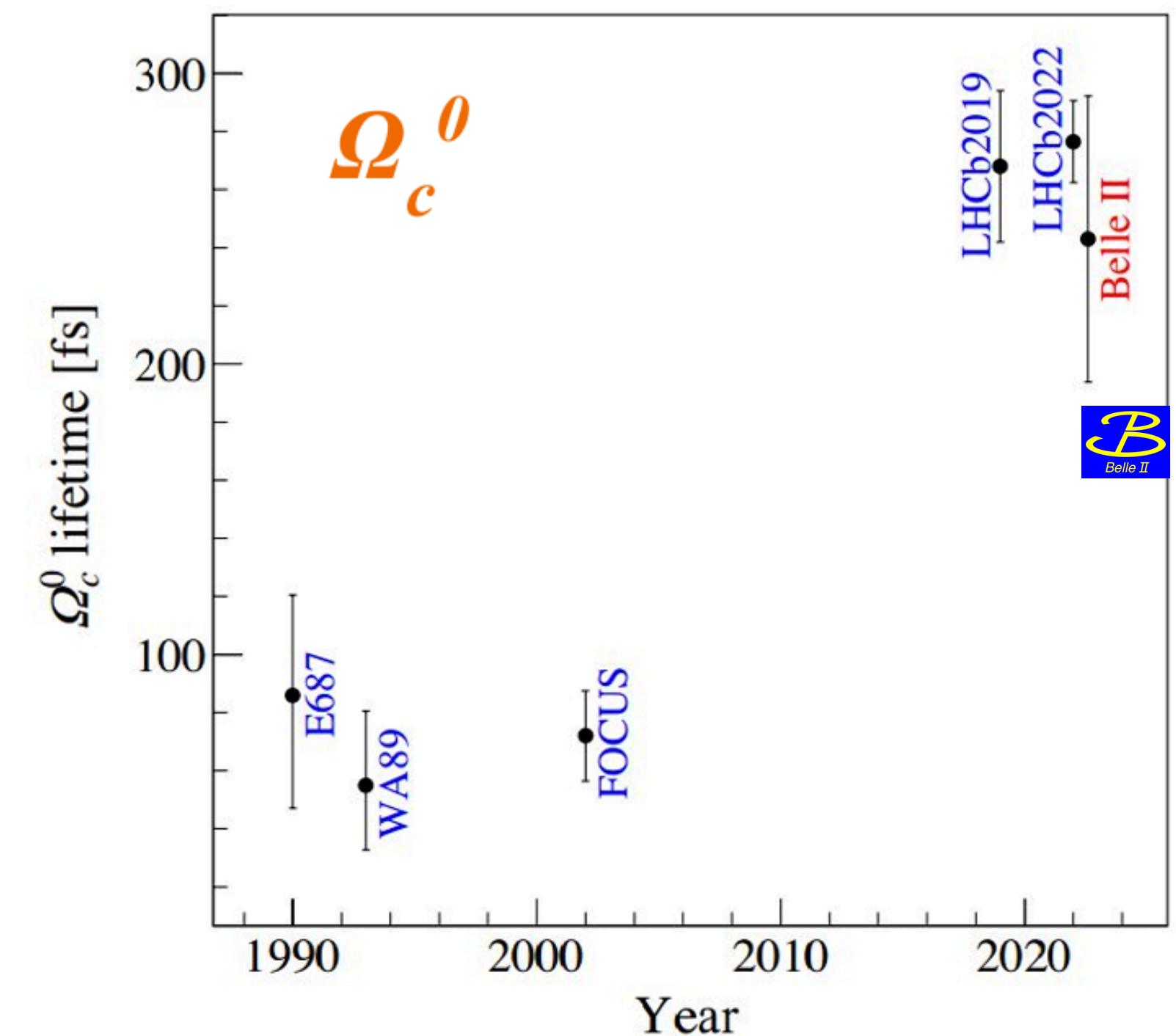
Measurement of Ω_c^0 Lifetime

- Dataset of 207.2 fb^{-1} is used to reconstruct $\Omega_c^0 \rightarrow \Omega^- \pi^+$, $\Omega^- \rightarrow \Lambda^0 K^-$, $\Lambda^0 \rightarrow p \pi^-$
- Applied unbinned likelihood fit to $m(\Omega^- \pi^+)$
- Derive lifetime from (t, σ_t) fit
- Result consistent with LHCb measurements but leave 3.4σ tension from old WA

PRD 107, L031103 (2023)



$$\tau(\Omega_c^0) = 243 \pm 48_{\text{stat}} \pm 11_{\text{syst}} \text{ fs}$$



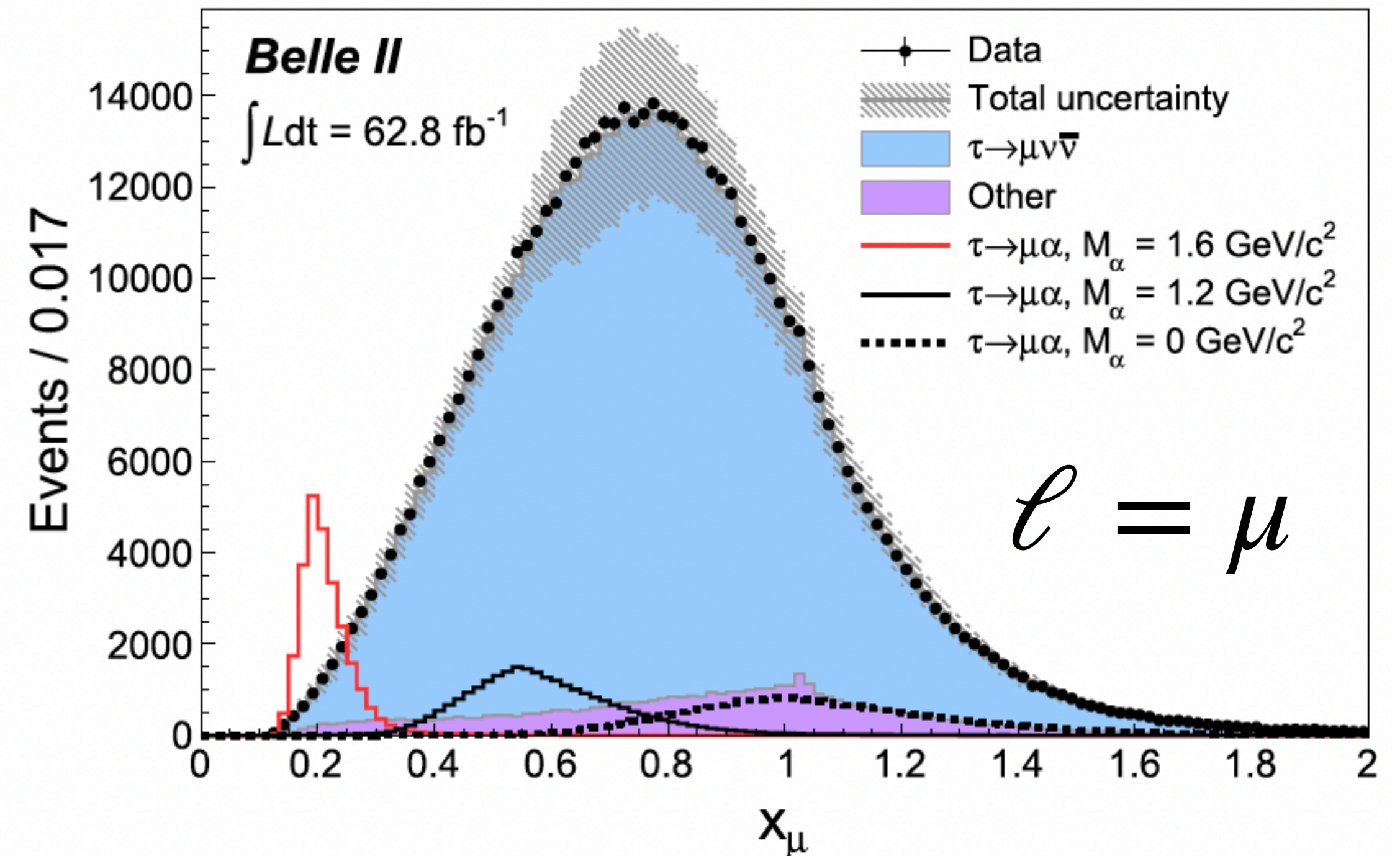
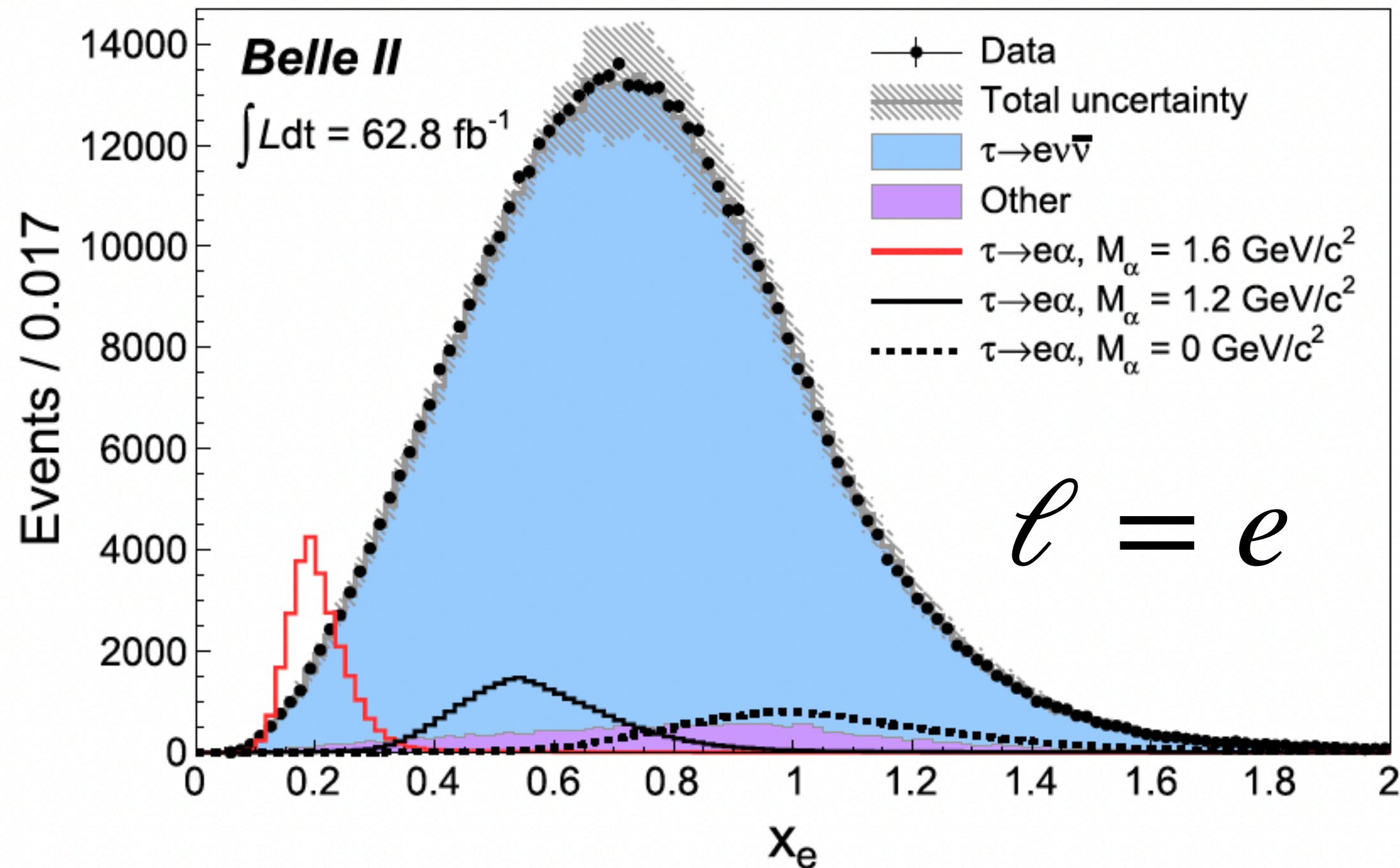
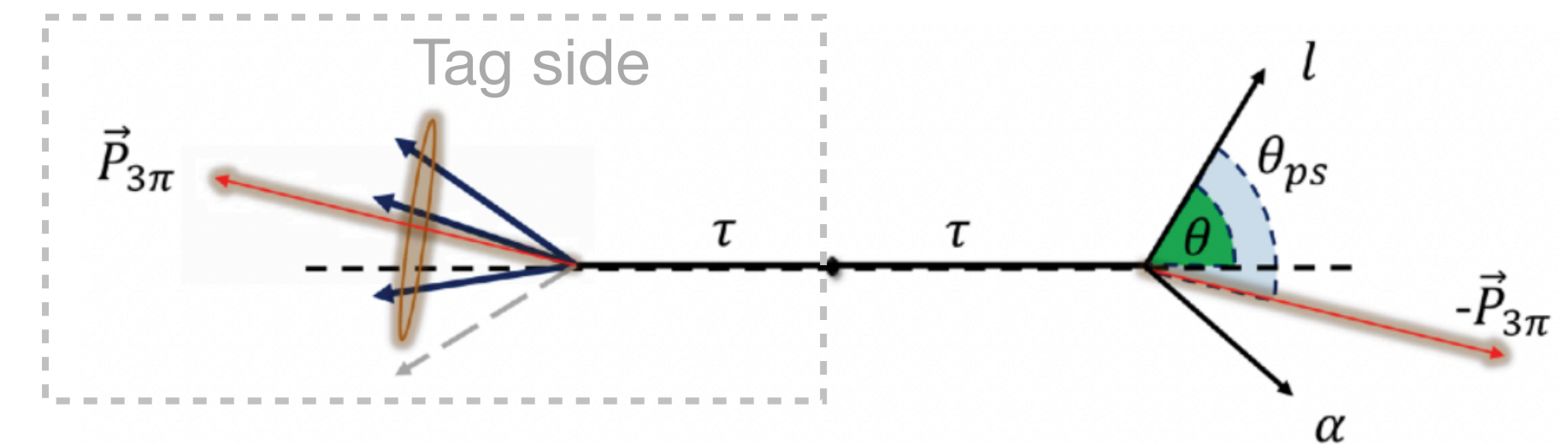
Lepton-flavor-violating $\tau \rightarrow \ell + \alpha$ decay

Search for LFV $\tau^- \rightarrow \ell^- + \alpha$

PRL 130, 181803 (2023)

- Use dataset of 62.8 fb^{-1} and tagged by $\tau \rightarrow h^- h^+ h^- \nu_\tau$
- Probe existence of a long-lived invisible gauge boson α
- Reconstruct τ pseudo rest frame based on $E_\tau = \sqrt{s}/2$, $\hat{p}_\tau \approx -\vec{p}_{3h}/|\vec{p}_{3h}|$
- Search for an excess of events on $\tau^- \rightarrow \ell^- \bar{\nu}_\ell \nu_\tau$ normalized lepton energy

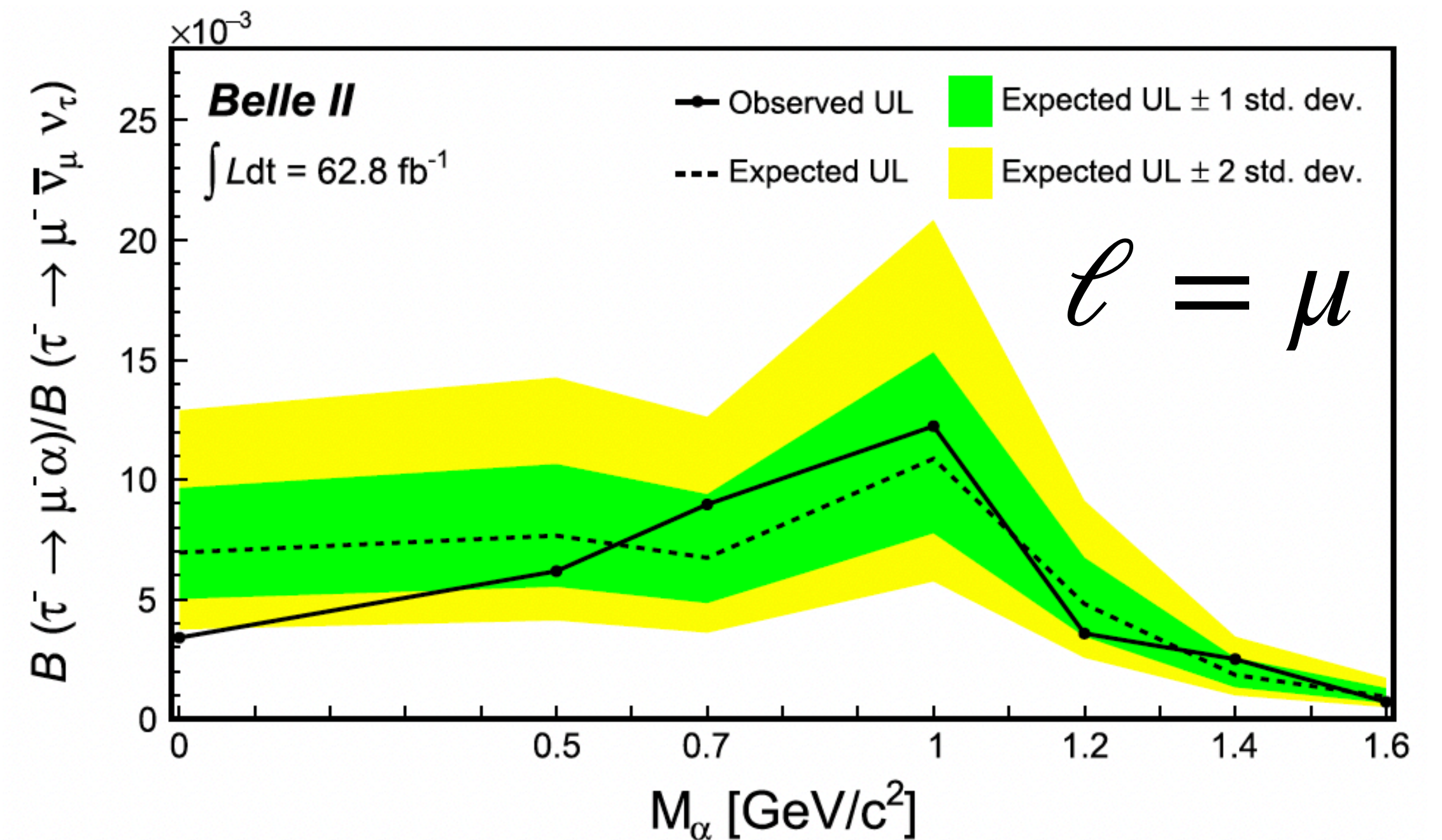
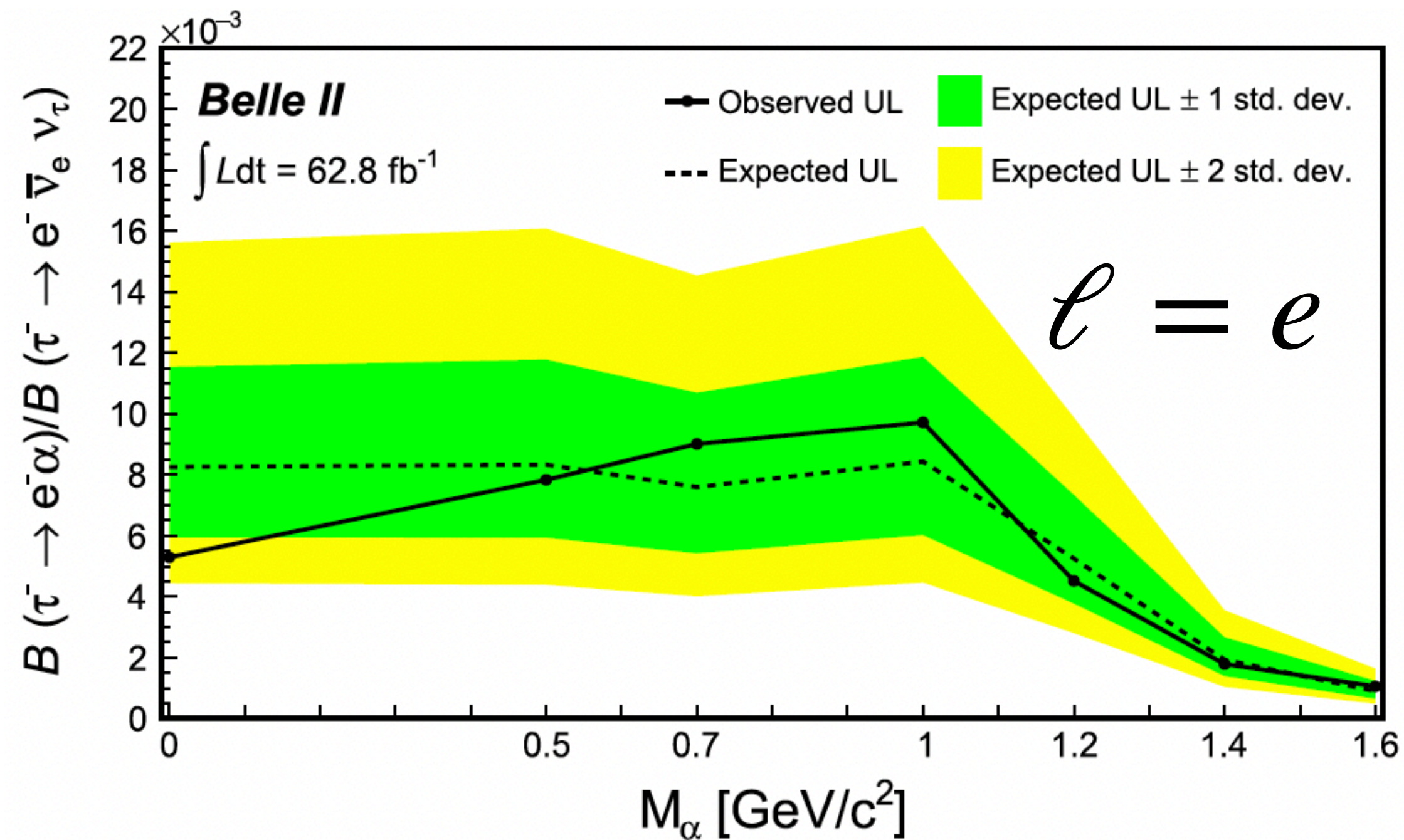
$$x_\ell = \frac{E_\ell^*}{m_\tau c^2/2}$$



Search for LFV $\tau^- \rightarrow \ell^- + \alpha$

PRL 130, 181803 (2023)

- No signal observed
- Set upper limit at 95% C.L. for $\mathcal{B}(\tau \rightarrow \ell \alpha) / \mathcal{B}(\tau \rightarrow \ell \bar{\nu}_\ell \nu_\tau)$
- World **best** limits to date



Summary & Prospects

- As luminosity frontier project, SuperKEKB/Belle II will search for physics beyond SM with ultimate sensitivity

- By Summer 2022, Belle II has achieved

$$L_{\text{peak}} = 4.7 \times 10^{34} \text{ cm}^{-2}\text{s}^{-1} \text{ (world record)}$$

$$L_{\text{int}} = 424 \text{ fb}^{-1} \text{ (similar to BarBar; } \sim \text{ half of Belle)}$$

- Many exciting physics results are on the way
 - Benefited by improved detector performance & analysis technique
 - Some of them are already world-leading
- After current shutdown period, we will try to achieve higher luminosity
 - During LS1, many components are to be improved

| Observables | Expected the. accuracy | Expected exp. uncertainty | Facility (2025) |
|--|------------------------|---------------------------|-----------------|
| UT angles & sides | | | |
| ϕ_1 [°] | *** | 0.4 | Belle II |
| ϕ_2 [°] | ** | 1.0 | Belle II |
| ϕ_3 [°] | *** | 1.0 | LHCb/Belle II |
| $ V_{cb} $ incl. | *** | 1% | Belle II |
| $ V_{cb} $ excl. | *** | 1.5% | Belle II |
| $ V_{ub} $ incl. | ** | 3% | Belle II |
| $ V_{ub} $ excl. | ** | 2% | Belle II/LHCb |
| CP Violation | | | |
| $S(B \rightarrow \phi K^0)$ | *** | 0.02 | Belle II |
| $S(B \rightarrow \eta' K^0)$ | *** | 0.01 | Belle II |
| $A(B \rightarrow K^0 \pi^0) [10^{-2}]$ | *** | 4 | Belle II |
| $A(B \rightarrow K^+ \pi^-) [10^{-2}]$ | *** | 0.20 | LHCb/Belle II |
| (Semi-)leptonic | | | |
| $B(B \rightarrow \tau \nu) [10^{-6}]$ | ** | 3% | Belle II |
| $B(B \rightarrow \mu \nu) [10^{-6}]$ | ** | 7% | Belle II |
| $R(B \rightarrow D \tau \nu)$ | *** | 3% | Belle II |
| $R(B \rightarrow D^* \tau \nu)$ | *** | 2% | Belle II/LHCb |
| Radiative & EW Penguins | | | |
| $B(B \rightarrow X_s \gamma)$ | ** | 4% | Belle II |
| $A_{CP}(B \rightarrow X_{s,d} \gamma) [10^{-2}]$ | *** | 0.005 | Belle II |
| $S(B \rightarrow K_S^0 \pi^0 \gamma)$ | *** | 0.03 | Belle II |
| $S(B \rightarrow \rho \gamma)$ | ** | 0.07 | Belle II |
| $B(B_s \rightarrow \gamma \gamma) [10^{-6}]$ | ** | 0.3 | Belle II |
| $B(B \rightarrow K^* \nu \bar{\nu}) [10^{-6}]$ | *** | 15% | Belle II |
| $B(B \rightarrow K \nu \bar{\nu}) [10^{-6}]$ | *** | 20% | Belle II |
| $R(B \rightarrow K^* \ell \ell)$ | *** | 0.03 | Belle II/LHCb |
| Charm | | | |
| $B(D_s \rightarrow \mu \nu)$ | *** | 0.9% | Belle II |
| $B(D_s \rightarrow \tau \nu)$ | *** | 2% | Belle II |
| $A_{CP}(D^0 \rightarrow K_S^0 \pi^0) [10^{-2}]$ | ** | 0.03 | Belle II |
| $ q/p (D^0 \rightarrow K_S^0 \pi^+ \pi^-)$ | *** | 0.03 | Belle II |
| $\phi(D^0 \rightarrow K_S^0 \pi^+ \pi^-) [^\circ]$ | *** | 4 | Belle II |
| Tau | | | |
| $\tau \rightarrow \mu \gamma [10^{-10}]$ | *** | < 50 | Belle II |
| $\tau \rightarrow e \gamma [10^{-10}]$ | *** | < 100 | Belle II |
| $\tau \rightarrow \mu \mu \mu [10^{-10}]$ | *** | < 3 | Belle II/LHCb |

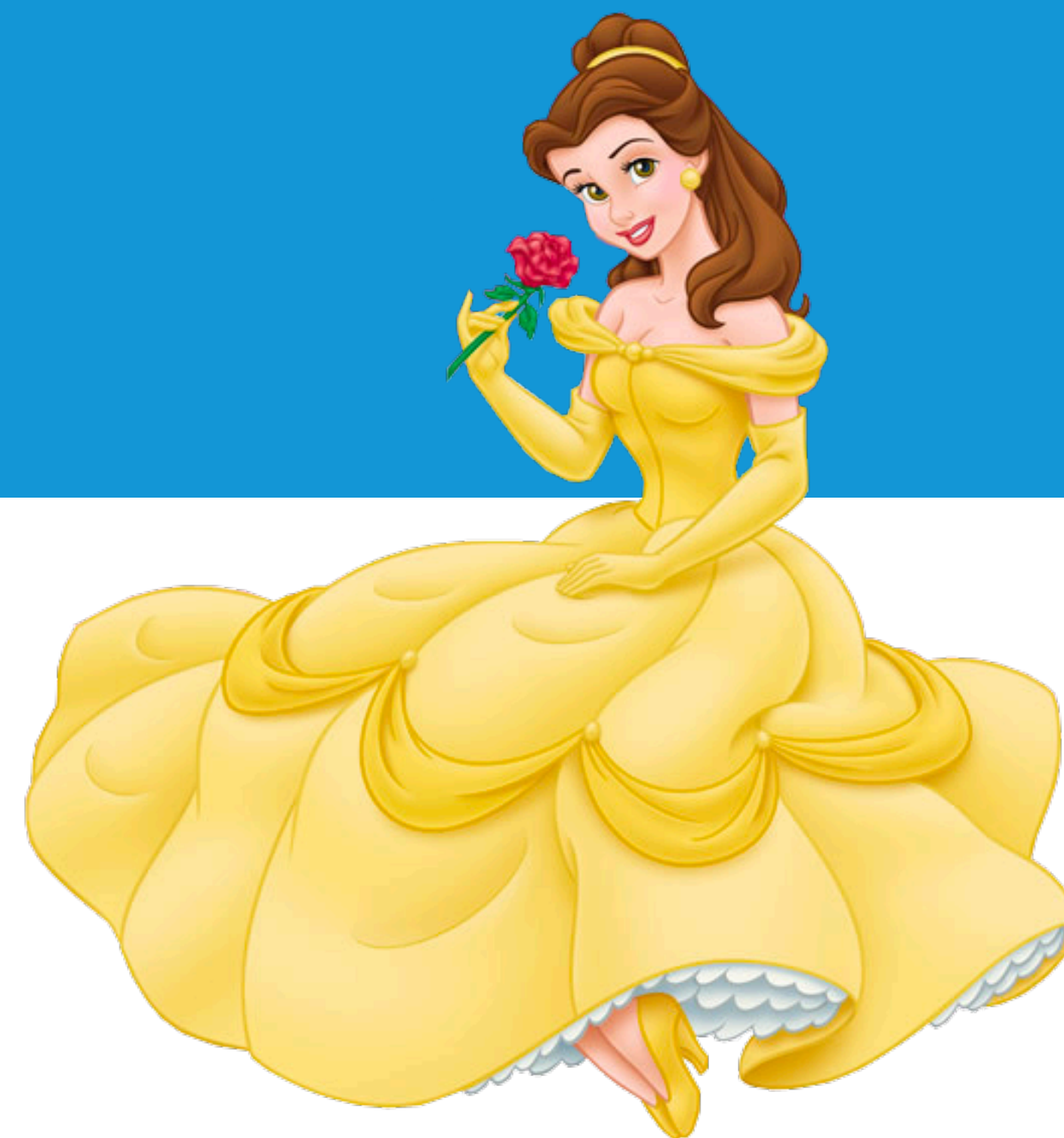
THANK YOU



Belle II Collaboration Meeting (February 13-17, 2023)



> 1100 active members
124 institutes
27 countries



Backup Slides

Table I: Statistical and systematic uncertainties on the value of $R(X_{e/\mu})$ from the most significant sources.

| Source | Uncertainty [%] |
|------------------------------------|-----------------|
| Sample size | 1.0 |
| Lepton identification | 1.9 |
| $X_c \ell \nu$ branching fractions | 0.1 |
| $X_c \ell \nu$ form factors | 0.2 |
| Total | 2.2 |

Measurement of Λ_c^+ Lifetime

PRL 130, 071802 (2023)

| Source | Uncertainty [fs] |
|--------------------------|------------------|
| Ξ_c contamination | 0.34 |
| Resolution model | 0.46 |
| Non- Ξ_c backgrounds | 0.20 |
| Detector alignment | 0.46 |
| Momentum scale | 0.09 |
| Total | 0.77 |

Major sources of systematic error:

- $\Xi_c^{0/+}$ contamination
- *Resolution Model*: Correlations between the decay time and the decay-time uncertainty are neglected.
- *Background model*: Sideband data that differ from the background in the signal region. Systematic is estimated using the differences in data-MC.
- *Alignment of the detector*: Periodic calibrations are necessary to account for detector misalignment. Misalignment can bias the measurement of the decay lengths.

Fit to (t, σ_t)

- Unbinned ML fit to (t, σ_t) for candidates in the signal region.
- PDF Model:

- Signal PDF :

$$pdf(t, \sigma_t | \tau, f, b, s_1, s_2) = pdf(t | \sigma_t, \tau, f, b, s_1, s_2) pdf(\sigma_t)$$

$$\propto \int_0^\infty e^{-t_{true}/\tau} R(t - t_{true} | \sigma_t, f, b, s_1, s_2) dt_{true} pdf(\sigma_t)$$

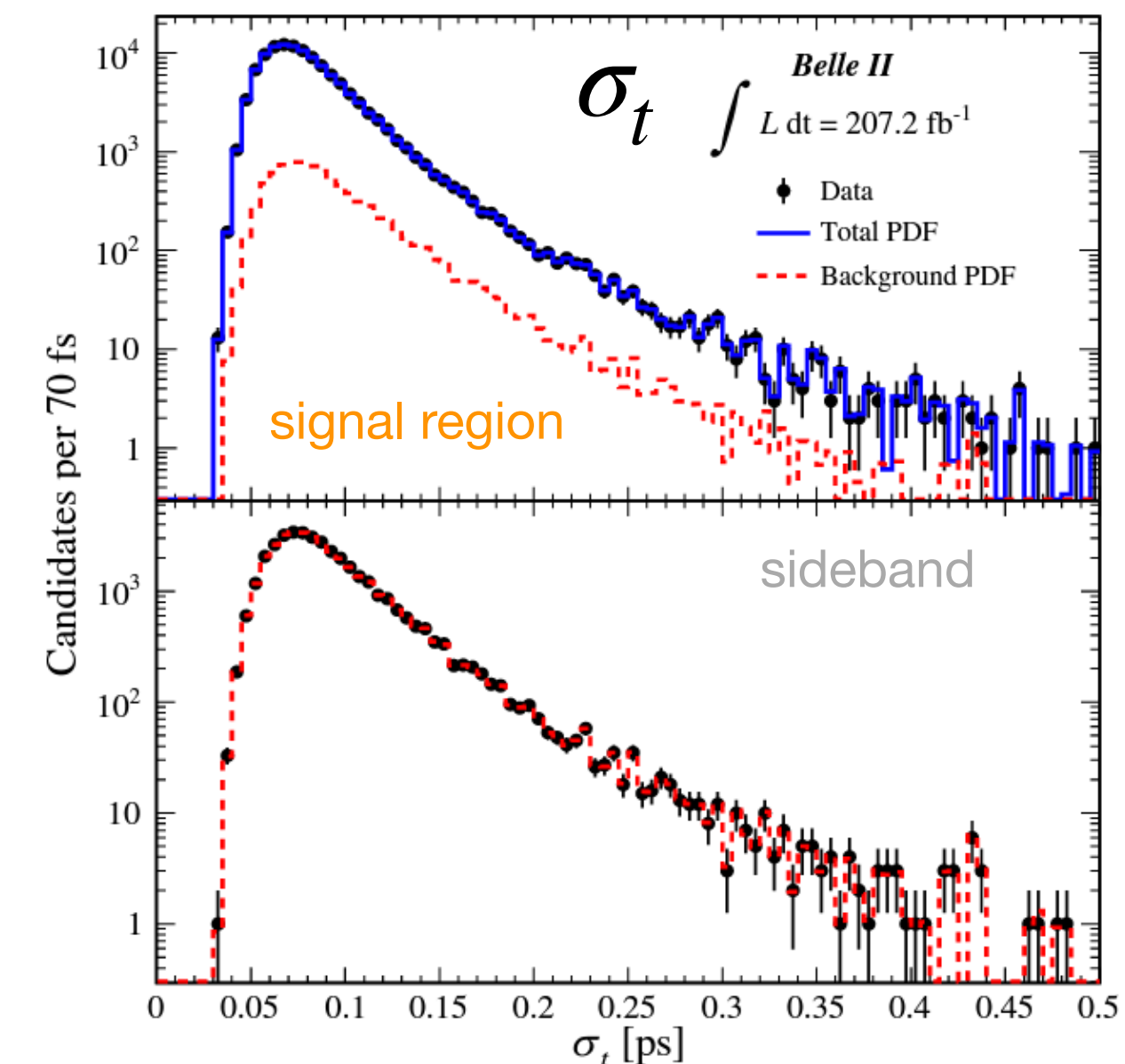
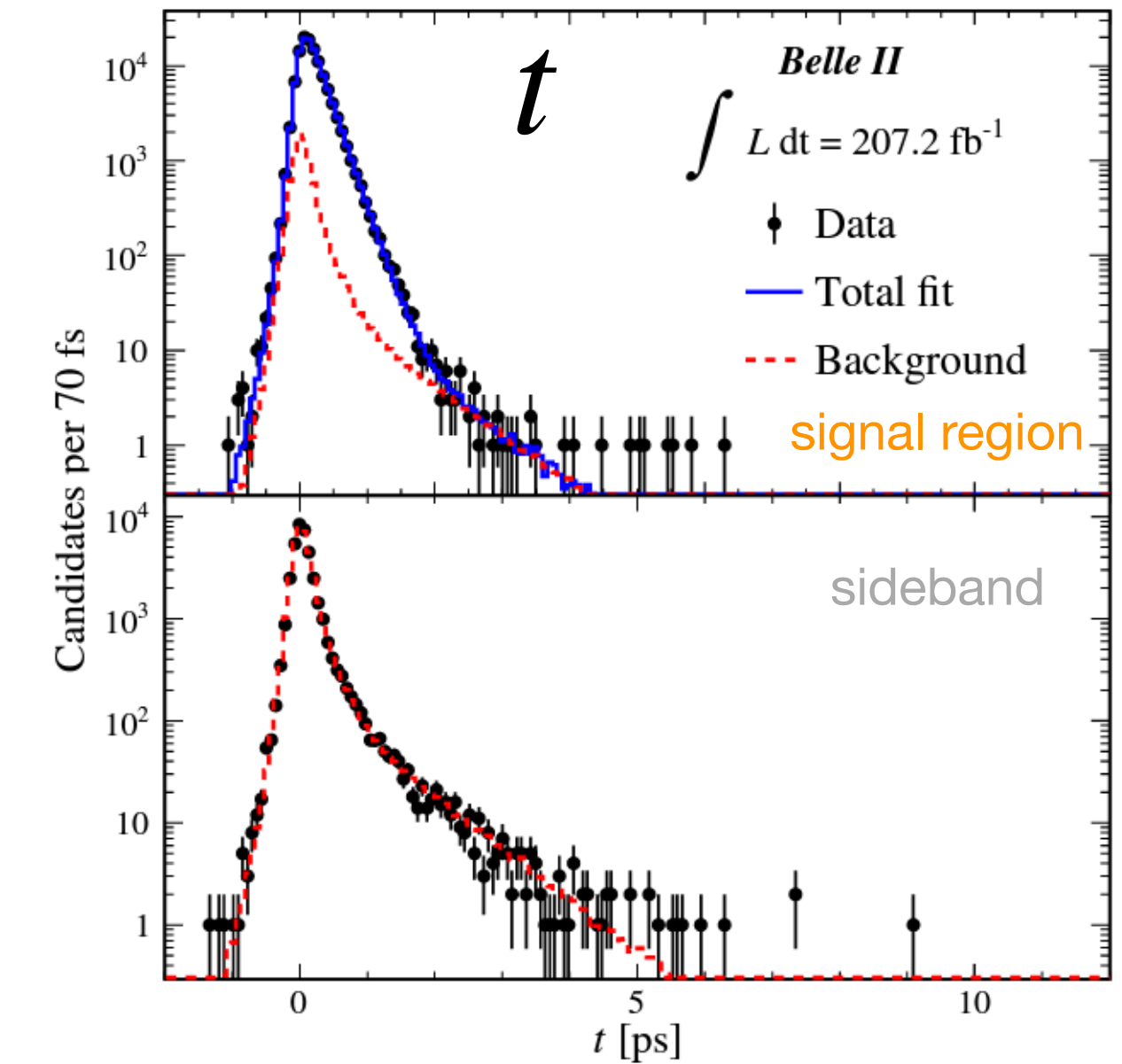
f is the fraction of events in the Gaussian, and b is a mean parameter for a possible bias in t . R is the resolution function as:

$$R(t - t_{true} | \sigma_t, f, b, s_1, s_2) = f G(t - t_{true} | b, s_1 \sigma_t) + (1 - f) G(t - t_{true} | b, s_2 \sigma_t)$$

$s_1 \sigma_t$ and $s_2 \sigma_t$ are the Gaussian widths.

- Background PDF:

- Empirical model of the sideband data, is the sum of two exponential functions convolved with Gaussian resolution functions.
- A simultaneous fit to the events in the signal region and sidebands is also performed.



| Source | Uncertainty (fs) |
|-------------------------|------------------|
| Fit bias | 3.4 |
| Resolution model | 6.2 |
| Background model | 8.3 |
| Detector alignment | 1.6 |
| Momentum scale | 0.2 |
| Input Ω_c^0 mass | 0.2 |
| Total | 11.0 |

Major sources of systematic error are:

- *Background model*: Sideband data that differ from the background in the signal region. Systematic is estimated using the differences in data-MC.
- *Resolution model*: Simulation shows that the resolution function has tails that are inconsistent with a Gaussian model.
- *Fit Bias*: Due to small sample size.

Search for LFV $\tau^- \rightarrow \ell^- + \alpha$

TABLE III. Central values with their uncertainties, 95% C.L., and 90% C.L. upper limits (UL) for the branching-fraction ratios $\mathcal{B}_{e\alpha}/\mathcal{B}_{e\bar{\nu}\nu}$ (top) and $\mathcal{B}_{\mu\alpha}/\mathcal{B}_{\mu\bar{\nu}\nu}$ (bottom) for various masses of the α boson. Corresponding absolute upper limits for $\mathcal{B}(\tau^- \rightarrow \ell^- \alpha)$, computed using standard-model branching fractions from Ref. [35], are provided in parentheses for convenience.

| M_α [GeV/ c^2] | $\mathcal{B}_{e\alpha}/\mathcal{B}_{e\bar{\nu}\nu}$ ($\times 10^{-3}$) | UL at 95% C.L. ($\times 10^{-3}$) | UL at 90% C.L. ($\times 10^{-3}$) |
|--------------------------|--|-------------------------------------|-------------------------------------|
| 0.0 | -8.1 ± 3.9 | 5.3(0.94) | 4.3(0.76) |
| 0.5 | -0.9 ± 4.3 | 7.8(1.40) | 6.5(1.15) |
| 0.7 | 1.7 ± 4.0 | 9.0(1.61) | 7.6(1.36) |
| 1.0 | 1.7 ± 4.2 | 9.7(1.73) | 8.2(1.47) |
| 1.2 | -1.1 ± 2.6 | 4.5(0.80) | 3.7(0.66) |
| 1.4 | -0.3 ± 1.0 | 1.8(0.32) | 1.5(0.26) |
| 1.6 | 0.2 ± 0.5 | 1.1(0.19) | 0.9(0.16) |
| M_α [GeV/ c^2] | $\mathcal{B}_{\mu\alpha}/\mathcal{B}_{\mu\bar{\nu}\nu}$ ($\times 10^{-3}$) | UL at 95% C.L. ($\times 10^{-3}$) | UL at 90% C.L. ($\times 10^{-3}$) |
| 0.0 | -9.4 ± 3.7 | 3.4(0.59) | 2.7(0.47) |
| 0.5 | -3.2 ± 3.9 | 6.2(1.07) | 5.1(0.88) |
| 0.7 | 2.7 ± 3.4 | 9.0(1.56) | 7.8(1.35) |
| 1.0 | 1.7 ± 5.4 | 12.2(2.13) | 10.3(1.80) |
| 1.2 | -0.2 ± 2.4 | 3.6(0.62) | 2.9(0.51) |
| 1.4 | 0.9 ± 0.9 | 2.5(0.44) | 2.2(0.38) |
| 1.6 | -0.3 ± 0.5 | 0.7(0.13) | 0.6(0.10) |